

**Fe₃O₄/Al₂O₃/ZrO₂ TERNARY OXIDE NANOCOMPOSITE:
SYNTHESIS, CHARACTERIZATION AND PHOSPHATE
DESORPTION STUDY FROM ACID SOIL USING DIALYSIS
MEMBRANE TUBES (DMTs)**

MSc THESIS

DAWIT ALEMU MAMMO

MAY 2018

HARAMAYA UNIVERSITY, HARAMAYA

**Fe₃O₄/Al₂O₃/ZrO₂ Ternary Oxide Nanocomposite: Synthesis,
Characterization and Phosphate Desorption Study from Acid Soil using
Dialysis Membrane Tubes (DMTs)**

**A Thesis Submitted to the Department of Chemistry, Postgraduate Program
Directorate
HARAMAYA UNIVERSITY**

**In Partial Fulfillment of the Requirements for the Degree of
MASTER OF SCIENCE IN CHEMISTRY (ANALYTICAL CHEMISTRY)**

Dawit Alemu Mammo

**May 2018
Haramaya University, Haramaya**

HARAMAYA UNIVERSITY
POSTGRADUATE PROGRAM DIRECTORATE

I hereby certify that I have read and evaluated this Thesis entitled “ $\text{Fe}_3\text{O}_4/\text{Al}_2\text{O}_3/\text{ZrO}_2$ Ternary oxide Nanocomposite: Synthesis, Characterization and Phosphate Desorption Study from Acidic soil using Dialysis Membrane Tubes (DMTs)” prepared under my guidance by Dawit Alemu. I recommend that it be submitted as fulfilling the thesis requirement.

Abi Tadesse (PhD)	_____	_____
Major Advisor	Signature	Date

Tesfahun Kebede (PhD)	_____	_____
Co-Advisor	Signature	Date

Isabel Diaz (Prof.)	_____	_____
Co-Advisor	Signature	Date

As a member of the Board of Examiners of the MSc Thesis Open Defense Examination, I certify that I have read and evaluated the thesis prepared by Dawit Alemu and examined the candidate. I recommend that the thesis be accepted as fulfilling the Thesis requirement for the degree of Master of Science in Chemistry (Analytical Chemistry).

_____	_____	_____
Chairperson	Signature	Date

_____	_____	_____
Internal Examiner	Signature	Date

_____	_____	_____
External Examiner	Signature	Date

DEDICATION

I dedicate this thesis manuscript to my late father Alemu Mammo.

STATEMENT OF AUTHOR

By my signature below, I declare and affirm that this thesis is my own work and I have followed all ethical and technical principles of scholarship in the preparation, data collection, data analysis and complication of this thesis. Any scholarly matter that is included in the Thesis has been given recognition through citation.

This Thesis is submitted in partial fulfillment of the requirements for MSc Degree in Analytical Chemistry at Haramaya University and is deposited at the University Library to be made available under rules of the Library. I solemnly declare that this thesis is not submitted to any other institution anywhere for the award of any academic degree, diploma, or certificate.

Brief quotations from this thesis are allowable without special permission provided that accurate acknowledgement of source is made. Requests for permission for extended quotation from or reproduction of this manuscript in whole or in part may be granted by the Head of the Department of Chemistry or the Director of Postgraduate Program Directorate when in his/her judgment the proposed use of the material is in the interests of scholarship. In all other instances, however, permission must be obtained from the author.

Name: Dawit Alemu:

Signature _____

Date: _____

Department: Chemistry

BIOGRAPHICAL SKETCH OF THE AUTHOR

The author was born in Debre Libanos Woreda, North Shewa Zone, Oromia, Ethiopia on September 11, 1988. He attended his elementary and junior education from 1994-2001 at Schools in Dehana Primary and Junior School and secondary education at Fiche Comprehensive Secondary and Preparatory School from 2002-2005. After completing high School, he joined Hawassa University in 2006 and graduated in July 2008 with B. Sc Degree in Applied Chemistry. Soon after graduation, the author was employed by the Somali Education Bureau as Chemistry teacher then after serving one year he joined Jijiga University and serve for 4 years as laboratory technician and graduate assistant. In 2016, he joined Postgraduate Program Directorate of the Haramaya University as a candidate for Master of Science in Chemistry (Analytical Chemistry).

ACKNOWLEDGMENTS

First, I would like to thank the Almighty God for giving me the life, patience, audacity wisdom from the beginning to the completion of this work.

I consider it a profound pleasure to express my deep sense of indebtedness; gratitude and profound thanks to my supervisors, Dr. Abi Tadesse and Dr. Tesfahun Kebede, without them the entire work would not have come into existence. Their critical comments and helpful guidance gave me a chance to explore further.

I thank the Chemistry Department of Haramaya University for hosting me to pursue my M.Sc. study and Ministry of Education for providing me the financial assistance.

I would like to thank Dr. Yonas Chebude and Dr. Negash Getachew from Addis Abeba University for FTIR and XRD characterization of the Nano composite.

I would also like to give great respect to Dr. Abi Tadesse and Prof. Isabel Diaz for their support in characterizing the as-synthesized samples using SEM and EDX conducted at the Instituto de Catálisis Y. Petroleoquímica, CSIC, C/Marie Curie 2, Madrid, Spain.

My special heartfelt gratitude also goes to Dr. Endale Teju for his guidance, consistent supervision, as well as suggestions during laboratory work.

I am forever grateful to my beloved Sisters Eskedar Mesfin and Rahel Alemu my Mother, Tsehay Tafese and my beloved brother Degafe Zeleke; they have always been constant source of my strength and hope in every aspect of my life.

My special acknowledgement extends to Wakshuma Yadesa (PhD Student in department of Soil Science, Haramaya University) for soil sample collection for this work. Lastly, I would like to thank my friends, Fantahun Gonfa, Hirpo Hinsene and Yebrehu Bogale for all their help, support throughout the study period.

ACRONYMS AND ABBREVIATIONS

ANOVA	Analysis of Variance
ATP	Adenosine tri-phosphate
DNA	Deoxyribonucleic Acid
RNA	Ribonucleic Acid
DMT HFO	Dialysis Membrane Tube-Hydrous Ferric Oxide
DMT-Fe-Al-Zr	Dialysis Membrane Tube-Iron Alumina Zircon
DMWCO	Molecular weight Cutoff
FAAS	Flame Atomic Absorption Spectroscopy
FTIR	Fourier Transforms Infrared
NMOs	Nano Sized Metal Oxides
SEM-EDX	Scanning Electron Microscope with Energy Dispersive X-ray
TEM	Transmission Electron Microscopy
UV-Vis	Ultraviolet-Visible Spectroscopy
XRD	X-ray Diffractometer

TABLE OF CONTENTS

STATEMENT OF AUTHOR	iv
ACKNOWLEDGMENTS	vi
ACRONYMS AND ABBREVIATIONS	vii
TABLE OF CONTENTS	viii
LIST OF TABLES	xi
LIST OF FIGURES	xii
LIST OF TABLES IN THE APPENDIX	xiii
LIST OF FIGURES IN THE APPENDIX	xiv
1. INTRODUCTION	1
2. LITERATURE REVIEW	5
2.1. Nanosized Metal Oxides	5
2.1.1. Iron Oxide	6
2.1.2. Aluminum Oxide	6
2.1.3. Zirconium Oxide	7
2.2. Multi Component Nanocomposite Metal Oxides as Sorbents	8
2.3. Synthesis Methods of Nanomaterials	9
2.3.1. Hydrothermal Synthesis Method	10
2.3.2. Sol-Gel Method	10
2.3.3. Co-Precipitation Method	11
2.4. Dialysis Membrane Tube	11
2.5. Phosphorus Desorption Kinetics	12
2.6. P- Species in Soil	14
2.7. Process of P Transformation in Soil	16
2.7.1. Sorption Process	17
2.7.2. Precipitation	19
2.8. Sorption Mechanisms of Phosphate to Metal Oxides	20
2.8.1 Electrostatic Force	20
2.8.2. Ion Exchange	21

Continues...

Continued...

2.8.3. Lewis Acid–Base Interaction	21
2.9. Sorption and Desorption of Phosphorus	22
2.10. Factors that affect P-sorption	24
3. MATERIALS AND METHODS	26
3.1. Description of Study Area and Experimental Site	26
3.1.1. Description of Soil Sampling Areas	26
3.1.2. Experimental Site	26
3.2. Instruments and Apparatus	26
3.3. Chemicals and Reagents	27
3.4. Experimental Procedures	28
3.4.1 Soil Sample Collection and Sample Preparation	28
3.4.2. Physicochemical Properties	29
3.4.3. Synthesis of Fe-Al-Zr Mixed Oxide Nanocomposite	30
3.4.4. Characterization of the As-synthesized Adsorbent	31
3.5. Desorption Study	32
3.6. Data Analysis	33
4. RESULTS AND DISCUSSION	34
4.1. Characterization of the Adsorbent	34
4.1.1. Powder X-ray Diffraction	34
4.1.2. FT-IR Analysis	35
4.1.3. Elemental Analysis	36
4.1.4. SEM and EDX Analysis	36
4.2. Physicochemical Properties of the Soil	38
4.3. Long Term Phosphate Desorption Study	43
4.4. Kinetics of Phosphorus Desorption	49
4.4.1. Correlation of Soil Parameter with Cumulative Desorption P	53
5. SUMMARY, CONCLUSION AND RECOMMENDATION	56
5.1. Summary and Conclusion	56
5.2. Recommendations	57

Continues...

6.REFERENCES

Continued...

58

7. APPENDIX

71

LIST OF TABLES

Table	Page
1. Actual yield and theoretical composition of the selected as-synthesized adsorbent	36
2. Selected physical and chemical properties of the soil samples studied	39
3. Desorption of Phosphorus from four different soil samples for 28 days with different P treatment (in triplicate)	44
4. Desorption of phosphorus from four different soil samples for 28 days with similar P treatment (in triplicate n = 3)	45
5. P desorption rate of soil samples studied	51
6. Correlation of desorbed phosphorus level and soil properties for Boji Dirmeji(B) and Mana Sibü (M) soil samples	54
7. Correlation of desorbed phosphorus level and soil properties for Kiltu Kara (K) and Nedjo (N) soil samples	55

LIST OF FIGURES

Figure	Page
1. Speciation distribution of phosphates	15
2. Bi-dentate arrangement	18
3. Phosphate sorption mechanisms of metal oxides	22
4. The availability of phosphorus as affected by soil pH	25
5. XRD pattern of $\text{Fe}_3\text{O}_4/\text{Al}_2\text{O}_3/\text{ZrO}_2$ mixed oxide	34
6. FTIR spectrum of the nano sized Fe-Al-Zr mixed oxide adsorbent.	35
7. Scanning electron microscopic images of $\text{Fe}_3\text{O}_4/\text{Al}_2\text{O}_3/\text{ZrO}_2$ with EDX spectrum	37
8. Cumulative desorbable P with time extracted using DMT-Fe-Al-Zr for the different treatments for Bojii Dirmejjii (B) soil sample over 28 days	47
9. Cumulative desorbable P with time extracted using DMT-Fe-Al-Zr for the different treatments for Mana Sibii (M) soil sample over 28 days	47
10. Cumulative desorbable P with time extracted using DMT-Fe-AlZr for the different treatments for Kiltu Kara (K) soil sample over 28 days	48
11. Cumulative desorbable P with time extracted using DMT-Fe-Al-Zr for the different treatments for Nedjo (N) soil sample over 28 days	48
12. Phosphorus desorption rates from soil to solution for Boji Dirmij (a) Mana Sibii (b), Kara Kiltu (c) and Nedjo (d) soil samples with different P treatment	52

LIST OF TABLES IN THE APPENDIX

Appendix Table	Page
1. Total correlation between soil properties and cumulative P desorbed for Bojii (B) soil	72
2. Total correlation between soil properties and cumulative P desorbed for Mana Sibiu (M) soil.	73
3. Total correlation between soil properties and cumulative P desorbed for Kara Kiltu (K) soil	74
4. Total correlation between soil properties and cumulative P desorbed for Nedjo (N) soil	75

LIST OF FIGURES IN THE APPENDIX

Appendix Figure	Page
1. Calibration curve for day 1 P desorption	76
2. Calibration curve for day 7 P desorption	76
3. Calibration curve for day 14 P desorption.	77
4. Calibration curve for day 21 P desorption.	77
5. Calibration curve for day 28 P desorption.	78
6. Calibration curve for total phosphorus	78
7. Calibration curve for Mn in soil for dithionate extractants	79
8. Calibration curve for Fe in soil for dithionate and oxalate extractants	79
9. Calibration curve for Mn in soil for oxalate extractants	80
10. Calibration curve for Zr in synthesized nano composite	80
11. Calibration curve for Fe in synthesized nano composite	81
12. Cumulative desorbable P with time extracted using DMT-Fe-Al-Zr for the different treatments for Boji Dirmeji (B) soil sample over 28 days	81
13. Cumulative desorbable P with time extracted using DMT-Fe-Al-Zr for the different treatments for Mana Sibiu (M) soil sample over 28 days	82
14. Cumulative desorbable P with time extracted using DMT-Fe-Al-Zr for the different treatments Kiltu Kara (K) for soil sample over 28 days	82
15. Cumulative desorbable P with time extracted using DMT-Fe-Al-Zr for the different treatments for Nedjo (N) soil sample over 28 days	83

**Fe₃O₄/Al₂O₃/ZrO₂ TERNARY OXIDE NANOCOMPOSITE: SYNTHESIS,
CHARACTERIZATION AND PHOSPHATE DESORPTION STUDY FROM ACIDIC
SOIL USING DIALYSIS MEMBRANE TUBES (DMTs)**

ABSTRACT

Phosphorus (P) is an essential element for plant and animal growth; although plant roots are capable of absorbing P from the soil solution at low P concentrations, most soils cannot supply sufficient amounts of P to the plant due to various factors. Knowledge of the effect of the P remaining in the soil (residual effect) is of great importance for fertilization recommendation. Phosphorous fixation to soil results in less P available to plants. Nano technology addresses the development of solutions to the existing environmental problems. For this purpose, Fe-Al-Zr ternary mixed oxide Nano composite adsorbent with 70, 25 and 5 percentage composition of Fe, Al, and Zr respectively was synthesized by co-precipitation method. The as-synthesized adsorbent was characterized by X-ray diffraction (XRD), Fourier transform-infrared (FT-IR), flame atomic absorption spectroscopy (FAAS) studies and Scanning Electron Microscope with Energy Dispersive X-ray (SEM-EDX). The study of phosphate desorption was carried out on four soil samples collected from West Wollega Zone, Oromia region namely, Kiltu Kara, Nedjo Boji, Dirmeji and Mana Sibiu which were incubated with 0, 50, 100 and 150 ppm phosphate. Selected physicochemical properties of soil were determined. The simulation of phosphate desorption from soil to plant was predicted by dialysis membrane tube filled with Iron-aluminum-Zirconium oxide (DMT-Fe-Al-Zr). The results suggest that the phosphorus treatment and desorption time had significant effect on the amount of desorbed phosphorus from the soils. The phosphate desorbed was found to be highest at Kiltu Kara soil with 150 mg/Kg treatment which has the value ranging (4.51-32.62.mg/Kg) and lowest in the control (1.42-15.591 mg kg⁻¹) at all levels of extraction time for all soil types. The releasing rate of phosphate from soil followed first order kinetics having highest desorption rate found on day 1 for Kiltu Kara soil sample with the value of 4.63 mg/Kg day⁻¹ and the lowest was observed on day 28th of Boji Dirmeji (B) with the value of 0.44 mg/Kg day⁻¹. Therefore, the DMT- Fe-Al-Zr method can serve as analytical tool to assess the availability of residual P in soil, which is essential to estimate available P for plants.

Keywords: Acid Soil, Dialysis membrane tubes, Fe-Al-Zr mixed oxide, Nano-composites, Phosphorus desorption,

1. INTRODUCTION

1.1. Background of the Study

Phosphorus (P) is a central element to life on earth. Living organisms rely on it, as it is crucially involved in most major metabolic processes for example; it takes on a prime role in energy transfer as adenosine tri-phosphate (ATP). As phospholipids, phosphorus being part of cell membranes and part of nucleotides, it is a major component to build up DNA and RNA. Furthermore, plants are dependent on phosphorus to secure energy production in photosynthesis (Ruttenberg, 2009). Due to the reasons mentioned above, the fundamental significance of phosphorus in agriculture and food production is beyond question.

Compared with the other major nutrients, phosphorus is by far the least mobile and available to plants in most soil conditions. It is, therefore, frequently a major or even the prime limiting factor for plant growth. Indeed, it is estimated that 5.7 billion of hectares worldwide contain too little available phosphorus for sustaining optimal crop production (Gaume, 2000). The poor mobility of soil inorganic phosphorus is due to the large reactivity of PO_4^{3-} ions relative to numerous soil constituents and to the consequent strong retention of most of soil phosphorus onto those. Therefore, only a marginal proportion of soil phosphorus is present as PO_4^{3-} ions in the soil solution.

Phosphorus deficiency in soils is a wide spread problem in the world (Harrison, 1987). It is believed to be the second most important soil fertility problem throughout the world next to nitrogen (Warren 1992). It is often the first limiting element in acid tropical soils (Buehler *et al.*, 2002). The amount of available soil P has been more frequently evaluated than the rate of its release when studying the P nutrition of plants. The term Available-P is often used to express the amount of soil P in solution, which can be extracted or mined by plant roots and utilized by the plant for growth and development during its life cycle. It is also referred to as labile P. The concentration of available-P is always low because of continuous plant uptake. This is further complicated by the slow replenishment of the extracted P from the soil solution by the labile pool which is dictated by the soil P equilibria (Holford, 1997).

It is however, favored by an application of P-amendment source like fertilizers or manure. The concentration of available-P pool is dictated by the prevailing soil conditions at a particular time and the ability of the crop to extract the P from the soil solution. Maintenance of plant-available P in the soil is very imperative to avoid over exploitation of soil P which will lead to P deficiency and consequently, low plant yield. This maintenance is a function of the concentration of P in the labile pool and how readily it is released into the soil solution from the solid phase. The availability of a nutrient to plants depends on the rate at which it released to replenish the soil solution (Raven and Hossner 1994). There can be a significant residual effect due to desorption of phosphate from the soil of long term fertilization history and this can lead to an underestimation of the benefit of phosphate fertilizer if not taken in to account (McKean and Warren, 1996).

Soil tests for plant available P is used worldwide to determine the current P status of soils so as to estimate fertilizer P requirements for specific yield goals. Soils receiving successive applications of fertilizer P or manure over a long-term, therefore, can accumulate large amounts of residual P. This represents not only an uneconomic practice, as phosphate ores are expected to be depleted within approximately 60-100 years, but also the risk of potential for P loss to surface waters via overland or subsurface flow and this in turn accelerate freshwater eutrophication (McDowell and Sharpley, 2002). The current P status is due to indigenous (native) P present in the soil and P from previous fertilizer P application (residual P) (Indiati, 2000). Since the actual plant available P is composed of solution P plus P that enters the solution as the result of desorption/dissolution from a solid phase, the conventional soil test methods have been unsatisfactory in predicting the plant P uptake (Beck and Sanchez, 1994).

Plant P availability of residual P in soils can be reliably estimated by consecutive cropping experiments carried out in field or green house conditions, where P is taken up until P deficiency occurs or a response to added P is measured (Indiati, 2000). Since this approach is very expensive and time consuming, successive soil extractions with P sink methods have been proposed to estimate residual P. According to these methods, a given soil is subjected to repeat P desorption using materials that can act as P sinks.

In order to evaluate long-term P desorption kinetics, it is necessary to suppress the re-sorption reaction. This can be done by introducing effective P sinks into the system. Several P sink methods have been devised since 1987. For example, Vander zee *et al.* (1987), proposed the use of Fe-oxide impregnated filter paper strips (Fe-oxide strips) as a promising method to study the P release kinetics of soils. However, this method was found to be not well applicable for long-term desorption studies as it may lead to errors due to adhesion of fine P rich particles to the paper strips and due to the mechanical instability of the paper when used for long term desorption studies (Freese *et al.*, 1995; Lookman *et al.*, 1995). To overcome this deficiency, use of dialysis membrane tube in place of resin/Fe- strips for studying long-term P dynamics has been proposed by Freese *et al.* (1995). Following the work of Freese *et al.* (1995). Reports on the long-term P desorption studies have been emerged from South African acid soils (Ochwoh *et al.*, 2005; Taddesse *et al.*, 2008) and recently for some acid soils from Ethiopia (Gemechu *et al.*, 2015). This method is similar to Fe-oxide impregnated filter paper strips but in this case the P sink (hydrated iron oxide) is placed in a dialysis membrane tube instead of being impregnated in the filter paper.

The phosphate sink in all the aforementioned cases however is hydrated ferric oxide which is an example of typical single component system. Such systems in amorphous and nanocrystalline form have been employed widely for phosphate sorption acting as sinks. On the other hand, different Fe_2O_3 as natural minerals exist in our natural environment usually not alone and they very often coexist with silicate and alumina in soil. The fraction of silicate and alumina in clay varies in a broad range from very low up to 75% (Li *et al.*, 2007). Multi-component sorbents comprising mixtures of metal oxides, clay, quartz and organic compounds are ubiquitous in soils and aquatic environments and have been shown to be significant in determining the environmental distribution of various contaminants and nutrients. Binary oxides of Fe-Al in both amorphous and crystalline forms have been reported for phosphate sorption study (Sausa *et al.*, 2012; Tofik *et al.*, 2016). Employment of ternary mixed oxides for phosphate sorption is also a recent approach (Liu *et al.*, 2013; Yu and Chen, 2015; Buzuayehu *et al.*, 2017).

Although sorption of phosphate using binary and ternary oxides nanocomposites have been attempted, there is no report in the literature regarding the use of such materials for desorption of phosphate except the recent attempt by Gemechu *et al.* (2015). Magnetic Fe–Zr binary oxide was used as adsorbent for removal of phosphate from aqueous solution. The adsorbent is collected with a high gradient magnet. The magnetic Fe–Zr binary oxide adsorbent possessed favorable adsorption capacity for phosphate and exhibited good regeneration property. Thus, it is expected that an iron–zirconium composite material originated from the combination of iron oxide and zirconium oxide may take full use of the advantages of both parent materials and have the potential for phosphate removal.

Given the affinity of zirconium based mixed oxide system, we attempted to evaluate the desorption property of ternary mixed oxide where zirconium is a component, Fe-Al-Zr. To the best of the researchers' knowledge, there is no report on the use of this ternary system for phosphate desorption study. We are inspired as the result to study the desorption of phosphate by using Fe-Al-Zr ternary Nanocomposite placed in dialysis membrane tubes. The aim of this work was, therefore, to evaluate desorption of phosphate from soil solution using Fe-Al-Zr mixed oxide system as Nano-sorbent placed in DMT to serve as phosphate sink.

1.2. Objectives of the Study

1.2.1. General Objective

- ✓ The general objective of this study was to synthesize characterize and to evaluate the phosphate desorption from soil using; Fe-Al-Zr Nanocomposite filled dialysis membrane tubes from selected acid soils.

1.2.2. Specific Objectives

- ✓ To synthesize Fe-Al-Zr mixed oxide Nanocomposite by employing co-precipitation method.
- ✓ To characterize the as-synthesized Nanocomposite using modern instrumental techniques including XRD, FTIR, SEM-EDX and FAAS.
- ✓ To study desorption of P from acid soils by filling the as- synthesized Nanocomposite adsorbent in DMT.

2. LITERATURE REVIEW

2.1. Nanosized Metal Oxides

Synthesis of various functional Nanomaterial's such as metals, semiconductors, magnetic materials and so forth has been of immense scientific and technological interest. Among them aluminum and iron oxide nanomaterial are well-known and widely used materials in ceramics manufacturing. These compounds have both cationic and anionic chemisorption properties and this can possibly be used to remove metal ions from the aqueous phase. While the sorption capabilities of these aluminum and iron compounds are known, they have not found wide usage in this capacity because their sorption capacities have been limited compared to other material already commercially available. However, the nanomaterial form of this aluminum and iron is anticipated to be more catalytically active than its bulk form and if indeed sorption is the key mechanism, then the substantial increase in surface area of the nano form would increase capacities very significantly (Ge *et al.*, 2009).

The current knowledge on oxide materials allows affirming that most of their physicochemical Properties display acute size dependence. Physico-chemical properties of special relevance in Chemistry are mostly related to the environmental and industrial use of oxides as sensors, ceramics, absorbents and/or catalysts. Metal oxides are used for both their redox and acid/base properties in the context of Absorption and Catalysis. The three key features essential for their application as absorbents or catalysts are (i) the coordination environment of surface atoms, (ii) the redox properties, and (iii) the oxidation state at surface layers. In a simple classification, oxides having only s or p electrons in their valence orbital's tend to be more effective for acid/base catalysis, while those having d or f outer electrons find a wider range of uses for example as adsorbent (Yang *et al.*, 2008). The goal of nanotechnology is to make nanostructures or nanoarrays with special properties, which do not exist in their bulk or single particle types. Oxide nanoparticles can present unique physical and chemical properties, because of their limited size and high density in their corner or edge surface site (Bhattacharje *et al.*, 2011).

Among the available adsorbents, nano sized metal oxides (NMOs), including nano sized ferric oxides, manganese oxides, aluminum oxides, titanium oxides, magnesium oxides and cerium oxides are classified as the promising for inorganic anions such as arsenic (Cumbal and SenGupta, 2005), fluoride (Zhang *et al.*, 2007) and phosphate (Zhang *et al.*, 2009) removal from environmental solution systems. This is partly because of their large surface areas, high capacity, and selectivity and high activities caused by the size-quantization effect. The size and shape of NMOs are both important factors to affect their adsorption performance (Agrawal and Sahu, 2006).

2.1.1. Iron Oxide

Research on iron oxide nano material has experienced a surge in the recent decade or two. This is likely due to new synthetic techniques as well as interest in new applications of iron oxides nano material. Iron oxides have been extensively studied in diverse fields. Recently, functionalized iron oxide nano particles have also been used in many advanced nano technological applications (Vincent *et al.*, 2012). The most important advantage of nanosized iron oxides among other nano materials are due to its relatively low toxicity and biodegradability. It is observed that generally, amorphous metal oxides show great industrial potential in many advanced applications such as solar energy transformation, electronics, electrochemistry, manufacture of magnetic storage media, sorption and purification processes and catalysis. The intensively studied iron oxides for heavy metals removal from water/wastewater include goethite (α -FeOOH) and hematite (α -Fe₂O₃) used for removal of Cu (II), (Chen and Li, 2010), amorphous hydrous Iron oxides for Ni(II), Cr(III), Cu (II) and Pd(II) (Fan *et al.*, 2005).

2.1.2. Aluminum Oxide

Alumina has many appealing properties which makes the material interesting for applications in many different areas. Alumina especially has a high melting point, high strength, corrosion resistance, chemical stability, low thermal conductivity and good electrical insulation properties. As a type of important structural ceramic material, alumina has applications in absorbent, catalyst, carrier and reinforcement of ceramic composites.

Alumina occurs in nature as the minerals, corundum (Al_2O_3); diaspore ($\text{Al}_2\text{O}_3 \cdot \text{H}_2\text{O}$); gibbsite ($\text{Al}_2\text{O}_3 \cdot 3\text{H}_2\text{O}$); and most commonly as bauxite, which is an impure form of gibbsite. Alumina (Al_2O_3) is a traditional adsorbent for heavy metals, and $\gamma\text{-Al}_2\text{O}_3$ is anticipated to be more adsorptive active than $\alpha\text{-Al}_2\text{O}_3$ (Li *et al.*, 2008). Nanosized $\gamma\text{-Al}_2\text{O}_3$ can be prepared by sol-gel method and has been employed as solid phase extraction material for separation or pre-concentration of trace metal ions (Chang *et al.*, 2003). Chemical or physical modification of $\gamma\text{-Al}_2\text{O}_3$ nanoparticles with certain functional groups containing some donor atoms such as oxygen, nitrogen, sulfur and phosphorus is expected to improve their sorption toward heavy metals. When a modifier is immobilized at the surface of alumina, the removal mechanism is changed accordingly. The target metals are not only removed by adsorption on the surface of the alumina but also by a surface attraction/chemical bonding interaction on the newly added chemicals (Shabani *et al.*, 2009).

2.1.3. Zirconium Oxide

Among the metal oxides, which are widely employed as catalysts and support, the most prominent are silica, alumina and zirconium dioxide. Zirconium dioxide is an important oxide which has been used extensively for heterogeneous catalytic reactions. Application of zirconium dioxide has been quite promising in catalysis and many other areas due to its versatile structural and surface chemical properties as well as good thermal stability (Song *et al.*, 1996). It has been reported as a better catalyst and catalyst support compared to classical materials such as Al_2O_3 , SiO_2 and TiO_2 . In addition, zirconium oxide was also a suitable adsorbent for phosphate removal due to its good efficiency of adsorption and desorption for recycling. Zirconia was one of the ceramic oxides and was used to adsorb arsenate and phosphate (Long *et al.*, 2011). Qiu *et al.* (2015) used zirconium oxide as phosphate removing and recovering agent when they study about fabrication of a biomass-based hydrous zirconium oxide nanocomposite for preferable phosphate removal and recovery. Hydrous zirconium oxide could also serve as an efficient adsorbent because it possesses a rich amount of hydroxyl groups and shows high capacity and specific adsorption through Lewis acid-base interaction toward phosphate (Su *et al.*, 2013).

2.2. Multi Component Nanocomposite Metal Oxides as Sorbents

Multi component sorbents comprising of mixtures of metal oxides, clay, quartz and organic compounds are ubiquitous in soils and aquatic environments and have been shown to be significant in determining the environmental distribution of various contaminants and nutrients. Characterization studies of multi component sorbents indicated that the physicochemical properties of these solids differ significantly from those of their single component constituents. It is this difference in physico-chemical properties that are believed to be primary reason for differences in sorption behavior between multi-component and single component solids. For example, Xu and Axe, (2005) attributed increase Ni adsorption in a Fe-oxide/ silica multi-component system (compared to a silica only system) to increases in surface area, porosity and surface charge distribution. Potter and Yong, (1999) attributed differences in the retention of Cu and Pb in Fe/Al oxide systems to differences in specific area and surface charge.

Mixed Al-Fe hydro (oxide) is among the most significant multi-component sorbents. In addition to being ubiquitous in soil and aquatic environments, where they occur as coatings on other particles or as discrete solids, mixed Al-Fe hydro (oxides) have high specific surface areas and surface functional groups capable of interacting with both cationic and anionic species. Although sorption characteristics of single-component Al or Fe hydro (oxides) have been widely studied, limited work has been conducted on the sorption characteristics of mixed Al-Fe hydro (oxide). Many studies have shown that in both soils and aquatic environments Al and Fe-hydro (oxides) often control the biogeochemical cycling of nutrients, such as phosphate, via colloidal transport and/or adsorption/desorption mechanisms (Shwe *et al.*, 2012). Since, naturally occurring oxides are typically co-precipitated mixtures; it is reasonable to postulate that co-precipitated mixed metal Al-Fe hydroxides are likely to play a major role in the geochemical cycling of nutrients and contaminants (Shaheen and Hong, 2002). ZrO_2 is an amphoteric oxide which displays surface acid-base properties. The acid-base properties of ZrO_2 have been exploited to carry out many organic reactions on its surface including, dehydration, hydrogen transfer reaction and Friedel Craft alkylation reactions.

In addition to its application in industrial applications ZrO_2 has many technological applications as catalyst and promoter in environmental catalytic processes and energy devices. The properties that strengthen the general behavior of Nano composite towards their substantial improvement include: mechanical properties, dimensional stability, decreased permeability to gases, chemical resistance, surface appearance etc. Aluminum oxide (alumina, Al_2O_3) is one of the most useful oxide ceramics (Cava *et al.*, 2007). It has been used in many fields of engineering such as coatings, heat resistant materials and advanced ceramics. This is because alumina is hard, highly resistant towards bases and acids, allows very high temperature applications and has excellent wear resistance. Apart from this alumina is also used in heterogeneous catalysis because it is thermally stable and allows the dispersion of active phases due to its high specific surface area.

2.3. Synthesis Methods of Nanomaterials

The interest in the properties of solids and the development of new materials has given rise to the development of a huge variety of methods for preparing them. The method chosen for any solid will depend not only on the composition of the solid but also on the form it is required in for its proposed use. For example, silica glass for fiber optics needs to be much freer of impurities than silica glass used to make laboratory equipment. Some methods may be particularly useful for producing solids in forms that are not the stable form under normal conditions; for example, the synthesis of diamond employs high pressures. Other methods may be chosen because they favor the formation of unusual oxidation states, for example, the preparation of chromium dioxide by the hydrothermal method, or because they promote the production of fine powders or, by contrast, large single crystals. For industrial use, a method that does not employ high temperatures could be favored because of the ensuing energy savings. There are many methods of synthesizing metal oxide nanoparticles. Among them some methods; such as hydrothermal, microwave synthesis; sol-gel processing and coprecipitation methods are mostly used due to purity, homogeneity, easy preparation and ease of introducing dopants.

2.3.1. Hydrothermal Synthesis Method

Hydrothermal synthesis is typically carried out in a pressurized vessel called an autoclave with the reaction in aqueous solution. The temperature in the autoclave can be raised above the boiling point of water, reaching the pressure of vapor saturation. Hydrothermal synthesis is widely used for the preparation of metal oxide nanoparticles which can easily be obtained through hydrothermal treatment of peptized precipitates of a metal precursor with water (Chen and Mao 2007). Hydrothermal method can be useful to control grain size, particle morphology, crystalline phase and surface chemistry through regulation of the solution composition, reaction temperature, pressure, solvent properties, additives and aging time (Carp *et al.*, 2004).

2.3.2. Sol-Gel Method

Sol-gel processing is a common chemical approach to produce high purity materials shaped as powders, thin film coatings, fibers, monoliths and self-supported bulk structures (Kashmiri *et al.*, 2006). The sol-gel process involves hydrolysis and condensation of the metal alkoxide followed by heat treatment at elevated temperatures, which induce polymerization, producing a metal oxide network (Verma *et al.*, 2005). The sol-gel method has several advantages over other synthesis techniques such as purity, homogeneity, ease of preparation and ease of introducing dopants, composition, and the ability to produce thin film coatings or porous powders. There are two possible routes for carrying out solgel synthesis, the non-alkoxide route and the alkoxide route. The non-alkoxide route uses inorganic salts as the starting material. This requires the removal of the inorganic anion to produce the required oxide. However, halides often remain in the final oxide material and are difficult to remove. The alkoxide route involves hydrolysis of a metal alkoxide, followed by condensation. The hydrolysis/condensation reactions typically form a three dimensional polymeric structure, that, upon calcination will result in anatase or rutile metal oxide crystals depending on the calcination temperature (Carp *et al.*, 2004).

2.3.3. Co-Precipitation Method

The co-precipitation method involves the separation of solid containing target metal ions from a solution phase. In the process of co-precipitation, the metal components of the superconducting materials are first dissolved in solution. The solution combines with the precipitants in the supersaturated condition to form ion associates or clusters. A homogeneous co-precipitation process results in the formation of crystal line or amorphous solids which depends upon the condition under which the precipitate has been formed, the individual characteristics of the particular substance and its aging after precipitation. The most important advantage of this technique is its feasibility for large-scale production as well as its simplicity and low cost). Co precipitation method also offers some other advantages: Simple and rapid preparation, easy control of particle size, composition, various possibilities to modify the particle surface state and overall homogeneity in mixed precipitates High specific surface of the products (Yanjun *et al.*, 2008).

2.4. Dialysis Membrane Tube

The term dialysis was first routinely used for scientific or medical purposes in the late 1800s and early 1900s, pioneered by the work of Thomas Graham. The first mass-produced man-made membranes suitable for dialysis were not available until the 1930s based on materials used in the food packaging industry such as Cellophane. In the 1940s, Willem kolff constructed the first dialyzer (artificial kidney), and successfully treated patients with renal failure using dialysis across semi-permeable membranes. Dialysis occurs throughout nature and humans have exploited the principles of dialysis for thousands of years using natural animal or plant based membranes. Today, dialysis tubing for laboratory applications comes in a variety of dimensions and molecular-weight cutoffs (MWCO). In addition to tubing, dialysis membranes are also found in a wide range of different preformatted devices, significantly improving the performance and ease of use of dialysis. Different dialysis tubing or flat membranes are produced and characterized as differing molecular-weight cutoffs (MWCO) ranging from 1-1,000,000 kDa. The MWCO determination is the result of the number and average size of the pores created during the production of the dialysis membrane.

The MWCO typically refers to the smallest average molecular mass of a standard molecule that will not effectively diffuse across the membrane upon extended dialysis. Dialysis tubing for laboratory use is typically made of a film of regenerated cellulose or cellulose ester. However, dialysis membranes made of polyethersulfone (PES), etched polycarbonate, or collagen are also extensively used for specific medical, food, or environmental application such as water treatment. Dialysis tubing is a cellulose material used in the removal of salts and low molecular during the purification of biomolecules. It is a thin polymeric membrane exhibiting maximum wet strength, compatibility with a wide variety of solvents, minimal polarity, and uniform pore size. Researchers Freese *et al.* (1995); Abi Taddesse *et al.* (2008) have studied it also used for the identification of phosphorus-rich and phosphorus-leaky soils to estimate the risk of phosphorus (P) using HFO-DMT.

2.5. Phosphorus Desorption Kinetics

The kinetics of P desorption is a subject of importance in soil and environmental sciences primarily because P uptake by plants occurs over a period of time. Thus, kinetic information is required to properly characterize the P supplying capacity of soils, to design P-fertilizer management to optimize efficiency, to reduce environmental pollution, to develop guidelines for the disposal of P-rich wastes onto the land and for kinetic studies to obtain information on reaction mechanisms. In order to assess long-term P desorption kinetics, it is necessary to sufficiently suppress the backward resorption reaction. This can be done by introducing effective P sink into the system. Van der Zee *et al.* (1987) proposed the use of Fe oxide impregnated filter paper strips (Fe-oxide strips) as a promising method to study the P release kinetics of soils acting as a sink for P, the Fe-oxide strips have a sounder theoretical basis than the chemical extractants in estimating available soil P (Sharpley, 1996). However, this method was not found to be suitable for long-term desorption studies as it may lead to errors due to adhesion of fine P-rich particles to the paper strips and due to the mechanical instability of the paper when used for long desorption studies (Freese *et al.*, 1995). Recently, use of dialysis membrane tubes filled with hydrous ferric oxide (DMT-HFO) in place of resin/Fe-oxide paper strips for studying long-term P dynamics has been proposed (De Jager & Claassens, 2005; Ochwoh *et al.*, 2005).

Nonetheless, relatively little information is available in the literature in relation to the use of this method. Lookman *et al.* (1995) studied the kinetics of P desorption using this procedure. They concluded that P desorption could be well described by a two component first order model. They also reported that no desorption maximum was reached in the entire period of desorption (1600 h). Research was also done which linked short-term soil P tests to long term soil P kinetics (Koopmans *et al.*, 2001).

Desorption kinetics theory

Desorption kinetics of soil as determined by DMT-HFO can be schematically represented as



Where SP is the solid phase P, P_{sol} is P in solution, P_{HFO} is P adsorbed by HFO, k_T is the rate constant of P transport through the membrane ($0.09 \pm 0.01 \text{ h}^{-1}$, Freese *et al.*, 1995) and k_R is the rate constant of P release (De Jager & Claassens, 2005).

The presence of two pools is assumed: the pool with the fast release kinetics is pool A (SP_A) and the pool with the slow release kinetics is pool B (SP_B). With this assumption, the mass balance equation for the total exchangeable solid phase soil P (SP_{total}) at time $t = 0$ is:

$$SP_{total\ 0} = SP_{A0} + SP_{B0} \quad (2)$$

Where SP_{A0} is initial amount of P in pool A and SP_{B0} is initial amount of P in pool B. The mass balance equation at time t will therefore be:

$$SP_{total(t)} = SP_{A(t)} + SP_{B(t)} \quad (3)$$

Assuming the decrease in SP_A and SP_B follow first order kinetics, the integrated rate laws for the decrease of SP_A and SP_B will be:

$$SP_{A(t)} = SP_{A0} e^{-k_A t} \text{ and } SP_{B(t)} = SP_{B0} e^{-k_B t} \quad (4)$$

Where k_A and k_B are conditional first order rate constants (day^{-1}) for P desorption from pools A and B respectively

The total solid phase soil P ($SP_{total}(t)$) remaining at time t will be given by:

$$SP_{total}(t) = SP_{A0} e^{-k_A t} + SP_{B0} e^{-k_B t} \quad (5)$$

The total amount of P released at time t is expressed as:

$$\begin{aligned} P_R(t) &= SP_{A0} - SP_A(t) + SP_{B0} - SP_B(t) \\ &= SP_{A0} - SP_{A0} e^{-k_A t} + SP_{B0} - SP_{B0} e^{-k_B t} \\ &= SP_{A0} (1 - e^{-k_A t}) + SP_{B0} (1 - e^{-k_B t}) \end{aligned}$$

It was assumed that the rate constant of P release from the soil was equal to the rate constant of P adsorption (k_A) by the DMT-HFO. The rate constant of P adsorption (k_A) by the DMT-HFO was obtained from a plot of the natural logarithm (\ln) of the P adsorbed by the DMT-HFO against time with the slope as k_A . As Zhang *et al.* (2006) found that the phosphate-loaded Fe–Mn binary oxide was desorbed using NaOH solutions of different concentrations. It is clear that the amount of phosphate desorption increased with the increase of alkalinity. More than 93% of adsorbed phosphate was desorbed into the solution when the concentration of NaOH increased to 0.1 M. The further increase in NaOH concentration (up to 0.5 M) did not significantly enhanced desorption of phosphate. He concluded that the adsorption of phosphate on Fe–Mn binary oxide is relatively reversible, and the bonding between the active sites and the adsorbed phosphate is not so strong. These results suggest that the phosphate-loaded material can be easily desorbed using a 0.1 M NaOH solution and has the potential to be used as an adsorbent for phosphate removal.

2.6. P- Species in Soil

Dominant P species in soil solution that plants take up are $H_2PO_4^-$ or HPO_4^{2-} in the pH range of common soils. In acidic soils, $H_2PO_4^-$ ions dominate and in alkaline soils HPO_4^{2-} ions present. P cycle in modern eco-system absolute quantity of soluble P is governed by input from organic and inorganic sources as well as the solid phases through precipitation and dissolution processes. Yet, at any one time, absolute quantity of soluble P is low compared to the plant requirement and without addition through fertilizer, the actual soil P reserves are not enough to support intensive crop cultivation (Horta and Torrent, 2007).

For optimum crop production use of fertilizer P becomes essential to replenish soil soluble P continuously. Nevertheless, fertilization use efficiency of the plant is depending on soil type and management due to different soil type affect the availability of P (Kolahchi and Jalali, 2012). The pH value can affect the phosphate species and the performance of precipitation or adsorption significantly. The distribution of major phosphate species in solution versus pH could be calculated by using the phosphate dissociation constants ($pK_{a1} = 2.13$, $pK_{a2} = 7.21$, $pK_{a3} = 11.66$), which is illustrated in speciation distribution diagram in Figure 1 (Karageorgiou *et al.*, 2007). It is clear from the Figure that $H_2PO_4^-$ and HPO_4^{2-} species are present in the pH region between 3 and 11. The concentration of $H_2PO_4^-$ species is high between 3 and 6 while HPO_4^{2-} species prevail at pH between 8 and 11, which means the $H_2PO_4^-$ ions are predominating at pH 3-6 and in the high pH range, the HPO_4^{2-} ions are dominating. Around pH 4 to 5, the highest fraction of $H_2PO_4^-$ exists (Karageorgiou *et al.*, 2007).

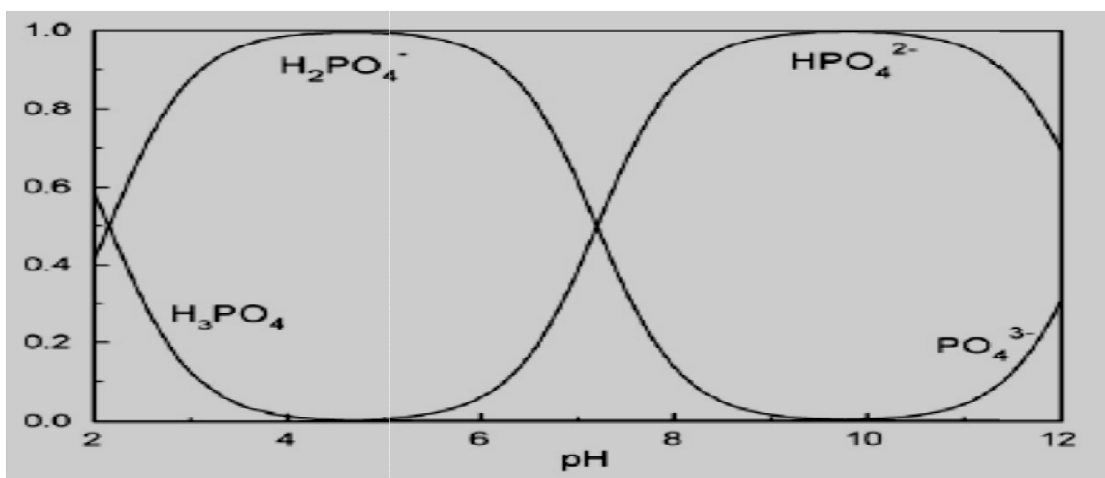
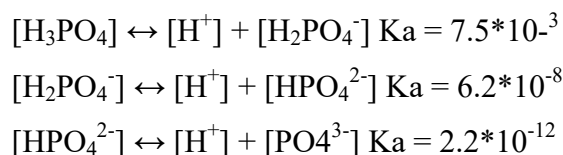


Figure 1. Speciation distribution of phosphates

The $H_2PO_4^-$ species are more easily adsorbed on metal hydroxide surfaces than HPO_4^{2-} species when pH is below 6, but HPO_4^{2-} species are more likely precipitated with Mg or Ca in the alkaline solution than $H_2PO_4^-$ species (Xiaofang *et al.*, 2007).

The acid-dissociation constants for phosphate are listed below (Stumm and Morgan, 1981).



2.7. Process of P Transformation in Soil

Soil transformations of P are complex and often ambiguous. Phosphorus availability has often been characterized in general terms: as solution, readily available/labile and non-labile P. The labile fraction might include easily mineralizable organic P, low energy sorbed P, and soluble mineral P. The non-labile fraction might include resistant organic P, high energy sorbed P and relatively insoluble phosphate minerals. As plants take up P from the solution, it is replenished from the labile fraction, which in turn is more slowly replenished by the non-labile fraction. Phosphorus is utilized in the fully oxidized and hydrated form as orthophosphate. Plants typically absorb either H_2PO_4^- or HPO_4^{2-} depending on the pH of the growing medium. However, under certain conditions plants might absorb soluble organic phosphates, including nucleic acids. A portion of absorbed inorganic P is quickly combined into organic molecules upon entry into the roots.

Phosphorus is important in energy storage and transfer in plant biochemical processes where the most notable are adenosine di phosphate and tri phosphate (ADP and ATP). Energy is released when a terminal phosphate is split from ADP or ATP for photosynthesis activity.

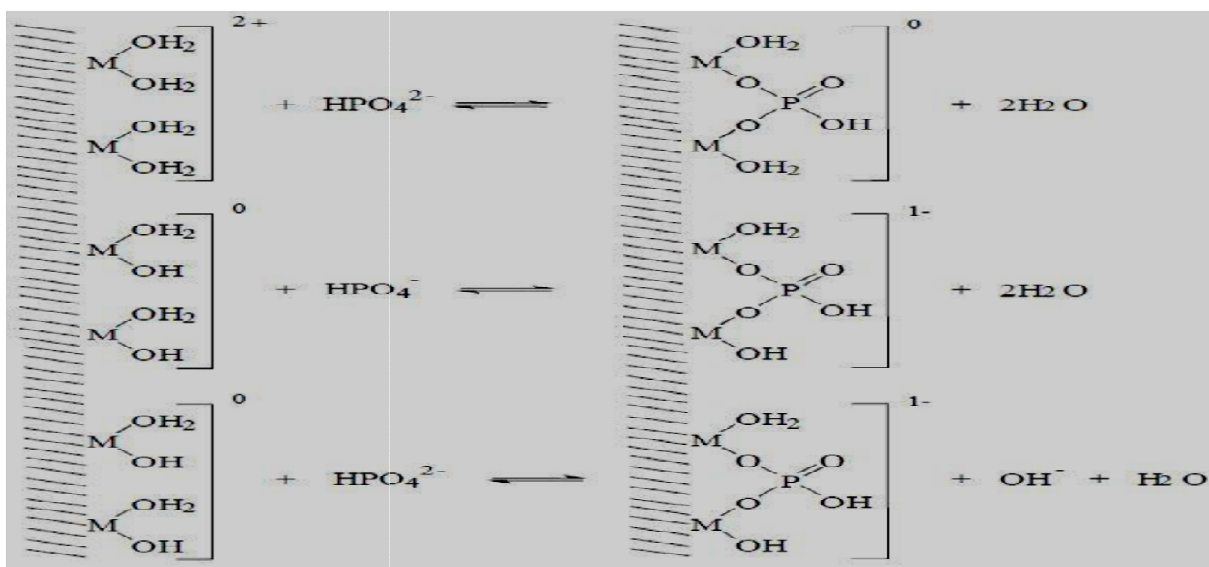
At the soil pH below 5.5, both Fe^{3+} and Al^{3+} ions precipitate P while at pH above 7.0, Ca^{2+} precipitate P. Maximum P availability is at a pH of 6.5 for mineral soils and about 5.5 for organic soils. Phosphate fixation and unavailability is a major fertility constraint in acid soils containing large amounts of free Fe and Al oxides of Oxisols and Ultisols soils (FAO, 2005). Phosphorus deficiency occurs in many soils of east Africa including Ethiopia due not only to P depletion through crop harvest and erosion but mainly to the prevalence of high P fixing soils in the region (Asmare, 2014).

2.7.1. Sorption Process

Sorption describes two processes (Haygarth and Sharpley, 2000): (a) adsorption, which occur when phosphate ions are adsorbed to the surface of particles and (b) absorption when adsorbed ions diffuse into the solid; and “sorption” is the general term used for these processes. Phosphate may become trapped on the surface of soil minerals under coating of iron oxide precipitates (Moazed *et al.*, 2012). The trapped phosphate is termed as occluded. Phosphate ions are more strongly sorbed by iron oxide surfaces due to their large surface area. Soluble P added to soil, initially undergoes a very rapid exothermic reaction (adsorption) followed by a slow reaction (absorption) resulting in occluded P. Occlusion takes place in then iron oxide structures. Phosphate sorption capacity increases with clay content, because clay particles have a large surface area on which phosphate can be sorbed (phosphate is an anion, therefore soil particles that have an anion exchange capacity will form strong bonds with phosphate). Clayey materials with more than 20% iron or aluminum oxides in their clay-size particles sorb large quantities of added phosphorus, transforming them into slowly soluble iron and aluminum phosphates that are not immediately available to plants.

High P retaining soils are often clayey with red or yellowish colors indicative of high contents of iron and aluminum oxides; usually, such soils have a strong granular structure (e.g., Ferralsols). High phosphorus retention is related to high clay content, therefore, most sandy red soils do not fall in this category (Sanchez *et al.*, 2003). Phosphate is chemisorbed on the reactive iron oxide surface groups through a binuclear bridging mechanism. An OH^- or H_2O molecule is released from the surface and phosphate bridging complexes are formed between HPO_4^{2-} ions and iron oxide surface. This sorption reaction is strongly non-reversible and the sorbed P is mostly unavailable for plant uptake (Gichangi *et al.*, 2008). At hydroxylated surfaces, a positive or negative charge is created by the adsorption or desorption of H^+ or OH^- ions, which is balanced by an equivalent amount of anion through specific adsorption. Sorption of P is occurs through ligand exchange on variable charge surfaces by the exchange of OH^- on the surface for phosphate ion. There is covalent bond between the metal ion and the phosphate ion.

Phosphate is considered to sorb mainly as an inner-sphere complex, which means that the sorption takes place at specific coordination sites on the oxides or hydroxides (Figure 2). These reactions are termed as “ligand exchange reactions” because the anion displaces OH^- or H_2O from coordination positions of iron or aluminum ion at the surface that are the sites of chemisorptions. The sorption reaction is strongly non-reversible and the sorbed phosphate is mostly unavailable for plant uptake (Gichangi *et al.*, 2008). The precise nature of these reactions depends on pH, which influences the proportions of H_2O and OH^- groups on the solid surface, and hence its surface charge. Unlike metal cations, sorption of oxyanions decreases with increasing pH. Phosphorus is more strongly surface-associated through covalent bonds formed by ligand exchange with oxide surfaces' OH^- groups compared to SO_4^{2-} which is a non-specifically bound oxy-anion and is weakly surface-associated due to electrostatic interaction. Phosphate adsorption continually decreased with increasing pH. Phosphorus interacts more strongly with goethite, probably following an adsorption process and was observed more evenly distributed at its surface (Ahmed *et al.*, 2008).



M = Al or Fe

Figure 2. Bi-dentate arrangement

As studied by Gichangi *et al.*(2008) on seven different soils sample in their capacities to sorb P with four of the soils classified as low P fixing and the remaining three (43%) as moderate P fixers and concluded that latter category may need management interventions to ensure that P availability to crops is not compromised. The contrasting differences in the P fixing capacities of the soils suggested that the use of blanket phosphate fertilizer recommendations may not be a good strategy for the region as it may lead to under application or over-application of P in some areas with the attendant consequences of compromised crop yields or freshwater quality. Paini *et al.* (1999) stated that soils differed markedly in their ability to hold P, though P adsorption was high in all observed soil when Fe oxides and Al oxides contents dissolved, reactive P could be found in percolating water in consequence of Fe solubility enhanced by reducing condition held P. A relationship between the iron content in high reactivity form and the adsorption of P resulting from a decreased P in solution was found. Therefore, after flooding- drained condition, P availability to plants decreased due to adsorption of P with recently precipitated high reactivity forms of irons oxides (Hernandez and Meurer, 2000).

2.7.2. Precipitation

Sorption of phosphate is commonly measured by the decrease in the amount of phosphate in solution phase after a period of time the solution was in contact with the solid phase. The decrease in phosphate content, results not only from sorption but also from precipitation of phosphate in solution phase if the product of the solution concentrations of the constituents of the precipitate exceeds the solubility product of the precipitate.

Surface precipitation of metal phosphates can occur even at solution concentrations of phosphate and metals lower than those expected to form metal precipitates in solution phase according to the thermodynamic solubility product principle (Sparks, 2001). In such cases, a finite volume adjacent to the mineral surface exists that is oversaturated with respect to precipitate formation. X-ray diffraction and scanning electron microscopic data provided evidence for the formation of surface precipitates of phosphate compounds of Ca, Fe, Al, and Zn on sorbents containing components of these metals (Bowden *et al.*, 2009; Koilraj and Kannan, 2010).

Precipitation of P as di-calcium phosphate and surface precipitation on solid CaCO_3 are the main processes in calcareous soils. High activity of calcium ions and high pH values favor the precipitation as relatively insoluble di-calcium phosphate di-hydrate $[\text{Ca}_{10}(\text{PO}_4)_6(\text{OH})_2]$ and other calcium phosphates such as hydroxy-apatite and carbonateo apatite. Calcium phosphate initially formed as mono-calcium phosphate precipitate, later transformed to dicalcium phosphate to octa-calcium phosphate and finally to hydroxyl-apatite or carbonateo-apatite, which has the least solubility. While the intermediate precipitates are unlikely to persist in soils. The amount, nature, and reactivity of carbonate minerals affect phosphate reactions only to limited extent (Zhang *et al.*, 2004).

2.8. Sorption Mechanisms of Phosphate to Metal Oxides

A mechanistic study of phosphate adsorption is of paramount importance for the understanding the adsorbate–sorbent interaction; it can lead to optimization of the adsorption process and the subsequent desorption and regeneration process. Mechanistic studies of phosphate adsorption by metal oxides have been carried out with either the assistance of analytical equipment or the postulation from comprehensive experimental observations on adsorption characteristics. Recently, it has been now recognized that chemisorption (ion-exchange and electrostatic attraction) is the most prevalent mechanism and that the pH is a main factor affecting adsorption. Surface precipitation and Lewis acid–base interactions are also proposed by a few recent studies.

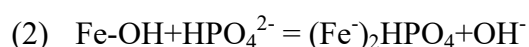
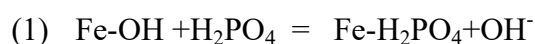
2.8.1 Electrostatic Force

The electrostatic forces between metal oxide sorbents and phosphate ions are dependent on the pH. The pH-dependent adsorption indicates that the adsorption is dominated by surface complexation (outer sphere complex) (Yu *et al.*, 2015). The electrostatic processes are illustrated in (Figure 3). At pH 2–12 When $\text{pH} < \text{pH}_{\text{pzc}}$, the increased H^+ in solution will react with the surface hydroxyl groups to form some protonated hydroxyl groups. The electrostatic attraction between a protonated hydroxyl group and phosphate will be favorable for adsorption (Su *et al.*, 2015). At the same time, electrostatic attraction can readily occur in conjunction with a specific chemical adsorption due to an exchange reaction occurring at a lower pH range.

When $\text{pH} > \text{pH}_{\text{pzc}}$, the surface of the sorbents is enriched with increasingly negative charges, which leads to the formation of de-protonated hydroxyl groups. As a result, the electrostatic repulsion between them and the phosphate increases with increasing pH (Lalley *et al.*, 2016). Moreover, competition between hydroxide ions and phosphate ions for the adsorption sites also occurs, which is not beneficial for the subsequent ion-exchange processes.

2.8.2. Ion Exchange

The presence of OH^- groups in metal oxides creates the possibility of phosphate–OH ion exchange, indicating a ligand exchange reaction. This may occur through inner sphere complexation, where when PO_4^{3-} anions create covalent chemical bonds with metallic cations on the surface of the metal oxides leading to the liberation of other anions that were formerly attached to the metallic ions. Based on the effect of pH and desorption results, ion exchange mechanism could be an important pathway for the removal of phosphorus. It is promising for P recovery as it is generally a reversible process and has high efficiency with high selectivity for the anions (Kuzawa *et al.*, 2006). The phosphate adsorption process which coincides strongly with the ion exchange mechanism, is presented in Figure (3) at $\text{pH} \leq \text{pH}_{\text{Pzc}}$. Zhou *et al.* (2012) reported, this mechanism for removing phosphorus using a hydrated ferric oxide-doped activated carbon fiber. At pH values greater than 2 the ion exchange took place between H_2PO_4^- , HPO_4^{2-} ions and the surface OH^- groups to form complexation as follows:



At $\text{pH} \leq \text{pH}_{\text{pzc}}$ or initial adsorption range (H_2PO_4 or HPO_4 solution), phosphate sorption onto sorbents is primarily the result of an ion exchange between phosphate and hydroxide groups on the surface of the sorbent (Liu *et al.*, 2011). But ion exchange increased solution pH because of the exchanged hydroxide groups. Thus it will be better to adjust solution pH to the initial range.

2.8.3. Lewis Acid–Base Interaction

At lower pH values, because of the presence of excess hydrogen ions in solution, metal active sites are protonated and become a weak acid (Lewis acid), acting as electron acceptors. Phosphate anions become a weak base (Lewis base), acting as electron donors.

At alkaline pH, the metal active sites are deprotonated and negatively charged along with phosphate species. Therefore, the metal active sites become a weak base (Lewis base), and phosphate anions become a weak acid (Lewis acid). This implies electron donor–acceptor and Lewis acid–base interactions exist between the metal active sites and phosphate anions (Figure 3). Moreover, in the Lewis acid–base interaction mechanism, it is likely that the metal active site reacts with oxygen anions in the phosphate to form M–O coordination bonds (Acelas *et al.*, 2015).

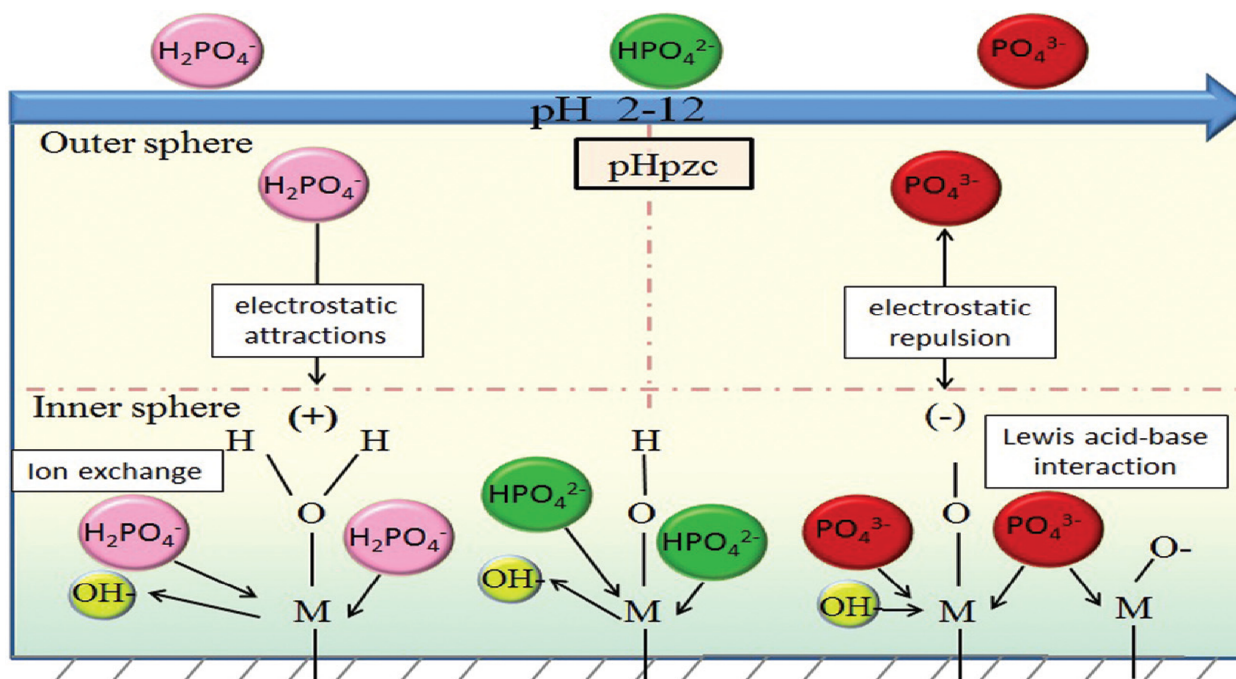


Figure 3. Phosphate sorption mechanisms of metal oxides

2.9. Sorption and Desorption of Phosphorus

Phosphorus sorption is the removal of labile P from the soil solution, due to the adsorption on, and absorption into the solid phases of the soil, mainly on to surfaces of more crystalline clay compounds, oxihydroxides, or carbonates (Hollford and Mattingly, 1975). While phosphorus desorption is a key process affecting inorganic P bioavailability; and desorption can also identify specific pools of bio-available P.

Extraction methods used in soil P characterization are based on 1) desorbing soil P from the sorption sites by creating circumstances where desorption is enhanced, 2) replacement of soil P with a compound having a stronger sorption affinity or 3) solubilisation of sorption components (Soinne, 2009).

The fundamental goal of soil P testing has always been to identify the “optimum” soil P concentration required for plant growth. The need for additional fertilization and the economic return on an investment in fertilizer P, could then be predicted. Adsorbed or precipitated inorganic P undergoes desorption or dissolution reactions when moving from the solid to the solution phase. Desorption is of particular importance in bioavailability evaluations, because this process controls what the plant can eventually access. Desorption is used to denote either the precise opposite of adsorption or the counterpart to sorption, which would include a combination of desorption and dissolution. Both soil and plant characteristics affect the extent and rate of desorption and dissolution for inorganic soil P. It is necessary, therefore, to understand these relationships in order to evaluate and predict P bioavailability and the fate of inorganic P.

According to Sato, (2003); Gemechu *et al.* (2015), phosphorus desorption can define P bioavailability. Prior studies on P sorption have outlined trends and provided a foundation for understanding sorption. However, bioavailability of P is a function of P desorption; not P sorption. Sorption and desorption reactions in the soil equilibrate P in solids with P in the soil solution. P can adsorb to the surfaces and edges of hydrous oxides, clay minerals and carbonates by replacing OH^- (De bolle, 2013). Adsorption of P in the soil is usually enhanced by presence of metal oxides of Fe or Al, collectively named sesquioxides, organic complexes of Al and Fe, edges of silicate clays and calcite (De bolle, 2013). Added inorganic P can be adsorbed weakly (electrostatically) or strongly (covalent bond) onto these variable charged surfaces. As mostly P species in soil solution are negatively charged, P will be sorbed to soil constituents that bear positive charges such as hydroxyl, carboxyl clays groups. Metal hydroxides have a variable charge, and their capacity to adsorb anions such as P ions will increase with decreasing pH, due to higher protonation at low pH (Barrow, 2016).

2.10. Factors that affect P-sorption

Organic matter: The application of OM can increase soil phosphorus (P) availability through decomposition and mineralization of included organic-P, or by abiotic processes such as ligand-exchange. However, presence of mineral-bound OM may also reduce phosphate adsorption capacity, favoring release of P in soil solution (Yusran, 2010). Three abiotic mechanisms are proposed to explain how addition of OM can reduce P sorption in soils. Firstly, soluble organic molecules may specifically adsorb to soil minerals by ligand exchange in competition with P (Fink *et al.*, 2016). Secondly, the soluble OM may react with bound Al^{3+} or Fe^{3+} at the surface of the soil mineral phase to form soluble complexes and release P which was previously sorbed or which was present as insoluble Al and Fe-phosphate (Yusran, 2010). Third, OM can be sorbed to soil particles, resulting in higher negative charge of the particles, and hence increased repulsion force for P anion

Mineralogy of the soil: has a great effect on P-sorption. Volcanic soils tend to have the greatest P-sorption of all soils since volcanic soils contain large amounts of amorphous minerals like Allophane with high content of Al^{3+} , Ca^{2+} , Fe^{3+} . These minerals also have a large surface area for P sorption.

Amount of clay: As the amount of clay increases in the soil, the P-sorption capacity increases as well since clay particles have a tremendous large surface area onto which phosphate sorption can take place. At smaller clay contents, the role of pedogenic Fe and Al becomes more important (Chintala *et al.*, 2014). That's why sandy soils are expected to have less P sorption capacity and the pedogenic Fe and Al then should be the primary binding sites for P.

Soil pH: There is a general relationship between soil pH and phosphorus availability, which is based on the kinds of o-P compounds associated with the various pHs. Reactions that reduce P availability occur in all ranges of soil pH but can be very pronounced in alkaline soils ($\text{pH} > 7.3$) and in acidic soils ($\text{pH} < 5.5$). At low pH, soils have greater amounts of Al and Fe in the soil solution, which form very strong bonds with P. In contrast, at high pH, P precipitates with calcium as Ca-P (Oelkers *et al.*, 2008).

Maintaining soil pH between 6 and 7 will generally result in the most efficient use of phosphate with maximum P availability (Busman *et al.*, 2009).

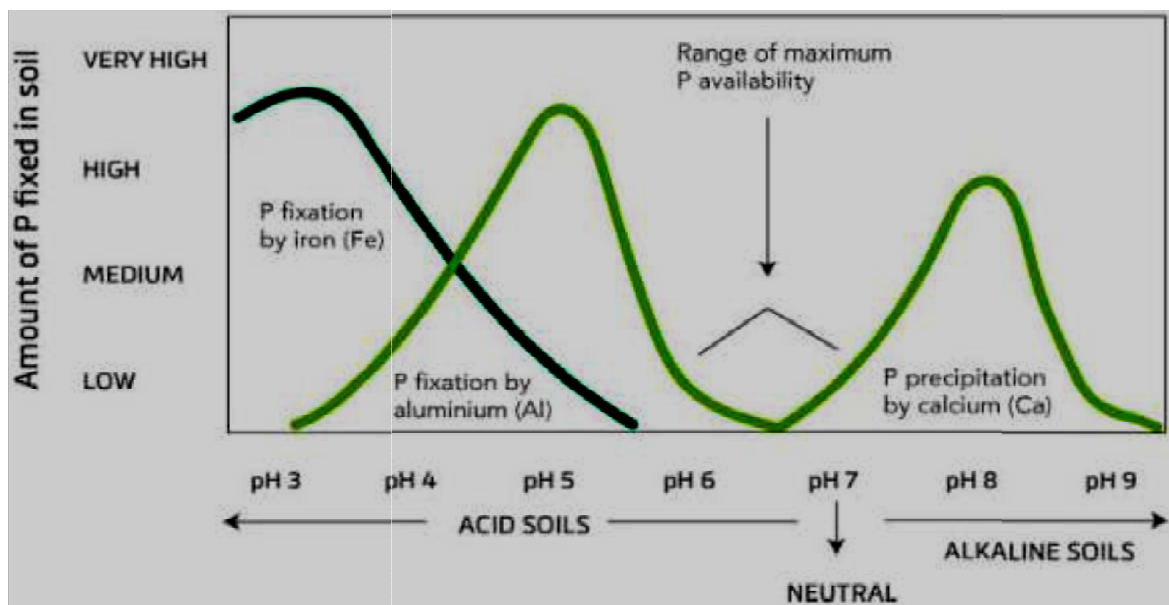


Figure 4. The availability of phosphorus as affected by soil pH

Presence of competing anions in soil solution. Ligands with higher affinity for the soil surface than phosphate will destabilize P minerals (Sato, 2003) and resulting desorption of P mostly occurs through ligand exchange reactions. An increase in the concentration of competing anions will shift the adsorption–desorption equilibrium towards enhanced desorption (Hinsinger, 2011). Anions such as silicates, carbonates, sulfates molybdate, and carboxyl-containing OM constituents compete with P for a position on the anion exchange site. Higher concentrations of competing ligands such as sulphate are however, needed for effective ligand exchange as P ions have a strong affinity to be adsorbed on the surface of positively charged minerals.

3. MATERIALS AND METHODS

3.1. Description of Study Area and Experimental Site

3.1.1. Description of Soil Sampling Areas

Soil samples were collected from four districts found in West Wollega Zone, Oromia region of Ethiopia located at about 477-575 Km west of Addis Ababa. The districts selected for sample collection were Mana Sibbu, Kiltu Kara, Nedjo and Boji Dirmeji. The altitudes, the mean annual rainfalls and the minimum and maximum temperature of these areas range from 1300 - 1800 masl, 1000 -2400 mm^{yr}⁻¹ and 12.5 - 29 °C respectively (MoA, 2010). The major soil type of western and south western Oromia is Oxisols. The major crops grown in the zone include cereals (Maize, Teff, Millet, Sorghum, and Barley), pulses (Faba bean and Field peas) and oil crops (Niger seed, Rapeseed and Sesame).

3.1.2. Experimental Site

Synthesis of Fe-Al-Zr mixed oxides Nanocomposite and the desorption experiments using the as-synthesized material were carried out at Haramaya University, Chemistry Department Research Laboratory. XRD and FTIR studies were conducted at the Addis Ababa University. SEM-EDX analysis of the as-synthesized Nanocomposite was conducted at the Instituto de Catálisis Y. Petroleoquímica, CSIC, C/Marie Curie 2, Madrid, Spain and UV-Vis spectroscopic technique was used for the determination of desorbed phosphorus at the Chemistry Department Research Laboratory, while analysis of soil samples was conducted at Haramaya University, Soil Science Laboratory.

3.2. Instruments and Apparatus

X-ray diffractometer (XRD, D8-Advanced, Germany, power 40 kW with 35 mA at 25°C) was used to determine the X-ray diffraction (XRD) pattern of the adsorbent from which to determine the phase composition and estimate the crystallite size of the powders. Fourier transform infrared spectrophotometer (FT-IR, Bruker Optics EQUINOX 55, at 25°C) was used for functional identification of the as-synthesized adsorbent and Flame atomic absorption spectroscopy (FAAS) was used for elemental determination of as-synthesized adsorbent.

UV-Vis spectrophotometer was used to determine the concentrations of phosphate. The morphology and particle size distribution of the solids were determined by scanning electron microscopy (SEM) using a Hitachi TM1000 with EDX detector Deionizer (B114), Dry oven (Gallenkamp made in UK), pH-meter (model 3310 JENWAY, Japan), Furnace (BIBBY Stuart, UK), DMT, hydrometer, conductivity meter and Orbital shaker S01 (Stuart, UK) were also used in this study. The common laboratory glassware which were used during the study include various sizes of beakers, Erlenmeyer flasks, burettes, funnels, graduated cylinders, volumetric flasks, test tubes, droppers, glass pipettes, measuring cylinders, spatula, magnetic stirrer, analytical balance, cotton wool, crucible dish, desecrator, mortar pestle and sieve were also used during laboratory work.

3.3. Chemicals and Reagents

The chemicals and reagents required for this study include Aluminum nitrate nanohydrate ($\text{Al}(\text{NO}_3)_3 \cdot 9\text{H}_2\text{O}$, Blulux LR), ferrous chloride tetra hydrate ($\text{FeCl}_2 \cdot 4\text{H}_2\text{O}$, Uni-chem chemical reagents), Ferric chloride hexahydrate ($\text{FeCl}_3 \cdot 6\text{H}_2\text{O}$, Blulux LR), zirconial chloride octahydrate ($\text{ZrOCl}_2 \cdot 8\text{H}_2\text{O}$, BDH chemicals Ltd, England), Potassium dihydrogen phosphate (KH_2PO_4 , 99 % CDH Laboratory reagents), Ammonium molybdate tetra hydrate ($(\text{NH}_4)_6\text{Mo}_7\text{O}_{24} \cdot 4\text{H}_2\text{O}$, 81-83 % Riedel-DeHaen AG), Potassium antimony tartarate ($\text{KSb} \cdot \text{C}_4\text{H}_4\text{O}_6$, 98.5 % BDH chemicals Ltd, England), ascorbic acid ($\text{C}_6\text{H}_8\text{O}_6$ 99 % Blulux laboratory reagents), Sodium sulphate (Na_2SO_4 , 99 %, Merck), sulfuric acid (H_2SO_4 , 98%, laboratory reagent, LOBA, India). Hydrochloric acid (HCl , 36-37%, BDH chemicals Ltd, England), Sodium hydroxide (NaOH , 97.5% BDH chemicals Ltd, England), Potassium dichromate ($\text{K}_2\text{Cr}_2\text{O}_7$, 99% BDH chemicals Ltd, England), KCl , CaCl_2 , Ferrous ammonium sulfate ($\text{Fe}(\text{NH}_4)_2(\text{SO}_4)_2 \cdot 6\text{H}_2\text{O}$ 97% BDH chemicals Ltd, England), Sodium sulfate (Na_2SO_4 , 99.5-100.5% BDH chemicals Ltd, England), copper sulfate ($\text{CuSO}_4 \cdot 5\text{H}_2\text{O}$, 98.5% BDH chemicals Ltd, England), selenium powder (Se, 99.7%, Germany), Boric acid (H_3BO_3 , 99.8% BDH chemicals Ltd, England). Dispersing agent (sodium hexa meta phosphate ($(\text{NaPO}_3)_6$, 97.5%, Germany), Sodium hydrosulfite (dithionite) ($\text{Na}_2\text{S}_2\text{O}_4$, 99.5% BDH chemicals Ltd Poole, England), Sodium citrate ($\text{Na}_3\text{C}_6\text{H}_5\text{O}_7 \cdot 2\text{H}_2\text{O}$, 99.6% BDH chemicals Ltd, England), Ammonium oxalate solution ($(\text{NH}_4)_2\text{C}_2\text{O}_4 \cdot \text{H}_2\text{O}$, 98% BDH chemicals Ltd Poole, England) Oxalic acid solution ($\text{H}_2\text{C}_2\text{O}_4 \cdot 2\text{H}_2\text{O}$, 99%, Switzerland). Ammonium fluoride (NH_4F)

3.4. Experimental Procedures

3.4.1 Soil Sample Collection and Sample Preparation

Surface soil samples (0-20 cm) were randomly collected from each of the sampling sites in each district. The randomly collected soil samples were thoroughly mixed to form one composite sample for each site and a total of four composite soil samples were collected and packed in plastic bags. After bringing to HU soil laboratory, the collected samples were air-dried and grinded to pass through a 2 mm sieve to be used for testing for the selected soil physico-chemical parameters which include; pH in (H₂O and KCl), organic carbon (organic matter) content, exchangeable acidity, exchangeable Al, exchangeable hydrogen, available phosphorus CEC, EC, total phosphorus, extractable nutrients (Fe_D, Mn_D, Fe_{Ox}, and Mn_{Ox}), and total nitrogen following standard laboratory procedures as described in section 3.4.2

Four soil samples were incubated with known amount of P since the total phosphorus in the soil is <20 ppm. The collected soil samples were incubated with known concentration of P in the form of KH₂PO₄. Four rates of P which has (0, 50, 100 and 150 mg kg⁻¹) amount of KH₂PO₄ were applied to soil and incubated for 112 days at 25 °C. At the end of the incubation period, soils were air dried again and extraction process of soil P using DMT-Fe-Al-Zr was conducted.

Experimental design

4 samples, 4 P rates and 3 replicates (**4x4x3 = 48**)

Code	Name	Description
B	Sample 1	Sample collected from Boji Dirmeji district
M	Sample 2	Sample collected from Mana Sibiu district
K	Sample 3	Sample collected from Kiltu Kara district
N	Sample 4	Sample collected from Nedjo district
P0	P -rate 0	0.00 mg P kg ⁻¹ (control)
P1	P-rate 1	50 mg P kg ⁻¹
P2	p-rate 2	100 mg P kg ⁻¹
P3	p-rate 3	150 mg P kg ⁻¹

3.4.2. Physicochemical Properties

Topsoil samples (0-20 cm) were collected from four different districts whose phosphorous added rate also differs. The collected samples were air-dried and ground to pass through a 2 mm sieve. Selected soil chemical parameters such as pH, organic carbon, total nitrogen, and available P and soil physical parameters such as texture and bulk density were determined by following the standard laboratory procedures.

Soil pH in water and potassium chloride (1 M KCl) was measured Potentiometrically using a pH meter with combined-glass electrode in a 1:2.5 soil to solution supernatant suspension (Peech, 1965).

Determination of soil organic matter was carried out by oxidizing the soil organic carbon under standard condition with potassium dichromate in Sulphuric acid solution as described by Walkely and Black, (1934) and it was obtained by multiplying percent soil OC by a factor of 1.724 following the assumptions that OM is composed of 58% carbon.

The EC of soil samples was determined electrometrically (soil water ratio being 1:5) by a conductivity meter. A 10 g of air dried soil was taken in a plastic container and 50 mL of distilled water was added to it. The suspension was stirred for 30 min intermittently and then allowed to stand for 30 min. Then the electrical conductivity was determined by an electrical conductivity meter (Calibrated with 0.01 N KCl solutions) (Anderson and Ingram, 1996).

Cation exchange capacity (CEC) is a measure of the quantity of readily exchangeable cations neutralizing negative charge in the soil. The cation exchange capacity (CEC) of the soil was determined using the ammonium acetate method (Rhoades, 1982).

Exchangeable acidity was determined by saturating the soil sample with potassium chloride (1 M KCl) solution and titrated with hydrochloric acid (0.02 M HCl). From the same extract, exchangeable Al in the soil samples was titrated with a standard solution of hydrochloric acid (0.02 M HCl). Finally, exchangeable H^+ was obtained by subtracting exchangeable Al from exchangeable acidity (Rowell, 1994).

Soil total nitrogen content was determined by the Kjeldahl method using micro-Kjeldahl distillation unit and Kjaldahl digestion stand (Jackson, 1958).

Available soil phosphorus was extracted by the Bray II procedure (Bray and Kurtz, 1945). Total soil P was determined on sub-samples of 0.5 g soil with the addition of 5 mL concentrated sulfuric acid (H_2SO_4) and heated to 360 °C on a digestion block with subsequent stepwise additions of 0.5 mL hydrogen peroxide (H_2O_2) until the solution became clear (Taddesse *et al.*, 2008a). Finally, the absorbance was measured by Spectrophotometry at wave length of 882 nm by preparing standard solution from KH_2PO_4 for calibration to determine P in soil.

The bounded Al and Fe to phosphorus in soil were determined by the dithionite–citrate and the acid ammonium oxalate methods (Mehra and Jackson, 1960). Such that dithionite–citrate removes organically complexed Al and Fe, amorphous inorganic Al and Fe, compounds and non-crystalline aluminosilicates (Guest *et al.*, 2002) while acid ammonium oxalate removes organically complexed and amorphous inorganic forms of Al and Fe (McKeague, 1967).

The soil texture was determined by hydrometer method after destroying organic matter and dispersing the soil (Bouyoucos, 1962) and bulk density was determined gravimetrically after oven drying for 24 h at 105°C (Day, 1965).

3.4.3. Synthesis of Fe-Al-Zr Mixed Oxide Nanocomposite

The adsorbent, ternary oxide nanocomposite was prepared by chemical co-precipitation method as reported by Liyuan *et al.*, (2013). Stoichiometric factors of Fe^{2+} and Fe^{3+} are very important for magnetic property of the composite products. For 0.5 $\text{Fe}^{2+} / \text{Fe}^{3+}$ mole ratio the product obtained was homogeneous magnetic particle with uniform size and composition. So, in all samples the mole ratio of $\text{Fe}^{2+} / \text{Fe}^{3+}$ was selected to be 0.5 (Anamaria *et al.*, 2012). $\text{Fe}_3\text{O}_4/\text{Al}_2\text{O}_3/\text{ZrO}_2$ with Fe:Al:Zr mole ratio of 70:25:5 which is the best adsorbent proportion was selected for synthesizing the nanocomposite. In the first step, Stoichiometrically calculated $\text{FeCl}_2 \cdot 4\text{H}_2\text{O}$ and $\text{FeCl}_3 \cdot 6\text{H}_2\text{O}$ were accurately weighed and the calculated amounts were dissolved in 100 mL of 0.3 M HCl solution. Then, the solution was added drop wise from Separatory funnel into the solution of 120 mL of 3 M NaOH (pH 11) over period of 2 h, under vigorous stirring at 80°C in N_2 atmosphere.

During this process, the pH of mixture kept at 11.0 using 0.1 M, 0.01 M and 0.001 M NaOH or HNO₃ solutions. The suspension was allowed to settle undisturbed for 4 h and then washed with deionized water for several times to obtain a suspension of Fe₃O₄ ferro-fluid. The magnetite –alumina – zirconia oxide nano composite of each sample was prepared by adding 100 mL of Al(NO₃)₃.9H₂O and ZrOCl₂.8H₂O (obtained by dissolving stoichiometric amounts of both salt in 100 mL of DI- water) into the prepared Fe₃O₄ suspension and ultrasonicated for 10min prior to use. The pH of the mixtures was adjusted to 8.0 using 0.1 M, 0.01 M and 0.001 M NaOH. Then the mixture was magnetically stirred under N₂ atmosphere for 1.5 h at 70°C. Finally each resulting magnetic compound was separated by permanent magnet, washed with deionized water for several times to remove impurities such as Cl⁻, NO₃⁻ and excess OH⁻ ions and then dried at 60°C for 24 h to obtain each of the desired products (Fekadu, 2015).

3.4.4. Characterization of the As-synthesized Adsorbent

3.4.4.1. X-ray powder Diffraction

The size of the primary crystallite (D_s) of the solid-phase (Fe₃O₄-Al₂O₃-ZrO₂) was calculated based on the XRD diffractometry results according to the Dubye Scherrer equation (Laurent *et al.*, 2008):

$$D_s = 0.9\lambda/\beta \cos\theta \quad 6$$

Where, D_s is mean crystallite size (nm), λ wavelength of the incident radiation ($\lambda = 0.15405\text{nm}$), β pure diffraction broadening (radians) and θ the Bragg angle (degrees, half-scattering angle). Usually, β is taken as the full width at half maximum of the major diffraction band (FWHM).

3.4.4.2. Elemental Analysis

The percentages of iron as iron oxide and zirconium as zirconium oxide in the selected as-synthesized powders were determined by flame atomic absorption spectrophotometer. For this purpose, 0.5 g of the as-synthesized powder in three replication were digested with a mixture of concentrated nitric acid (7 mL), concentrated hydrochloric acid (4 mL) and hydrogen peroxide (2 mL) using acid digestion tube till clear solution appeared.

The samples were transferred to 100 ml volumetric flasks and brought to volume using deionized water. 1 mL of this solution was diluted further to 50 mL and the concentration of iron and zirconium were read from the solution in 50 mL volumetric flasks by using FAAS. Similarly, the standard solutions were prepared from the precursors ($\text{Fe}(\text{NO}_3)_3 \cdot 9\text{H}_2\text{O}$ and $\text{ZrOCl}_2 \cdot 8\text{H}_2\text{O}$) from which the results were calculated.

3.4.4.3. FTIR Analysis of Nano Composite

A Fourier transform infrared spectrum of the as-synthesized powder was recorded by using a FT-IR spectrometer at room temperature (Li *et al.*, 2007).

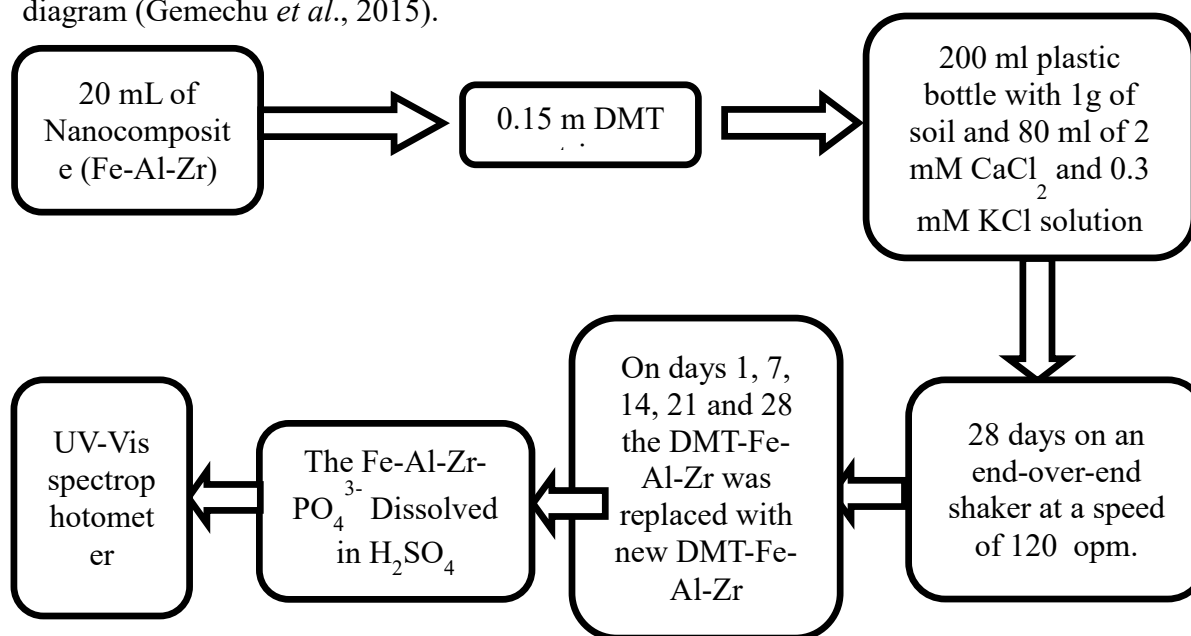
3.4.4.4. SEM and EDX Analysis

The surface morphology of the Fe-Al-Zr mixed oxide nano composite samples was studied by scanning electron microscopy (SEM) and the presence of Fe, Al and Zr elements in the mixed nano composite was determined by the EDX analysis.

3.5. Desorption Study

A desorption study was carried out using dialysis membrane tubes (Visking, size $3^{20/32}$ inches, Approximate pore size 2.5-5.0 nm; membrane thickness 3 μm , Medicell membranes Ltd, UK) filled with Fe-Al-Zr as described by Freese *et al.*, (1995); Taddesse *et al.*, (2008a, b); and Gemechu *et al.*, (2015). In this case the 0.15 m of DMT strip was filled with 20 mL of 0.1 g Fe-Al-Zr oxide ternary nanocomposite (sorbent). The sorbent suspension was stirred vigorously during the filling. The Fe-Al-Zr-DMT was placed in 200 ml polyethylene containers with 1 g of soil and 80 mL of 2 mM CaCl_2 and 0.3 mM KCl solution. All the experiments were carried out in complete randomized design (CRD) having three replications. The polyethylene containers were continuously shaken for 28 days on an end over-end shaker at 120 oscillations per minute (opm). Shaking at 120 opm created the required perturbation yet the tubes could be shaken for 14 days without physically damaging the dialysis tubes (Taddesse *et al.*, 2008).

At each of seven days intervals: 1, 7, 14, 21 and 28, the DMT- Fe-Al-Zr was replaced with new DMT-Fe-Al-Zr. In doing so, a glass rod was used to remove any attached soil from the dialysis membrane tubes. At each time interval, three of the tubes were removed, opened and the contents transferred to glass bottles. The suspension was dissolved by adding 1 mL of concentrated sulfuric acid. P in solution was determined calorimetrically with the molybdate blue method using ascorbic acid as a reductant as shown schematically in the following diagram (Gemechu *et al.*, 2015).



3.6. Data Analysis

To compare the effects of the treatments statistical analysis of variance (ANOVA) was computed to determine the existence of any statistical difference among the treatments using Statistical Analysis System, 2004 software (SAS version 9.1). Separations of significant differences among means was made by least significant differences at $\alpha = 0.05$. A simple correlation and regression analysis were conducted using Statistical Package for Social Science (SPSS, version 20) to test the relationship between desorbed P (P-Fe-Al-Zr) and other selected soil parameter including; pH in (H₂O and KCl), organic carbon (organic matter) content, exchangeable acidity, exchangeable Al, exchangeable hydrogen, available phosphorus, total phosphorus, extractable nutrients (Fe_D, Mn_D, Fe_{Ox}, and M_{Ox}) and total nitrogen.

4. RESULTS AND DISCUSSION

4.1. Characterization of the Adsorbent

4.1.1. Powder X-ray Diffraction

The x-ray diffraction study of the as-synthesized Fe-Al-Zr mixed oxide nanoparticle powder was carried out with Bruker D8 Advance X-ray diffractometer. As shown in Figure 5, the diffraction pattern shows very weak intensities on a broad background suggesting the amorphous nature of the adsorbent. However, the presence of some low intensity peaks at 2θ values of 36.03, 43.6, 53.87 and 63.54 evidenced presence of magnetite (Fe_3O_4) (Khayat *et al.*, 2012). The presence of weak intensity peaks at 2θ values indicated above exhibits the formation of some crystal at very small scale up on formation of Nanocomposite structure (Bamlaku *et al.*, 2016). No specific peaks were observed that can be attributable to alumina (Al_2O_3) and zirconia (ZrO_2) implying that both might exist in amorphous forms at the temperature of synthesis. These results indicated that the principal component of the magnetic Fe-Al-Zr ternary oxides nano composite is found to be magnetite (Fe_3O_4). Determination of the crystalline sizes of the samples were made from the full-width at half maximum (FWHM) method of the strongest reflection peak 2θ value of 36.03, using the Scherer approximation method, which assumes the small crystallite size to be the cause of line broadening. The reflection peak at $2\theta = 36.03^\circ$ is chosen to calculate the average crystallite size of the nanocomposite and was found to be ≈ 21.98 nm which is in agreement with literature (Fei *et al.*, 2011).

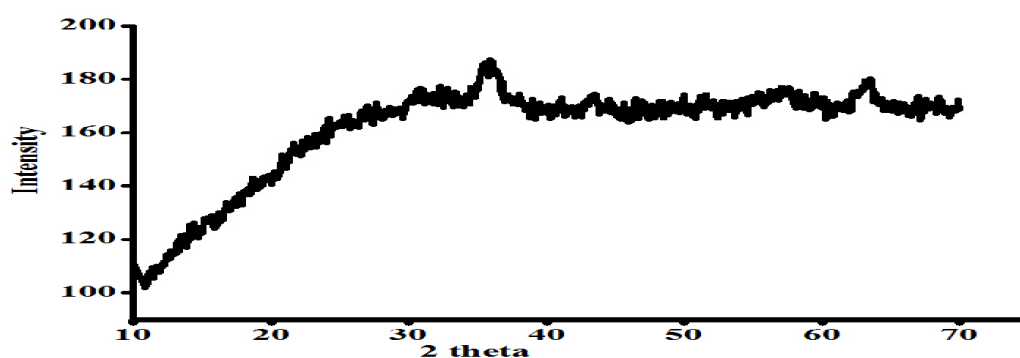


Figure 5. XRD pattern of $\text{Fe}_3\text{O}_4/\text{Al}_2\text{O}_3/\text{ZrO}_2$ ternary mixed oxide Nanocomposite

4.1.2. FT-IR Analysis

The surface functional groups of the adsorbent were determined by running the sample in KBr medium using spectrum-65 FT-IR (Perkin Elmer) in the range of 4000-400 cm^{-1} and the results were shown in Figure 6. The analysis was carried out to identify the surface functional groups of the adsorbent with the main absorption peaks located at 3434, 1384, 1022, and 585 and 441 cm^{-1} . The strong and broad band at 3800–3100 cm^{-1} region (O-H stretching vibration) may be assigned for the presence of hydroxyl of coordinated water molecules (Long *et al.*, 2011). Accordingly, the absorption peak at 3434 cm^{-1} represents O-H stretching vibration of the adsorbed water molecules (Sujana and Anand, 2010). The band that appeared at 1384 cm^{-1} corresponds to bending vibration of Al-O (Angel *et al.*, 2012). In addition to this the peak located at 1022 cm^{-1} may correspond to Al-O stretching vibration (Fei *et al.*, 2011). The second predominant broad band at 585 cm^{-1} may be assigned to Fe-O stretching vibration for magnetite because of the fact that the frequency of this vibration may be considered as indicative of involvement of Fe-O band in the Phosphate adsorption process (Taavoni-Gilan *et al.*, 2010). Another important adsorption band can be observed at 441 cm^{-1} , which corresponds to the vibration of the Zr-O bond in the Fe-Al-Zr powders (Julio *et al.*, 2012).

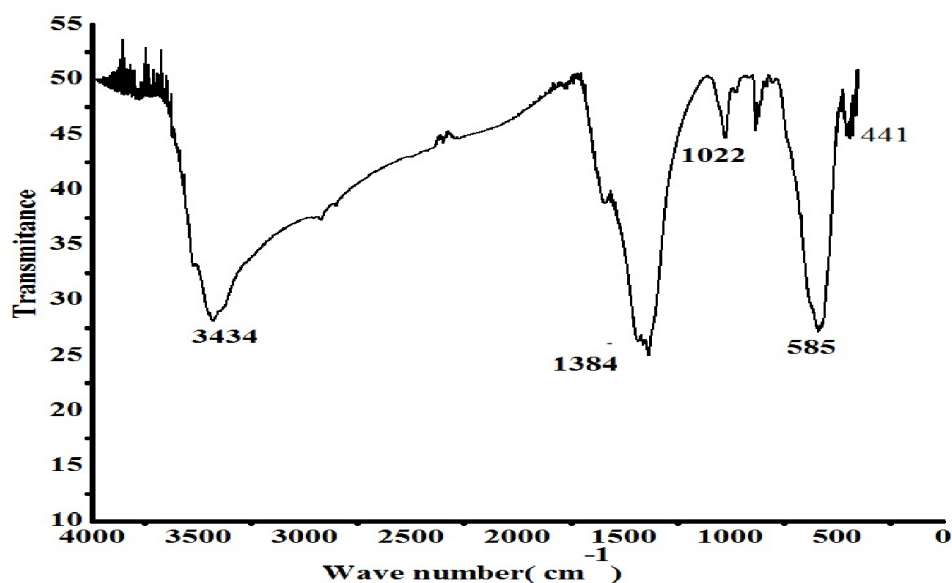


Figure 6. FTIR Spectrum of the nano sized Fe-Al-Zr mixed oxide adsorbent.

4.1.3. Elemental Analysis

Elemental analysis was performed by flame atomic absorption spectrophotometer using a standard solution of each analyte prepared at a series of concentrations. For the analysis of the metal contents of the as-synthesized powder, it was primarily dissolved by an acid digestion method and then diluted with deionized water to 100 mL. Determination of concentration of each metal ion was carried out using measured volume of the unknown solution making use of the calibration plot of each analyte metal ion prepared from the concentration of the standards versus absorbance readings. The FAAS results indicated the percentage compositions of Fe and Zr in the as-synthesized Nanocomposite were found to be shown in the following table, (Table 1).

Table 1. Actual yield and theoretical composition of the selected as-synthesized adsorbent

Sample code	Element	Theoretical composition (%)	Actual composition (%)
DA-HU-70-25-5	Fe	70	72.1
	Al	25	Not determined
	Zr	5	3.75

The FAAS results indicated that the percentage compositions of Fe, and Zr in the as synthesized selected nanocomposite were found to be 72.1 and 3.75%, respectively, but the expected values of the oxides are 70% for iron, and 5% for zirconium and this is not far from the theoretical compositions of the metals: Fe and Zr, respectively. The difference in the percentage compositions of iron and zirconium (between actual and theoretical values) may be due to insufficient dissolution, vaporization and lack of atomization. Concentration of Al was not determined due to lack of oxidant (nitrous oxide gas).

4.1.4. SEM and EDX Analysis

Scanning electron microscopy coupled with energy dispersive X-ray detector (SEM-EDX) was used to observe the morphology, and composition of Fe-Al-Zr ternary oxide nanosorbent. The SEM micrograph of the $\text{Fe}_3\text{O}_4/\text{Al}_2\text{O}_3/\text{ZrO}_2$ ternary oxide is shown in Figure 7. The SEM micrographs showed irregular particles with no distinct morphology.

The micrographs A to C revealed that the particles are generally characterized as of flake morphology, irregular shape, or uneven and rough with abundant protuberances and lots of pores which favored the adsorption of phosphate to its surface (Fei *et al.*, 2011).

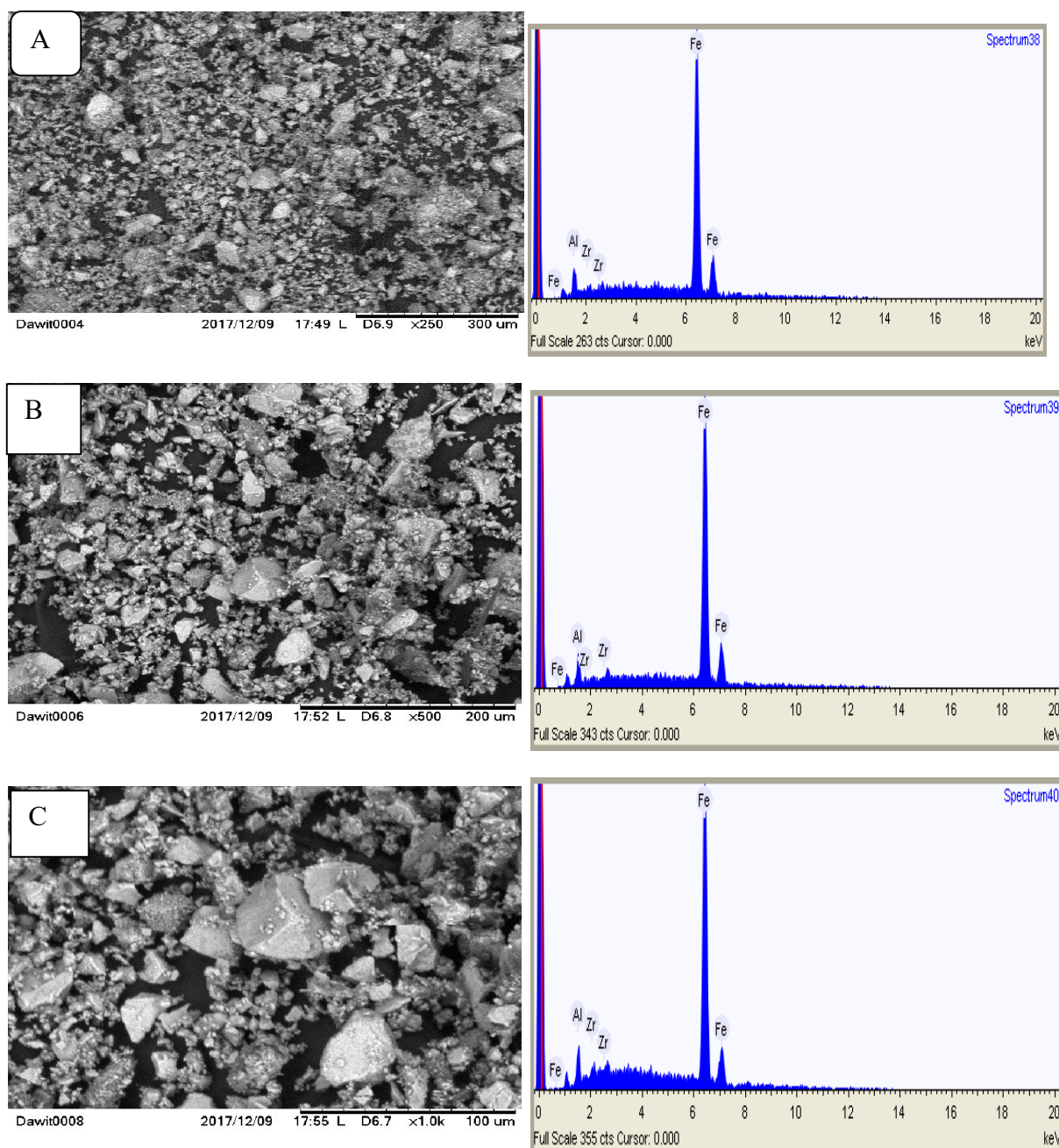


Figure 7. Scanning electron microscopic images of $\text{Fe}_3\text{O}_4/\text{Al}_2\text{O}_3/\text{ZrO}_2$ with EDX spectrum

A close look at the brighter part of the image indicates the presence of zirconia particles in the micrograph phase while alumina particles appear as a dark phase (Biamino *et al.*, 2006).

The EDX elemental analysis of these micrographs showed the presence of all the three metal constituents in the ranges of 94.7 – 96.6% (Fe) 2.5 – 3.5% (Al) and 0.9 – 1.8% (Zr). The observed slight variation of the Fe- Al- Zr metals percent weight ratio distribution might be due to the dispersion technique employed in the co-precipitation method (Nedkov *et al.*, 2006). Despite this variation, the narrow range of each element scanned on the Nanocomposite evidences the homogeneity of the as-synthesized Nanocomposite.

4.2. Physicochemical Properties of the Soil

Soil parameters including both physical and chemical parameters used for characterization of the soil sample collected from four different areas have been analyzed. These include pH in (H₂O and KCl), organic carbon (organic matter) content, exchangeable acidity, exchangeable Al, exchangeable hydrogen, available phosphorus soil texture, CEC, EC total phosphorus, extractable nutrients (Fe_D, Mn_D, Fe_{Ox}, and Mn_{Ox}), and total nitrogen. The physico-chemical properties of the soil samples considered in this study are presented in Table 2

Soil pH is one of the most common and important measurements in standard soil analyses. Many soil chemical and biological reactions are controlled by the pH of the soil solution in equilibrium with the soil particle surfaces and it is a measure of the acidity, which plays an important role in determining the solubility of important elements and processes from soils. In this study, both pH (H₂O) and pH (KCl) of the treatments were analyzed at ($\alpha = 0.05$). The soil samples studied were acidic with pH values ranging from 4.24 – 5.03 and 3.32 – 3.53 pH both in water and pH KCl solution, respectively. Even though the pH variation is not so large, and in acidic range, there is a significant difference among the treatments that Kiltu Kara (K)(4.24) is very strongly acidic and all the other treatment are rated as strongly acidic nature according to (Tekalign, 1991). The order of the soil samples according to increasing pH was Nedjo(N) < Mana Sibum(M) < Boji Dirmeji(B) < Kiltu Kara(K) and these were significantly different ($\alpha = 0.05$) (Table 2). The acidic nature of the soils caused that added P adsorbed to varied degrees by Al and Fe oxihydroxides that lowered desorption of P. Lower pH of soils influences both the degree of ionization of orthophosphate ions and the oxide surface charge which is the main factors lowering the P desorption capacity of the soils (Eze and Longathan 1990).

Table 2. Selected physical and chemical properties of the soil samples studied

Parameters		Treatments				RSD	LSD
		B. Dirmaj	Nedjo	K. Karra	M. Sibou		
pH (1:2.5)	H ₂ O	4.30 ^c	5.03 ^a	4.24 ^b	4.65 ^b	0.080	0.098
	KCl	3.32 ^c	3.51 ^a	3.36 ^b	3.53 ^a	0.030	0.029
Ex.A	meq/ 100g	4.17 ^a	2.44 ^d	3.36 ^c	3.54 ^b	0.211	0.052
Ex.A1		3.75 ^a	2.23 ^c	2.74 ^b	2.73 ^b	0.222	0.046
Ex.H		0.42 ^c	0.21 ^d	0.62 ^b	0.81 ^a	0.501	0.029
%C		0.843 ^b	0.92 ^a	0.57 ^c	0.45 ^d	0.324	0.025
% OM		1.44 ^b	1.54 ^a	0.98 ^c	0.77 ^d	0.310	0.026
%TN		0.18 ^b	0.03 ^c	0.17 ^b	0.21 ^a	0.543	0.016
EC(μ S/cm)		42.50 ^d	48.46 ^b	54.80 ^a	44.83 ^c	0.112	0.224
CEC(meq/100g)		20.60 ^b	24.63 ^b	17.73 ^d	27.63 ^a	0.192	0.312
Av.P	mg Kg-1	2.140 ^d	9.95 ^b	10.03 ^a	5.63 ^c	0.548	0.065
TP		384.10 ^d	714.05 ^a	691.33 ^b	670.28 ^c	0.251	1.611
Fe _D	g Kg-1	0.83 ^b	1.01 ^a	0.80 ^c	0.30 ^d	0.414	0.021
Mn _D		0.10 ^b	0.03 ^d	0.07 ^d	0.42 ^a	1.154	0.002
Fe _{Ox}		0.26 ^a	0.26 ^a	0.13 ^b	0.103 ^c	0.443	0.005
Mn _{Ox}		0.071 ^b	0.11 ^a	0.056 ^d	0.074 ^b	0.294	0.009
BD	g/cm ³	1.15 ^c	1.33 ^a	1.27 ^b	1.17 ^c	0.068	0.024
Soil texture	%clay	27	20	21	20		
	%silt	14	9	12	16		
	%sand	59	71	67	64		
	class	Sandy clay loam	Sandy clay loam	Sandy clay loam	Sandy clay loam		

Av.P = Availability of P, Ex.A = Exchangeable acidity, Ex.H = exchangeable hydrogen, C = carbon, OM =organic matter, TN = Total nitrogen, EC electrical conductivity, CEC=cation exchange capacity. TP = Total phosphorous, Fe_D = Iron extracted by Dithionite, Mn_D extracted by Dithionite, Fe_{ox} = Iron extracted by Oxalate, Mn_{ox} = manganese extracted by oxalate. BD= bulk density. RSD relative standard deviation, LSD = least significance difference, at P = 0.05. Mean values in rows with different letters a, b, c and d are significantly difference.

The pH (KCl) test is the more accurate of the two pH tests, as it reflects what the plant experiences in the soil. The values of pH (KCl) have similar trend with pH (H₂O): A useful, but not consistently accurate, conversion is to subtract 1 unit from the pH (H₂O) to obtain a pH (KCl) value (Gavriloaiei, 2012). pH (KCl) of the soil sample also followed the same trend as pH (H₂O) in which (Nedjo (N) < Mana Sibiu (M) < Bojii Dirmiji (B) < Kiltu Kara(K) but lower than pH (H₂O) (Table 2). Decrease in soil pH thus increasing the solubility of iron complexes that cause lower pH. In addition, soil acidity converts some available soil nutrients into unavailable form and consequently acidic soils are poor in their basic cations such as Mg, Ca, and K. The optimum pH range for most plants in soil range from 6 to 7.5 as suggested by Hazelton and Murphy, (2007).

Exchangeable acidity is the important parameter to describe the acidity of soil, which is the combined total exchangeable aluminum and reactive hydrogen ions. According to this study it showed very acidic soil in which all soil types have > 2 meq/100g. High exchangeable acidity was observed at Boji Dirmeji (B) with the value of 4.17 meq/100g and the lowest observed at < Kiltu Kara (K) with the value of 2.44 meq/100g (Table 2). This may be attributed to the fact that, phosphate anion in acidic soils can form strong bond with the oxides and hydroxides of Al generating H ion through hydrolysis reaction that lowers the pH (Achalu *et al.*, 2013).

Soil organic carbons were determined to estimate the amount of organic matter in the soil. Organic matter has an important influence on soil physical and chemical characteristics, soil fertility status, plant nutrition and biological activity in the soil (Brady and Weil, 2002). In this study, organic matter was significantly different at ($\alpha = 0.05$) between the treatments that Mana Sibiu (M) < Kiltu Kara (K) < Boji Dirmeji (B) < Nedjo (N) in order of increasing OM (Table 2). Even though a significant difference was observed among the treatments, the organic matter of the soil is deficient for plant growth according to Landon (2014). The C content of the soils in this study were very low which range from 0.45 to 0.92 which means less than 2% and is rated as very low according to Landon (2014). Such lower % soil OM and C in the soils may hinder Fe and Al oxides from formation of complex compounds with organic acids rather complexing with phosphates and decrease the releasing capacity of phosphates from the soils (Habtamu, 2015).

Total nitrogen contents of the soils were analyzed and there is no significant difference at ($\alpha = 0.05$) among the treatment Boji Dirmeji(B) and Kiltu Kara but there is significance different among the other two that is Mana Sibiu (M) and Nedjo (N) (Table 2). In this study, % TN was found to have the following value ranging from 0.03% to 0.21% for Nedjo ((N) and Mana Sibiu (M) soil and 0.18 to 0.17 for Boji Dirmeji (B) and Kiltu Kara (K). Total N for Boji dirmeji (B) (0.18%) and Kiltu Kara (K) (0.17%) and Mana Sibiu (M) (0.21%) soils was rated as medium and for that of N (0.03%) was rated as low according to Landon (2014).

Electrical conductivity (EC) is a reliable way to assess how salts affect plant growth. The EC of the soil is influenced by the concentration and composition of dissolved salts. In the present study, all of the soils collected from different districts were analyzed and small values of electrical conductivity recorded for Boji Dirmeji (B) soil sample having 42.5 $\mu\text{S}/\text{cm}$ and a maximum of 54.8 $\mu\text{S}/\text{cm}$ was recorded for the soils collected from Kiltu Kara (K) District. In the present study, all of the soils collected from different districts rated as small electrical conductivity values hence the soil samples are non-saline soils (Achal, 2014).

The Cation exchange capacity (CEC) of soils sample of Boji Dirmeji (B) and Nedjo (N) have no significant difference ($\alpha = 0.05$) but when comparison was made between Kiltu Kara (K) and Mana Sibiu (M) significant difference was observed at $\alpha = 0.05$ which their value range from (17.73 – 27.63) (Table 2). As Hazelton and Murphy (2007), suggest the CEC value of all of the soils of the present study categorized under low status of CEC value. This low CEC value of the soils leads to the accumulation of low percent organic carbon and has lower capacity to hold cations thereby resulted lower potential fertility in the soil (Achal, 2014).

Plant obtains phosphorus (P) from the soil solution through its roots and available P is composed of solution P plus P that enters the solution during the period used to define availability. Phosphorus may enter the solution by desorption or dissolution of inorganic P associated with the soil's solid phase or by the mineralization of organic P. Variations in available P content in soils are related with the intensity of soil weathering or soil disturbance, the degree of P fixation with Fe and Ca and continuous application of mineral P fertilizer sources as indicated by Paulos, (1996).

The available and total phosphorus contents were determined calorimetrically from the soil and analyzed under the significant level ($\alpha = 0.05$). Available phosphorous was estimated according to Bray II (Bray and Kurtz, 1945). Significant difference ($\alpha = 0.05$) was observed between all soil sample and showed the following increasing order such that Bojii Dirmeji (B) < Mana sibu (M) < Nedjo (N) < Kiltu Kara (K) (Table 2) Low available P status related mainly to the presence of low pH and high exchangeable acidity (Abreha, 2012). The available phosphorous in soil samples is low (< 10ppm) in three of the treatments except Kiltu Kara based on the criteria developed by Landon, (1984) for Bray II method. Such a low P status indicated that the soils under investigation are highly phosphorous fixing due to inherent low soil pH. Such high phosphorous fixing tends to maintain low phosphorous concentration in soil solution and is a characteristic feature of Fe/Al dominated clay soil that agree with previous report; (Sanchez *et al.*, 2003; Gemechu *et al.*, 2015). Total phosphorus contents were determined calorimetrically from the soil and analyzed under the significant level ($\alpha = 0.05$). Under this condition, there is significant difference among the different treatment with low total P observed at Bojii Dirmeji with the value of 384.1 mg/Kg and maximum value of 714 mg/Kg for Nedjo district soil sample. As per the ratings of Landon (1984), medium total P content was observed in all acidic soil of the studied districts.

The percentages of the Fe and Mn extracted through the Dithionite citrate bicarbonate and the Acid ammonium oxalate methods are shown in Table 2. The percentages of Fe, extracted by the dithionite citrate bicarbonate method was more than the percentage of Fe, extracted by the acid ammonium oxalate method and this observation agrees with Gemechu *et al.* (2015) that higher percentages of free iron should be extracted by the dithionite citrate bicarbonate method. The Al and Fe extract ratios for soils, stream sediments and lake sediments are well in excess of thresholds, indicating a strong retention capacity for P by these substrates (Kopáček *et al.*, 2005). The high content of extractable Fe is consistent with the acidic nature of these soils, as the solubility of Fe increases at low pH (Kiflu *et al.*, 2016). In our finding there was significance difference between each soil types among extractable nutrients (Fe_D , Mn_D , Fe_{Ox} , and Mn_{Ox} ($\alpha = 0.05$). Phosphorus/Mn interactions can develop when soil Mn availability increases with higher soil P levels. On some soils this is believed partially due to increased soil acidity from high rates of P.

Even though the dithionite citrate bicarbonate extracted elements are higher, also, ammonium oxalate extracted elements were high in quantities that it is thought to be selective for poorly crystalline and amorphous forms of Fe and Al in soils.

The relative percentage of soil separates that is % Sand, % Silt and % Clay of a given soil is called soil texture and influence the physical and chemical properties of the soil (Kiflu *et al.*, 2016). The results reveals that on average, the soil samples studied appeared to be sandy clay loam in texture with the value of (59, 14, 28) for Boji Dirmeji, (71, 9, 20) for Nedjo (67, 12, 21) for Kiltu Kara and (64, 16, 20) for Mana Sibiu in terms of % Sand, % Silt and % Clay respectively. The Bulk density value of the soils samples were significantly different for each different soil sample at ($\alpha = 0.05$) with lowest value of (1.15 g/cm^3) for Boji Dirmeji and highest (1.33 g/cm^3) value of bulk density was at the Kiltu Kara soil sample.

4.3. Long Term Phosphate Desorption Study

Phosphate desorption study was carried out using the DMT-Fe-Al-Zr mixed oxide nano-composite particle on four different soils samples with four different amount of P treatment for each soil (Table 3). The amount of P desorbed by DMT-Fe-Al-Zr was significantly influenced ($\alpha = 0.05$) both by P treatments and extraction time for all soil samples (Table 3). In all soil sample, where no P was added, lower P was extracted as DMT-Fe-Al-Zr-P whereas, significantly higher P was extracted with increasing P application rate and desorption time. This result is in agreement with the previous finding of Taddesse *et al.* (2008); Gemechu *et al.* (2015); Ochwoh *et al.* (2016). In our finding the cumulative P desorbed was higher at Kiltu Kara (K) soil with 150 mg/Kg treatment which has the value of 4.51–32.62 mg/Kg and Nedjo (N) with the same treatment which has comparable result with the value of 4.63 – 32.06 mg/Kg with no significant difference among the two soil samples and lower in the control (1.42 – 15.89 mg /Kg) at all levels of extraction time for all soil types (Table 3). Lower phosphate desorbed amount was observed in Boji Dirmeji district soil sample. Generally the amount of phosphate desorbed from each district follow the following increasing order such that Boji Dirmeji < Mana sibiu < Nedjo < Kiltu Kara (Table 3).

When comparison were made on the amount of P desorbed between the same soil types with different P treatments significance difference was observed at ($\alpha = 0.05$) and this may be due to different applied P on each treatments (Table 3).

Table 3. Desorption of phosphorus from four different soil samples for 28 days with different P treatment (in triplicate)

Soil Type (Code)	P Treatment (mg Kg ⁻¹)	P desorbed per Days				
		1	7	14	21	28
BP0	0	z1.42 ^c	y3.80 ^c	x5.91 ^d	w8.51 ^d	v12.38 ^d
BP1	50	z3.11 ^b	y6.95 ^b	x11.41 ^c	w16.166 ^c	v21.65 ^c
BP2	100	z3.59 ^a	y7.73 ^a	x12.72 ^b	w17.705 ^b	v23.72 ^b
BP3	150	z3.83 ^a	y8.05 ^a	x14.78 ^a	w21.50 ^a	v28.14 ^a
MP0	0	z2.12 ^d	y4.57 ^d	x7.12 ^d	w10.31 ^d	v13.33 ^d
MP1	50	z3.35 ^c	y7.17 ^c	x13.05 ^c	w18.32 ^c	v23.86 ^c
MP2	100	z3.67 ^b	y8.04 ^b	x14.21 ^b	w19.99 ^b	v26.90 ^b
MP3	150	z4.27 ^a	y8.94 ^a	x15.57 ^a	w22.38 ^a	v29.70 ^a
KP1	0	z2.01 ^d	y5.07 ^d	x7.28 ^d	w11.36 ^d	v14.91 ^d
KP2	50	z3.23 ^b	y7.98 ^c	x13.29 ^c	w19.53 ^c	v26.85 ^c
KP3	100	z3.89 ^c	y8.79 ^b	x15.19 ^b	w21.89 ^b	v29.56 ^b
KP4	150	z4.51 ^a	y9.56 ^a	x16.75 ^a	w23.82 ^a	v32.62 ^a
NP0	0	z2.26 ^c	y5.32 ^c	x7.93 ^d	w11.80 ^d	v15.89 ^d
NP1	50	z4.03 ^b	y8.55 ^b	x14.13 ^c	w20.31 ^c	v27.33 ^c
NP2	100	z4.19 ^b	y8.90 ^b	x14.97 ^b	w21.72 ^b	v29.04 ^b
NP3	150	z4.63 ^a	y9.71 ^a	x17.24 ^a	w24.39 ^a	v32.06 ^a

Mean values in rows with different letters z, y, x, w and v are significantly different ($\alpha = 0.05$) Mean values in columns per soil sample with different letters a, b, c and d are significantly different ($\alpha = 0.05$). for the same soil types at ($P < 0.05$). B= soil sample from Boji Dirmeji, M = soil sample from Mana Sibiu, K=soil sample from Kiltu Kara, N=Soil Sample from Nedjo

When we compare the amount of phosphate desorbed from the Kiltu Kara soil to other soils it is found to be a relatively higher than all others suggesting that high available and total P. present at Kiltu Kara soil sample was behind this high P desorption which is in agreement with the work of Gemechu *et al.* (2015). The amount of extracted P over different periods of extractions indicate that less phosphorus was extracted from Bojii dirmiji(B) soil compared to the other soil. The reason might be due to less available and total phosphorous compared to other soil in addition to this, it has relatively high content of clay in which the adsorbed phosphate was tightly held by the soil particles since clay particles have a tremendous large surface area onto which phosphate sorption can take and tends to release P slowly. Generally,

Cumulative P desorbed was higher with treatments of (150 mg/kg) and lower in the control (0 mg/kg) at all levels of extraction time (28 days) for all soils.

When we compare similar P treatment among different soil samples, there is significant difference between each soil type on 28th day of desorption for control soil sample of all soil types. However, there is a little significant difference among the other P treatments (Table 4). This significance difference might be due to difference in their physicochemical properties and in their rate of desorbed P by DMT-Fe-Al-Zr which can influence desorption in different manner (Gemechu *et al.*, 2015). The results also showed that there is significant difference between the amount of phosphate desorbed and extraction time for all soil sample studied.

Table 4. Desorption of phosphorus from four different soil samples for 28 days with similar P treatment (in triplicate (n = 3))

Soil Type	P Treatment (mg Kg ⁻¹)	P desorbed per days					Average P (mgKg ⁻¹)
		1	7	14	21	28	
BP0	0	z1.42 ^a	y3.80 ^c	x5.91 ^c	w8.51 ^c	v12.38 ^d	6.40
MP0	0	z2.12 ^{ba}	y4.57 ^b	x7.12 ^b	w10.31 ^b	v13.33 ^c	7.49
KP0	0	z2.01 ^b	y4.57 ^a	x7.28 ^{ba}	w11.36 ^a	v14.91 ^b	8.02
NP0	0	z2.26 ^a	y5.32 ^a	x7.93 ^a	w11.80 ^a	v15.89 ^a	8.64
BP1	50	z3.11 ^c	y6.95 ^c	x11.41 ^c	w16.16 ^d	v21.65 ^c	11.85
MP1	50	z3.35 ^b	y7.17 ^c	x13.05 ^b	w18.32 ^c	v23.86 ^b	13.15
KP1	50	z3.23 ^{cb}	y7.98 ^b	x13.29 ^b	w19.53 ^b	v26.85 ^a	14.17
NP1	50	z4.03 ^a	y8.55 ^a	x14.13 ^a	w20.31 ^a	v27.33 ^a	14.87
BP2	100	z3.59 ^b	y7.73 ^b	x12.72 ^c	w17.70 ^c	v23.72 ^c	13.09
MP2	100	z3.67 ^b	y8.04 ^b	x14.21 ^b	w19.99 ^b	v26.90 ^b	14.56
KP2	100	z3.89 ^{ba}	y8.79 ^a	x15.19 ^a	w21.72 ^a	v29.04 ^a	15.72
NP2	100	z4.19 ^a	y8.90 ^a	x14.9 ^{ab}	w21.89 ^a	v29.14 ^a	15.80
BP3	150	z3.83 ^c	y8.05 ^c	x14.78 ^c	w21.50 ^c	v28.14 ^a	15.26
MP3	150	z4.27 ^b	y8.94 ^b	x15.57 ^b	w22.38 ^b	v29.70 ^b	16.17
KP3	150	z4.51 ^{ba}	y9.56 ^a	x16.75 ^a	w23.82 ^a	32.62 ^a	17.45
NP3	150	z4.63 ^a	y9.71 ^a	x17.24 ^a	w24.39 ^a	32.069 ^a	17.61

Mean values in rows with different letters z, y, x, w and v are significantly different ($\alpha = 0.05$)

Mean values in columns per soil sample with different letters a, b, c and d are significantly different ($\alpha = 0.05$) B= soil sample from Boji Dirmeji, M = soil sample from Mana Sibiu,

K=soil sample from Kiltu Kara, N=Soil Sample from Nedjo.

Generally, cumulative desorption of P for all soil sample extracted by DMT-Fe-Al-Zr within 28 days was very low as compared to the total P, but it is larger as compared to the availability

of P (Table 3 and 4). The result showed that there were high adsorption of P on the soils and leads to low desorption as compared to the applied P (Table 3). This may be because of incubation effect, in which solution and labile P decreased with time of incubation and leads to an increase in adsorbed, occluded and residual P (Ochwoh *et al.*, 2016). In addition to this, in most acidic soil Fe and Al forms complex with phosphate ions in acidic soils as a result of incubation and those phenomenon caused a small phosphate desorption as compared to applied P (Ochwoh *et al.*, 2016). This indicated that as time of desorption increases the method can extract residual P, because the available P of all soils was small as compared to the desorbed P on 28th day. In general long term phosphate desorption study is essential since routine soil extractable (labile) P alone, does not provide adequate information on the P status of the soil especially in terms of the long term capacity of the soil to supply P for plant growth. Therefore, the successive DMT-Fe-Al-Zr-P extraction procedure could provide a convenient laboratory method for characterizing phosphate desorption from soil by simulating plant P uptake (Taddesse *et al.*, 2008a; Gemechu *et al.*, 2015).

Linear relationship was observed between the total P and initial P released from soil during consecutive extraction using DMT-Fe-Al-Zr (Figure 8-11) meaning as the rate of added P to the soil increases, the amount of initial and total P released also increases (Achalu *et al.*, 2013). That means, as the rate of applied P (0, 50, 100 and 150 mg kg) across all the soil sample increased, desorption of P with consecutive extraction have also increased. The results of how the successive DMT-Fe-Al Zr-P extractions influenced by the P treatments and desorption time are presented in Table 3 and 4 as well as Figure 8,9,10 and 11. According to the ANOVA and LSD values, there were highly significant responses ($P = 0.05$) in the successive DMT-Fe-Al Zr extracted P, from all the different Phosphorus treatments. The data fitted to regression equations and the R^2 values indicated very good correlations between treatments and P extractions.

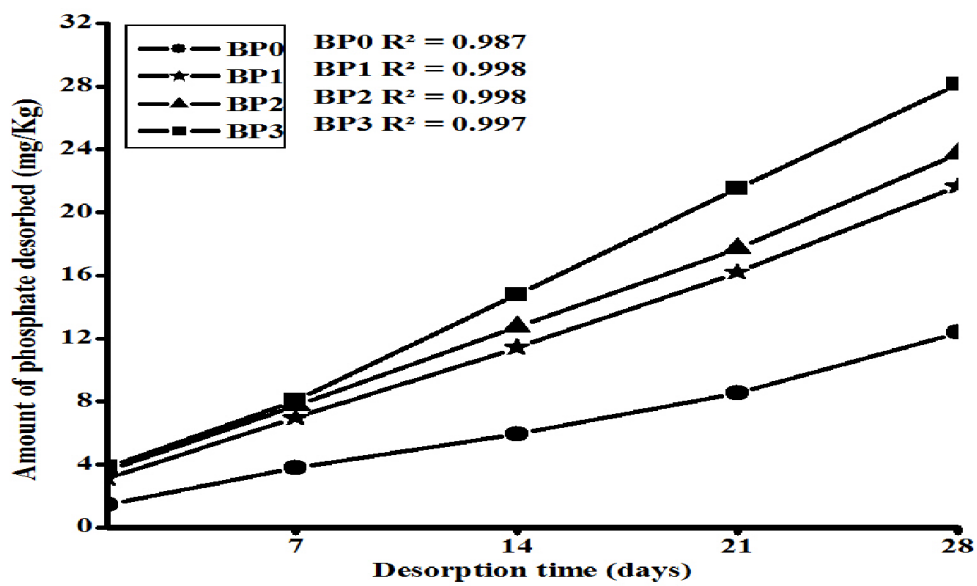


Figure 8. Cumulative desorbable P with time extracted using DMT-Fe-Al-Zr for the different treatments for Bojii Dirmejii (B) soil sample over 28 days

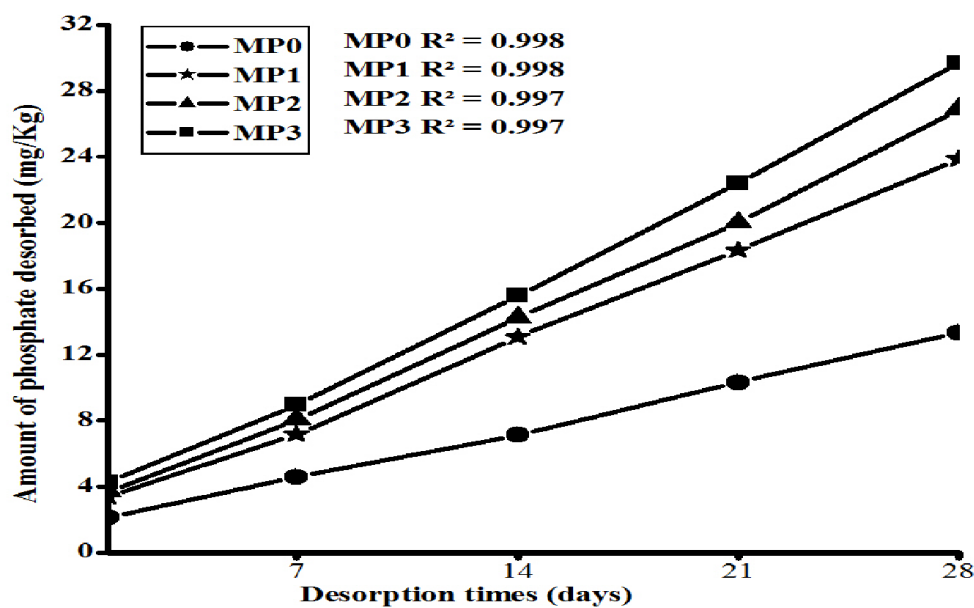


Figure 9. Cumulative desorbable P with time extracted using DMT-Fe-Al-Zr for the different treatments for Mana Sibü (M) soil sample over 28 days

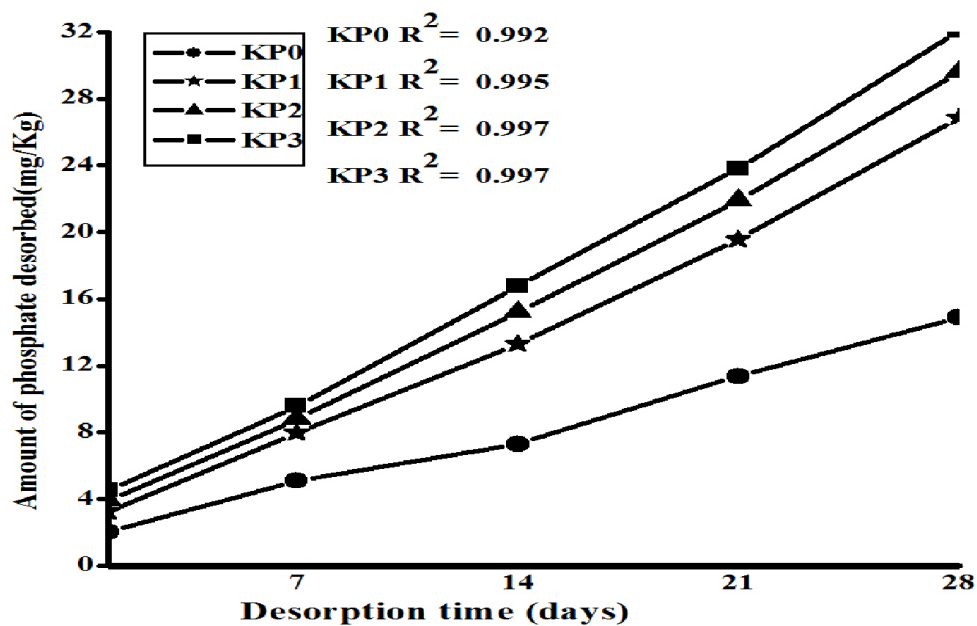


Figure 10. Cumulative desorbable P with time extracted using DMT-Fe-Al-Zr for the different treatments for Kiltu Kara (K) soil sample over 28 days

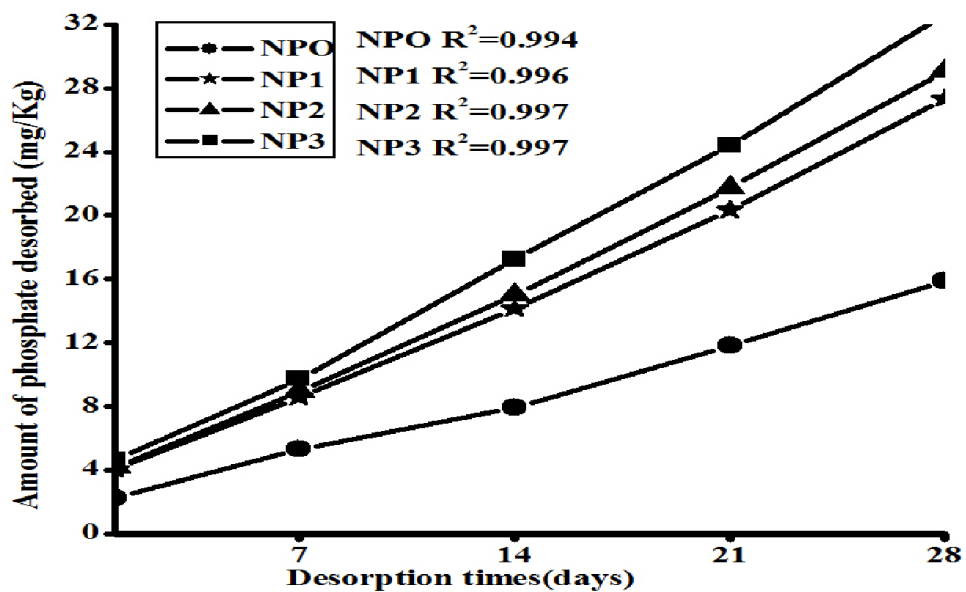
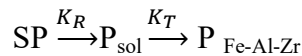


Figure 11. Cumulative desorbable P with time extracted using DMT-Fe-Al-Zr for the different treatments for Nedjo (N) soil sample over 28 days

4.4. Kinetics of Phosphorus Desorption

The kinetics of phosphate desorption was investigated using DMT-Fe-Al-Zr method. The cumulative P released with time followed the same pattern for all soils from Nedjo, Kiltu Kara Bojii Dirmiji and Mana Sibiu with different treatment with an initial rapid release of P followed by a slower release. Desorption kinetics of soil as determined using the DMT-Fe-Al-Zr as the sorbent can be schematically represented as follows.



Where, SP is solid phase P, P sol is P in solution, P Fe-Al-Zr is P adsorbed by Fe-Al-Zr k_T is rate constant of P transport through the membrane ($0.09 \pm 0.01 \text{ h}^{-1}$, Freese *et al.*, 1995) and k_R is the rate constant of P release. In our case k_d is the rate of P desorption and was found to be ($0.022-0.025 \text{ h}^{-1}$) which were obtained from a plot of the natural logarithm (ln) of the P adsorbed by the DMT-Fe-Al-Zr against time with the slope as k_d (Freese *et al.*, 1995). It was assumed that the rate constant of P release from the soil was equal to the rate constant of P adsorption (k_A) by the DMT-Fe-Al-Zr. The presence of two pools is assumed; the pool with the fast release kinetics is pool A (SP_A) and the pool with the slow release kinetics is pool B (SP_B). With this assumption, the mass balance equation for the total exchangeable solid phase soil P (SP_{total}) at time $t = 0$ is:

$$SP_{total\ 0} = SP_{A0} + SP_{B0} \text{ at time } = 0$$

$$SP_{total(t)} = SP_{A(t)} + SP_{B(t)} \text{ at time } = t$$

Assuming the decrease in SP_A and SP_B follow first order kinetics as equation (3)

$$SP_{total} = SP_{A0} + SP_{B0}$$

Where SP_{A0} is initial amount of P in pool A and SP_{B0} is initial amount of P in pool B. The mass balance equation at time t will therefore be:

$$SP_{total(t)} = SP_{A(t)} + SP_{B(t)}$$

Assuming the decrease in SP_A and SP_B follow first order kinetics, the integrated rate laws for the decrease of SP_A and SP_B will be:

$$SP_{A(t)} = SP_{A0} e^{-k_A t} \text{ and } SP_{B(t)} = SP_{B0} e^{-k_B t}$$

Where, k_A and k_B are conditional first order rate constants (day^{-1}) for P desorption from pools A and B respectively

The total solid phase soil P ($SP_{\text{total}(t)}$) remaining at time t equation (4):

$$SP_{A(t)} = SP_{A0} e^{-k_A t} + SP_{B0} e^{-k_B t}$$

For a long term desorption study (28 days), one might expect the two pools, pool A and pool B to play their role. However, in this study only rapid release of P was observed perhaps due to the better sorption capacity of the P- sink employed in this study (Fe-Al-Zr) and due to the short desorption time (28 days); not enough experimental days were available to attain both kinetics. This implies that longer equilibration time is required to observe the effect of the less labile pool (Pool B). In previous reports related to this work demonstrated the presence of two pools (de Jager and Claassens, 2005; Ochwoh *et al.*, 2005; Tadesse *et al.*, 2008). In the reports, the authors found two distinct pools of soil P within 56 days, one with rapid release kinetics and the other with slower desorption kinetics. The fast P pool presumably represents P bound to reactive surfaces, directly in contact with the aqueous phase. The slow P release rate from the second pool is either the result of slow dissolution and/or diffusion kinetics from interior sites inside oxyhydroxide particles (McDowell and Sharpley, 2003). In the latter reports, they employed a single system (hydrated ferric oxide-HFO). In our case we used ternary component system with better sorption capacity as compared to the single counterpart. As shown in Figures 12a – 12d, the P desorption kinetic of soil was found to follow first order model (first order kinetic) which schematically showed at equation (1):

$$SP_{A(t)} = SP_{A0} e^{-k_d t}$$

The rate of desorption k_d is ranged from ($0.023 - 0.025 \text{ h}^{-1}$) for Kiltu Kara, ($0.022 - 0.024 \text{ h}^{-1}$) for Mana Sibul ($0.022 - 0.025 \text{ h}^{-1}$) for Boji Dirmeji and ($0.023 - 0.024 \text{ h}^{-1}$) for Nedjo soil samples. Tadesse *et al.*, (2008) have reported in the range of ($0.00034 - 0.0004 \text{ hr}^{-1}$) for the UP soils and $0.009 - 0.005 \text{ h}^{-1}$ for Ermelo soils under the studies of kinetics of residual phosphate desorption from long-term fertilized soils of South Africa. According to our findings, highest desorption rate is found on day 1 of Kiltu Kara soil sample with the value of $4.63 \text{ mg/Kg day}^{-1}$ and the lowest is observed on day 28th of Boji Dirmeji (B) with the value of $0.44 \text{ mg/Kg day}^{-1}$.

Generally there were significant decreases in the desorption rate after day one desorption to the day 28th of desorption in which the highest rate observed on day 1 and lowest rate on day 28th for all soil types. The results are in agreement with the findings of Ochwoh *et al.* (2016).

Table 5. P desorption rate of soil samples studied

Soil Type (Code)	P Treatment (mg Kg ⁻¹)	P desorption rate (mg/Kg).day ⁻¹				
		1	7	14	21	28
BP0	0	1.42302	0.543714	0.422729	0.405276	0.442276
BP1	50	3.11709	0.993761	0.815127	0.769981	0.773254
BP2	100	3.59542	1.105323	0.908626	0.843167	0.84719
BP3	150	3.83458	2.115625	1.056054	1.024209	1.005194
MP0	0	2.12058	0.654173	0.508604	0.491016	0.476199
MP1	50	3.35625	1.025226	0.932226	0.872468	0.852235
MP2	100	3.67514	1.149133	1.015396	0.952334	0.960812
MP3	150	4.27304	1.277777	1.112721	1.066058	1.060919
KP1	0	2.01295	0.725254	0.520572	0.541051	0.532773
KP2	50	3.23667	1.140531	0.949804	0.930312	0.95911
KP3	100	3.89437	1.256101	1.085383	1.042405	1.055878
KP4	150	4.51221	1.365979	1.196898	1.134386	1.145324
NP0	0	2.26009	0.76056	0.566513	0.562182	0.567668
NP1	50	4.03388	1.221997	1.009395	0.967327	0.976289
NP2	100	4.19332	1.271791	1.069654	1.034633	1.03735
NP3	150	4.63179	1.388466	1.231715	1.161667	1.165075

B= soil sample from Boji Dirmeji ,M = soil sample from Mana Sibiu, K=soil sample from Kiltu Kara, N=Soil Sample from Nedjo.

Desorption rates of all soil samples decreased rapidly in the first 14 days and were almost the same after day 21 and approaches zero after day 28 (De Jager and Claassens, 2005) and this indicated that a fair amount of applied P could be extracted over the first 14 days with DMT-Fe-Al-Zr (Ochwoh *et al.*, 2016). For the longer DMT-Fe-Al-Zr extraction period (28th day), the desorption rate was less than 1 mg kg⁻¹ day⁻¹ and very little differences in desorption rates were found from the different P applications. Figure (12a-d) showed that there were significant decreases in the desorption rates after one day of extraction from the different P application rates, which varied from 4.63 mg kg⁻¹ day⁻¹ at the highest P rate (150 mg kg⁻¹) to only 0.442 mg kg⁻¹ day⁻¹ with no P application at the start of the incubation.

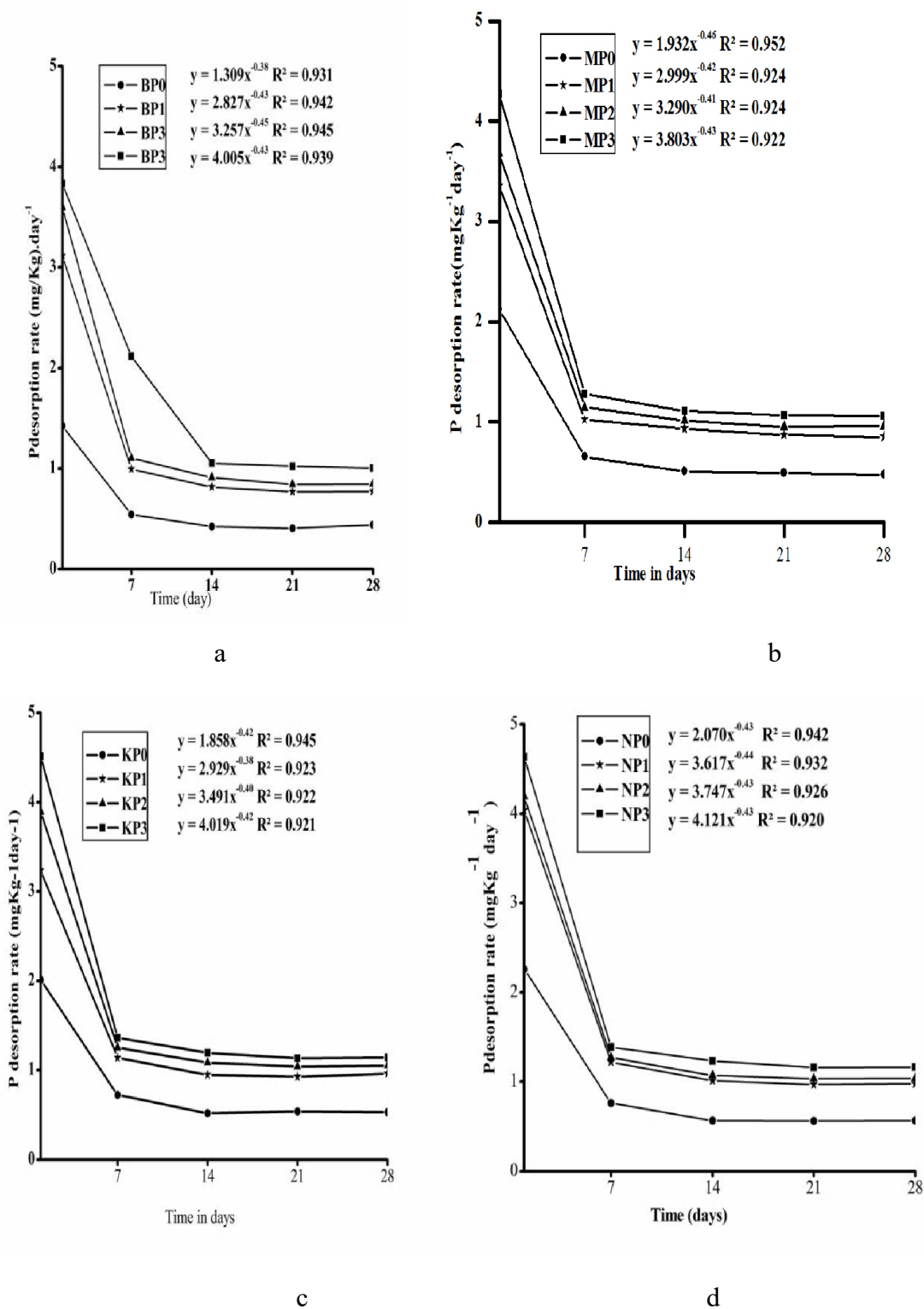


Figure 12. Phosphorus desorption rates from soil to solution for Boji dirmij (a) Mana Sibü (b), Kara kiltu (c) and Nedjo (d) soil samples with different P treatment

4.4.1. Correlation of Soil Parameter with Cumulative Desorption P

Correlation between cumulative phosphate desorption contents and selected soil properties of the treatments are shown in Table 6 and 7 and total correlation between soil properties and cumulative P desorbed was shown in Appendix table 1-4 for all soil sample. The low P-release was observed when compared with total phosphorus. Such a low P status indicated that the soils under investigation are highly phosphorous fixing due to inherent low soil pH. Such high phosphorous fixing tends to maintain low phosphorous concentration in soil solution and is a characteristic feature of Fe/Al/Mn dominated soil (Sanchez *et al.*, 2003). The result in this case showed that there is positive and significant correlation exist between cumulative desorbed P and BP1 with Fe_{Ox} and Mn_D for Boji dirmeji soil which has the value of ($r=0.952$) and ($r=0.992$) respectively (Table 6). In this study positive and high significant correlation between BP1 and pH-H₂O ($r = 0.998$) was also observed. In addition there is significant correlation exist between cumulative desorbed P for soil sample BP0 with pH-KCl, Av.P, TP and TN with the following correlation value ($r= -0.948$), ($r=-0.953$), ($r=0.874$) and ($r=0.948$), respectively (Table 6).

For the case of Mana sibu soil sample positive and significant correlation between MP2 and Exchangeable acidity ($r=0.990^{**}$) exist. There is also negative and significant correlation between MP1 and OM of that soil with($r=-0.971$). In addition, negative significant correlation between KPO and pHH₂O ($r = -0.981$) and Ex A ($r =-0.981$) was observed (Table 7) for Kiltu Kara soil while appositive significant correlation exist between KP3 and TP ($r=0.961$), TN ($r=0.961$) and FeD ($r =0.948$) for the same soil sample.

Generally the physicochemical properties of the soils were highly correlated with cumulative desorbed P either negatively, positively or not significantly Correlated as shown in the Table 6 and 7 based on the criteria that near +1 or -1 means a good relation between two variables . Correlation around zero means no relationship between them at a significant level of both 0.05 and 0.01 if $r > 0.7$ it is strongly correlated whereas, r values between 0.5 and 0.7 means moderate correlation between two different parameters exists (Sharma and Raju, 2013).

Table 6. Correlation of desorbed phosphorus level and soil properties for Boji Dirmeji(B) and Mana Sibiu (M) soil samples

Corr	pH H ₂ O	pH KCl	Ex.A	Ex. Al	C	OM
BP0	-0.94	-0.94	-0.61	-0.84	-0.98	-0.01
BP1	0.99	0.99	0.27	0.98	0.83	0.38
BP2	0.42**	0.42**	0.99	0.19	0.81	0.71**
BP3	0.77**	0.77**	0.85	0.59	0.98	0.34**
Corr	TN	AvP	TP	FeD	MnD	MnOx
BP0	0.94	-0.95	0.87	0.69	-0.71	-0.61
BP1	-0.99	0.99	0.99	-0.37	0.92	0.27
BP2	0.42**	0.43	0.25	1.00	0.01**	0.99**
BP3	0.77**	0.78	0.64	-0.90	0.41**	0.85**
Corr	pH H ₂ O	pH KCl	Ex.A	Ex. Al	C	OM
MP0	0.34	-0.34	1.00	-0.51	-0.64	0.98
MP1	-0.27	0.27	0.99	0.45	0.69	-0.97
MP2	0.18	-0.18	0.99**	-0.37	-0.75	0.94
MP3	-0.28	0.28	0.99	0.45	0.69	-0.97
Corr	TN	Av P	TP	FeD	MnD	MnOx
MP0	1.00	0.73	0.14	-0.01	-0.01	-0.98
MP1	0.99	-0.69	0.07	-0.05	0.08	0.99
MP2	-0.99	0.62**	0.01	0.14	-0.17	1.00
MP3	.099	-0.69	0.07	-0.04	0.08	0.99

** . Correlation is significant at the 0.01 level (2-tailed). And * . Correlation is significant at the 0.05 level (2-tailed) Corr. = Correlation, Av.P = Availability of P, Ex.A = Exchangeable acidity, C = carbon, OM =organic matter, TN = Total nitrogen, TP = Total phosphorous, Fe D = Iron extracted by Dithionite, by Dithionite, Mn D extracted by Dithionite, Fe Ox = Iron extracted by Oxalate, Mn Ox = manganese extracted by oxalate. B= soil sample from Boji Dirmeji M = soil sample from Mana Sibiu P0=Cumulative Phosphate desorbed from control,P1= Cumulative Phosphate desorbed from 50 mg kg⁻¹, P2 Cumulative Phosphate desorbed from 100 mg kg⁻¹, P3= Cumulative Phosphate desorbed from 150 mg kg⁻¹

Table 7. Correlation of desorbed phosphorus level and soil properties for Kiltu Kara (K) and Nedjo (N) soil samples

Corr	pH H ₂ O	pH KCl	Ex.A	Ex Al	C	OM
KP0	-0.98	0.32	-0.23	-0.89	0.96	0.04
KP1	-0.39	0.99	1.00	0.24	0.47	0.98
KP2	-0.80	0.91	-0.87	-0.27	0.85	0.77
KP3	-0.50	-0.49	0.57	-0.92	0.42	-0.71
Corr	TN	Av P	TP	Fe D	Mn D	Mn Ox
KP0	0.84	0.70	0.45	0.86	0.77	0.14
KP1	-0.35	0.83	0.77	-0.31	0.78	-0.93
KP2	0.16	0.99	0.35	0.20	0.98	-0.63
KP3	0.96	-0.06	0.97	0.94	0.03	0.83
Corr	pH H ₂ O	pH KCl	Ex.A	Ex Al	C	OM
NP0	0.95	0.93	-0.97	0.71	0.74	-0.74
NP1	0.73	0.99	-0.98	0.34	0.95**	-0.95
NP2	0.97	0.63	-0.72	0.96	0.30	-0.30
NP3	0.93	0.50	-0.60	0.99	0.15**	-0.15
Corr	TN	AvP	TP	Fe D	Mn D	Mn Ox
NP0	-0.02	-0.74	0.83	0.85	0.41	0.85
NP1	0.39	-0.95	0.98	0.99	-0.01	0.99
NP2	-0.52	-0.30	0.44	0.47	0.81	0.47
NP3	-0.64	-0.15	0.29	0.33	0.89	0.33

** . Correlation is significant at the 0.01 level (2-tailed). And * . Correlation is significant at the 0.05 level (2-tailed) Corr. = Correlation, Av.P = Availability of P, Ex.A = Exchangeable acidity, C = carbon, OM =organic matter, TN = Total nitrogen,. TP = Total phosphorous, Fe D = Iron extracted by Dithionite, Mn D Manganese extracted by Dithionite, Fe Ox = Iron extracted by Oxalate, Mn Ox = Manganese extracted by oxalate. K=soil sample from Kiltu Kara, N=Soil Sample from Nedjo P0=Cumulative Phosphate desorbed from control,P1=Cumulative Phosphate desorbed from 50 mg kg⁻¹, P2 Cumulative Phosphate desorbed from 100 mg kg⁻¹, P3= Cumulative Phosphate desorbed from 150 mg kg⁻¹

5. SUMMARY, CONCLUSION AND RECOMMENDATION

5.1. Summary and Conclusion

The P releasing soil test is fundamentally different from other soil tests in that it does not chemically extract P from soils; rather it removes P by sorption from solution into DMT filling with Fe-Al-Zr ternary oxide Nanocomposite. For this purpose Fe-Al-Zr ternary Nanocomposite adsorbent was synthesized by co-precipitation method. The surface structure of this oxide was investigated using XRD, FT-IR, FAAS, and SEM-EDX. FT-IR spectrometry shows the surface functional groups of the Nanocomposite. X-ray diffraction pattern indicated that the as-synthesized materials are in the Nano range. The percentage compositions of Fe and Zr were 72.1 and 3.75 respectively.

Soil samples were collected from West Wollega Zone, Oromia region namely, Kiltu Kara, Nedjo, Boji Dirmeji and Mana Sibru which are incubated with 0, 50, 100 and 150 ppm phosphate and their selected physicochemical properties of soil including; pH in (H₂O and KCl), EC, CEC, %C, %OM, TN, Exchangeable acidity Extractable metals (Fe and Mn) available phosphorus (Av. P) TP, soil texture was determined due to the fact that the phosphate sorption capacity of soils depends on soil physicochemical properties. Generally The result showed that all soils are in the range of strong and very strong acidic soil category which greatly affect phosphate sorption.

The phosphate adsorption to Fe-Al-Zr ternary oxide nano composite and its release from this ternary Nanocomposite is essential as it mimics the plant to absorb the phosphate from soil which this in turn useful for soil and environmental sciences primarily because P uptake by plants occurs over a period of time. The amount of P desorbed by DMT-Fe-Al-Zr was significantly influenced ($\alpha = 0.05$) both by the treatments and extraction time for all soil samples; Nedjo (N) ,Mana Sibru (M) , Boji Dirmeji (B), Kiltu Kara (K). Where no P was added, little P was extracted as DMT-Fe-Al-Zr -P but significantly more P was extracted with increasing P application rate and desorption time. The amount of extracted P over different periods of extractions; indicate that less Phosphorus was extracted from Boji Dirmeji (B) soil compared to the other soil and higher at Kiltu Kara (K) soil.

Generally cumulative desorption of P for all soil sample extracted by DMT-Fe-Al-Zr within 28 days was very low as compared to the total P, but it is larger as compared to the availability of P.

According to this study, cumulative P released with time followed the same pattern for all P treated soils, with an initial rapid release of P, approximately within the first two weeks, followed by a slower release that was still continuing after 28 days of extraction. The p desorption kinetic for all soil types considered was found to follow first order kinetic. The rate of the desorption P was founded in the Kiltu Kara range from(0.571 -0.613) day⁻¹for Mana Sibü (0.535- 0.581) day⁻¹ for Boji Dirmeji (0.547-0.613) day⁻¹ and for Nedjo (0.554-0.57) day⁻¹ in their respective P treatment. Generally the DMT- Fe-Al-Zr method can serve as analytical tool to assess the availability of residual P in soils in doing so the information obtained is essential to properly characterize the P supplying capacity of soils, to design P-fertilizer management to optimize efficiency, to reduce environmental pollution, and to develop guidelines for the disposal of P-rich wastes.

5.2. Recommendations

The result of the Nano-sized ternary mixed oxide adsorbent indicated that the adsorbent was capable of desorbing phosphate ions from acidic soil by filling it in DMT which mimicking the plant mode of action to access P to the plant. Therefore, the following recommendations are made as a result of the outcome of this study:

- ❖ Carry out the research on the desorption capacity of this Nano-sorbent other than acidic soil that is for neutral and basic soil.
- ❖ Cary out the research on the effect of competing anions in soil solution like as silicates, molybdate, carbonates and sulfates with phosphate
- ❖ Cary out the research longer than day 28 to assess the availability of residual P in soils.
- ❖ Cary out a research on quaternary mixed metal oxides Nanocomposite adsorbent to further enhance the adsorption efficiency of the Nanocomposite.

6. REFERENCES

- Abreha kidanemariam, Heluf Gebrekidan, Tekalign Mamo and Kibebew Kibret. 2012. Impact of altitude and land use type on some physical and chemical properties of acidic soils in tsegede highland, north Ethiopia. *Open Journal of Soil Science*, 2(3): 223-233.
- Acelas, N.Y. Martin, B. D., Lopez, D. and Jefferson, B. 2015. Selective removal of phosphate from wastewater using hydrated metal oxides dispersed within anionic exchange media. *Chemosphere*, 119: 1353–1360.
- Achalu Chimdi, Heluf Gebrekidan, Abi Tadesse and Kibebew Kibret. 2013. Phosphorus Desorption Patterns of Soils from Different Land Use Systems of East Wollega, Ethiopia. *Middle-East Journal of Scientific Research*, 17 (2): 245-251.
- Achalu Chimdi, Heluf Gebrekidan, Kibebew Kibret and Abi Tadesse. 2012a. Status of selected physicochemical properties of soils under different land use systems of Western Oromia, Ethiopia. *Journal of Biodiversity and Environmental Sciences*, 2(3): 57-71.
- Achalu Chimdi. 2014. Assessment of the Severity of Acid Saturations on Soils Collected from Cultivated Lands of East Wollega Zone, Ethiopia. *Science, Technology and Arts Research Journal*, 3(4): 42-48.
- Agrawal, A. and Sahu, K. 2006. Kinetic and isotherm studies of cadmium adsorption on manganese nodule residue. *Journal of Hazardous Materials*, 137: 915-924.
- Ahmed, M. F., Kennedy, I. R., Choudhury, A., Kecskes, T. L. and Deaker, R. 2008. Phosphorus adsorption in some Australian soils and influence of bacteria on the desorption of phosphorus. *Communications in Soil Science and Plant Analysis*, 39: 1269-1294.
- Anamarai, D., Mariana, P., Bogdan, C., Anamaria Duedureanu Anheluta, Mariana pinte alad Bogdan, C. and Simionencu. 2012. Tailored and functionalized magnetic particles for biomedical and industrial application. *Materials Science and Technology*, 7:150-178
- Anderson, J. M. and Ingram, J. S. I. 1996. Tropical Soil Biology and Fertility: A Handbook of Methods, 2nd edition, CAB International, Wallingford, U.K.
- Angel, J.D., Aguilera, A. F., Galindo, I. R., Martínez, M. and Viveros, T. 2012. Synthesis and characterization of alumina-Zirconia powders obtained by sol-Gel method: Effect of solvent and water addition rate. *Materials Sciences and Applications*, 3: 650-657.

- Angel, J.D., Aguilera, A. F., Galindo, I. R., Martínez, M. and Viveros, T. 2012. Synthesis and characterization of alumina-Zirconia powders obtained by sol-Gel method: Effect of solvent and water addition rate. *Materials Sciences and Applications*, 3: 650-657.
- Asmare Melese, Heluf Gebrekidan, Markku Yli-Halla and Birru Yitaferu. 2015. Phosphorus status, inorganic phosphorus forms, and other physicochemical properties of acid soils of Farta District, Northwestern Highlands of Ethiopia. *Applied and Environmental Soil Science*, 2015:1-12.
- Bamlaku Semagne, Isabel, D., Tesfahun Kebede, Abi M. Taddesse. 2016. Synthesis, characterization and analytical application of polyaniline tin(IV) molybdophosphate composite with nanocrystalline domains. *Reactive and Functional Polymers*, 98: 17–23.
- Barrow, J. 2016. The effects of pH on phosphate uptake from the soil. *Journal of Plant and Soil Science*, 2: 1-10.
- Beck, M. A. and Sanchez, P. A. 1994. Soil phosphorus dynamic fractions during 18 years of cultivation on a Typic Paleudult. *Journal of Soil Science*, 34: 1424-1431.
- Bhattacharjee, C. R., Purkayastha, D. D., Bhattacharjee, S. and Nath, A. 2011. Homogeneous chemical precipitation route to ZnO nanosphericals. *Journal of Physical Science and Technology*, 7(2): 122-127.
- Biamino, S., Fino, P., Pavese, M. and Badini, C. 2006. Alumina/zirconia/yttria nanocomposites prepared by solution combustion synthesis. *Ceramics International*, 32:509–513.
- Bouyoucos, G. J. 1962. Hydrometer method improved for making particle size analysis of soil. *Journal of Agronomy*, 54: 464-465.
- Bowden, L. I., Jarvis, A. P., Younger, P. L. and Johnson, K. L. 2009. Phosphorus removal from waste waters using basic oxygen steel slag. *Environmental Science. Technology*, 43: 2476–2481.
- Brady, N. C. and Weil, R. R. 2002. *Nature and Properties of Soils*. 13th ed. New York, USA.
- Bray, R. H. and Kurtz, L.T. 1945. Determination of total, organic, and available forms of phosphorus in soils. *Soil Science*, 59: 39-45.
- Bruce, R. C. and Rayment, G. E. 1982. Analytical methods and interpretations used by the agricultural chemistry branch for soil and land use surveys. Queensland Department of Primary Industries. Bulletin QB8 (2004), Indooroopilly, Queensland.

- Buehler, S., Obeson. A., Rao, I. M., Friessen, D. K. and Frossard, E. 2002. Sequential phosphorus extraction of a ^{33}P –labeled oxisol under contrasting agricultural systems. *Soil Science. Society of American Journal*, 66: 868-877.
- Bushman. L, John L, Gyles R, George. R and Michael. S, (2009). The nature of phosphorus in soils. *Canadian Journal of Soil Science*, 83:11–23.
- Buzuayehu Abebe, 2012. Synthesis, characterization and sorption study of nano sized Iron/Aluminum/Manganese mixed oxide sorbent system for removal of phosphate from aqueous solution. MSc Thesis, Haramaya University, Haramaya, Ethiopia.
- Carp, O., Huisman, C. L. and Reller, A. 2004. Photoinduced reactivity of Titanium dioxide. *Progress in Solid State Chemistiry*, 32: 33-177.
- Cava, S., Tebcherani, M., Souza, I. A., Pianaro, S. A., Paskocimas, C. A., Longob, E. and Varela, J. A. 2007. Structural characterization of phase transition of Al_2O_3 Nanopowders obtained by polymeric precursor method. *Materials Chemistry and Physics*, 103: 394–399.
- Chang, G., Jiang, Z., Peng ,T. and Hu, B. 2003. Preparation of high specific surface area nanometer sized alumina by sol–gel method and study on adsorption behaviors of transition metal ions on the alumina powder with ICP-AES. *Acta Chimica Sinica-Chinese*, 61(1): 100-103.
- Chen, X. and Mao, S. S. 2007. Titanium Dioxide Nanomaterials: Synthesis, Properties, Modifications and Applications. *Chem. Rev*, 107: 2891(95).
- Chen, Y. H. and Li, F. A. 2010. Kinetic study on removal of copper (II) using goethite and hematite nano-photocatalysts. *Journal Colloidal of Interface. Science*. 347: 277–281.
- Chintala, R., Schumacher, T., McDonald, L., Clay, D. E., Malo, D., Papiernik, S and Julson, J. 2014. Phosphorus sorption and availability from biochars and soil/biochar mixtures. *Clean–Soil, Air, Water*, 42: 626-634.
- Crittenden, J. C., Trussell, R. R., Howe , K. J. and Tchobanoglous, G. 2005. Water treatment: Principles and practice 2nd edition. Hoboken, NJ: John Wiley and Sons.
- Cui, H., Li, Q., Gao, S. A. and Shang, J. K. 2012. Strong adsorption of arsenic species by amorphous zirconium oxide nanoparticles. *Journal of Industrial and Engineering Chemistry*, 18: 1418-1427.

- Cumbal, L. and SenGupta .A. K. 2005. Arsenic removal using polymer-supported hydrated iron (III) oxide nanoparticles: role of Donnan membrane effect. *Environmental Science Technology*, 39: 6508-6515.
- Day, P. R. 1965. Particle fractionation and particle size analysis. In C. A. Black, editor. Methods of soil analysis. *American Society of Agronomy, Madison, Wisconsin, USA* 545-566p.
- De Bolle, S. 2013. Phosphate saturation and phosphate leaching of acidic sandy soils in Flanders: analysis and mitigation options. Doctoral dissertation, Ghent University.
- De Jager, P. C. and Claassens, A. S. 2005. Long-Term Phosphate Desorption Kinetics of an Acid Sandy Clay Soil from Mpumalanga, South Africa. *Communications in Soil Science and Plant Analysis*, 36(1-3): 309-319.
- Eze, O.C. and Longanthan, P. 1990. Effects of pH on phosphorus sorption of some Paleudults of southern Nigeria. *Soil Science*, 153(1990): 279-288.
- Fan, M., Boonfueng, T., Xu Y., Axe L. and Tyson, T.A. 2005. Modeling Pb sorption to microporous amorphous oxides as discrete particles and coatings. *Journal of Colloid Interface Science* ,281: 39–48.
- FAO (Food and Agriculture Organization). 2006. Plant nutrition for food security: A guide for integrated nutrient management. FAO, Fertilizer and Plant Nutrition. *Bulletin 16. FAO, Rome, Italy*.
- Fei L., Jilai G., Guang-Ming Z., Long C., Xi-Yang, W., Jiu-Hua, D., Qiu-Ya, N., Hui- Ying, Z. and Xiu-Rong, Z. 2011. Removal of phosphate from aqueous solution by magnetic Fe–Zr binary oxide. *Chemical Engineering Journal*, 171: 448–455.
- Fekadu Kassahun Bahiru, 2015. Synthesis and Characterization of $Al_2O_3/Fe_3O_4/ZrO_2$ Hetrojunction Terinary Oxide Nanocomposite for nitrate sorption from aqueous aolution. Thesis,Haremaya University.
- Freese, D., Lookman, R., Merckx, R. and van Riemsdijk, W. H. 1995. New method for the Assessment of long term phosphate desorption from the soil. *Soil Science of American Journal*, 59: 1295-1300.
- Gaume, A. 2000. Low-P tolerance of various maize cultivars: the contribution of the root exudation. *PhD Dissertation, Swiss Federal Institute of Technology, Zürich, Switzerland*.

- Gavriloaiei, T. 2012. The Influence of Electrolyte Solutions on Soil pH Measurements. *Revista de Chimic-Bucharest*, 63 (4): 396-401.
- Ge, S., Shi, X., Sun, K., Li, C., Uher, C., Baker, J. R. Jr., Holl, M. M. B. and Orr B.G., 2009. Facile hydrothermal synthesis of Iron Oxide nanoparticles with tunable magnetic properties. *Journal of Physics and Chemistry C*, 113: 13593–13599.
- Gemechu Shumi, Abi Tadasse, Tesfahun Kebede. 2015. Phosphorus desorption study using dialysis membrane tube filling Fe-Al-Mn ternary mixed nanocomposite from different farming practice of acidic soil. *Chemistry and Materials Research*, 7 (8): 82-91.
- Gichangi, E. M., Mnkeni, P. N. S. and Muchaonyerwa, P. 2008. Phosphate sorption characteristics and external P requirements of selected South African soils. *Journal of Agriculture and Rural Development in the Tropics and Subtropics*, 109(2): 139-149.
- Guo, Z., C. Yan, J. Xu and Wu. W. 2009. Sorption of U (VI) and phosphate on γ -alumina: Binary and ternary sorption systems, Colloids and Surfaces. *Physicochemical Engineering Aspects*, 336: 123–129.
- Habtamu Admas Desta. 2015. Reclamation of phosphorus fixation by organic matter in acidic soils: A review. *Global Journal of Agriculture and Agricultural Sciences*, 3 (6): 271-278.
- Harrison, A. F., 1987. Soil organic phosphorus- A review of world literature. CAB Intl, Wallingford,U.K.
- Haygarth, P. M. and Sharpley, A. 2000. Terminology for phosphorus transfer. *Journal of Environmental Quality*, 29:10-15.
- Hazelton, P. and Murphy, B. 2007. *Interpreting soil test results: 2nd Edition*.pp. 152.CSIRO Publishing.
- Hernandez, J. and Meurer, E. J. 2000. Phosphorus availability in six Uruguayan soils affected by temporal variation of oxidizing-reducing conditions. *Revista Brasileira of CienciadoSolo*, 24: 19-26.
- Hinsinger, P., Brauman, A., Devau, N., Gérard, F., Jourdan, C., Laclau, J. P., and Plassard, C. 2011. Acquisition of phosphorus and other poorly mobile nutrients by roots. Where do plant nutrition models fail. *Plant and Soil*, 348, 29.
- Holford, J. C. R. 1997. Soil phosphorus: its measurement, and its uptake by plants. *Australia Journal of Soil Resource*, 35: 227-239.

- Hollford, I. C. R. & Mattingly, G. E. G., 1975. The high and low energy phosphate adsorbing surfaces in calcareous soils. *Journal of Soil Science*, 26: 407-417.
- Horta, M. C. and Torrent, J. 2007. Phosphorus desorption kinetics in relation to Phosphorus forms and sorption properties of Portuguese acid. *Soil Science*, 172(8): 631-638.
- Hu, D., Zhang, J., Graff, G. L., Liu, J., Pope, M. A. and Aksay, I. A. 2010. Ternary self-assemble of ordered metal oxide-graphene Nanocomposites for electrochemical energy storage. *Journal of American Chemical Society*, 4(3): 1587–1595.
- Indiati, R. 2000. Addition of phosphorus to soils with low to medium phosphorus retention capacities and effect on soil phosphorus extractability. *Communication of Soil Science Plant Analysis*, 31: 2591-2606.
- Jackson, M. L., 1958. Soil Chemical Analysis: Prentice-Hall, Englewood Cliffs, 498p.
- Jianbo, L., Huijuan, L., Zaho, X., Liping, S. and Jihu, Q. 2013. Adsorptive removal of phosphate by a nanostructured Fe-Al-Mn trimetal oxide sorbent. *Powder Technology*, 233: 146-154.
- Jones, J. B. 2003. Agronomic Handbook: Management of crops, soils, and their fertility. pp. 482. CRC Press LLC, Boca Raton, Florida, USA.
- Karageorgiou, K., Paschalis, M. and Anastassakis, G. N. 2007. Removal of phosphate species from solution by adsorption onto calcite used as natural adsorbent. *Journal of Hazardous Material A*, 139: 447-452.
- Keshmiri, M.; Troczynski, T. and Mohseni, M. 2006. Properties of amorphous and crystalline titanium dioxide from first principles. *Journal of Hazardous Material*, 3: 128-130.
- Khayat, Z. and Khayat, S. 2012. Synthesis and Magnetic Properties Investigations of Fe₃O₄ Nanoparticles. *Proceedings of the 4th International Conference on Nanostructures (ICNS4) 12-14 March, 2012, Kish Island, I.R. Iran.*
- Kiflu Alemayehu¹, Beyene Sheleme and Jeff Schoenau. 2016. Characterization of problem soils in and around the south central Ethiopian Rift Valley. *Journal of Soil Science and Environmental Management*, 7(11):191-203.
- Koilraj, P. and Kannan, S. 2010. Phosphate uptake behaviour of ZnAlZr ternary double hydroxides through surface precipitation. *Journal of Colloid Interface Science*, 341: 289–297.

- Kolahchi, Z. and Jalali, M. 2012. Speciation of phosphorus in phosphorus-amended and leached calcareous soils using chemical fractionation. *Polish Journal Environmental Study*, 21(2): 395-400.
- Koopmans, G. F., Van der zeew, M. E., Chardon, W. J. and Dolfing, J. 2001. Selective extraction of labile phosphorus using dialysis membrane tubes filled with hydrous iron hydroxide. *Soil Science*, 166: 475-483.
- Kopáček, J., Borovec, J., Hejzlar, J., Ulrich, K., Norton, S. A. and Amirbahman, A. 2005. aluminum control of phosphorus sorption by lake sediments. *Environmental Science and Technology*, 39: 8784-8789.
- Kuzawa, K., Jung, Y. J., Kiso, Y., Yamada, T., Nagai, M., and Lee, T. G. 2006. Phosphate removal and recovery with a synthetic hydrotalcite as an adsorbent. *Chemosphere*, 62(1): 45–52.
- Lalley, J., Han, C., Li, X., Dionysiou, D. D. and Nadagouda, M. N. 2016. Phosphate adsorption using modified iron oxide-based sorbents in lake water: Kinetics, equilibrium, and column tests. *Chemical Engineering Journal*, 284: 1386–1396.
- Landon, J. R. 1984. Booker tropical soil manual: A handbook for soil survey and agricultural land evaluation in the tropics and subtropics. *Booker Agriculture International Limited*,. 48p.
- Landon, J. R. 2014. A handbook for soil survey and agricultural land evaluation in the tropics and sub tropics. pp. 474. *In: Wiley, J. and Sons (eds.), Booker Tropical Soil Manual*. New York.
- Laurent, S., Forge, D., Port, M., Roch, A., Robic, C., Elst, L. and Muller, R. N. 2008. Magnetic iron oxide nanoparticles: synthesis, stabilization, vectorization, physicochemical characterizations, and biological applications. *Chemical Review*, 108: 2064-2110.
- Li, F. B., Li, X. Z., Liu, C. S. and Liu, T. X. 2007. Effect of alumina on photocatalytic activity of iron oxides for bisphenol A degradation. *Journal of Hazardous Materials*, 149:199-207.

- Liu, J., Wan, L., Zhang, L., and Zhou, Q. 2011. Effect of pH, ionic strength, and temperature on the phosphate adsorption onto lanthanum-doped activated carbon fiber. *Journal of Colloidal Interface Science*, 364(2): 490–496.
- Liyuan, C., Yuan, W., Zhhao, Na., Weichum, Y. and Xiangyu, Y. 2013. Sulfate doped Fe₃O₄/Al₂O₃ nanoparticles as a novel adsorbent for fluoride removal from drinking water. *Water Research*, 47: 4040-4049.
- Lookman, R., Freese, D., Merckx, K., Vlassak, K. and van Riemsdijk, W. H. 1995. Long-term kinetics of phosphate release from soil. *Environmental Science and Technology*, 29(6): 1569-1575.
- Lu, J., Liu, H., Liu, R., Zhao, X., Sun, L. and Qu, J. 2013. Adsorptive removal of phosphate by a nanostructured Fe-Al-Mn trimetal oxide adsorbent. *Powder Technology*, 233:146-154.
- Mäkidea, P., Persson, P. and Österlunda, L. 2013. Adsorption of trimethyl phosphate and triethyl phosphate on dry and water pre-covered hematite, maghemite, and goethite nanoparticles. *Colloid Interface Science*, 392: 349-358.
- McDowell, R. W. and Sharpley, A. 2002. Phosphorus transport in over land flow in response to position of manure application. *Journal of Environmental Quality*, 31:217-227.
- McDowell, R.W. and Stewart, I. 2006. The phosphorus composition of contrasting soils in pastoral, native and forest management in Otago, New Zealand: Sequential extraction and ³¹P NMR. *Geoderma*, 130(1-2): 176-189.
- McKeague, J. A. 1967. An evaluation of 0.1M pyrophosphate and pyrophosphate–dithionite in comparison with oxalate as extractants of the accumulation products in Podzols and some other. *Canadian Journal of Soil Science*, 47: 95-99.
- Mckean S. J. and Warren, G. P. 1996. Determination of soil phosphate desorption characteristics in soils using successive resin extraction. *Communication of Soil Science. Plant Analysis*, 27: 2397-2417.
- Mehra, O. P. and Jackson, M. L. 1960. Iron oxide removal from soils and clays by Dithionitecitrate system buffered with sodium bicarbonate. *Clays Clay Mineral*, 7: 317-327.
- Mishra, B. G. 2008. Colloid and surfaces adsorption. *Journal of Hazardous Materials*, 4:317-234.

- Moazed, H., Hoseini, Y., Naseri, A. A. and Abbasi, F. 2010. Determining phosphorus adsorption isotherm in soil and its relation to soil characteristics. *Journal of Food, Agriculture and Environment*, 8 (2): 1153-1157.
- Nedkov, T., Merodiiska, L., Slavov, R. E., Vandenberghe, Y. and Kusano, J. T. 2006. Surface oxidation, size and shape of nano-sized magnetite obtained by co-precipitation. *Journal of Magnetism and Magnetic Materials*, 300: 358–367.
- Ochwoh, V. A., Claassens, A. S. and De Jager, P. C. 2005. Chemical changes of applied and native phosphorus during incubation and distribution into different soil phosphorus pools. *Communication in Soil Science and Plant Analysis*, 36: 535-556.
- Ochwoh, V. A., Nankya, E., De Jager, P.C. and Claassens, A. S. 2016. The impact of phosphorous applications and incubation periods on p-desorption characteristics with successive DMT-HFO-P extractions on P fixing soils. *International Journal of Plant and Soil Science*, 13(6): XX-XX
- Oelkers, E. 2008. Phosphate mineral reactivity: from global cycles to sustainable development *Mineralogical Magazine* 72, 337 - 340.
- Paini, R., Castelli, F. and Panichi, A. 1999. Phosphorus retention and leaching in some sand soils of northern Italy. *Italian Journal of Agronomy*, 3(2):101-107.
- Paulos Dubale. 1996. Availability of phosphorus in the coffee soils of southwest Ethiopia. The Resource Base for Survival. *Proceeding of the 2nd Conference of the Ethiopian Society of Soil Science*, 23-24 September 1993, Addis Ababa, Ethiopia.
- Peech, M. 1965. Hydrogen-ion activity Methods of Soil Analysis *American Society of Agronomy, Madison*, 2:914-926
- Pierzynski, G. M., Sims, J. T. and Vance G. F. 1994. Soils and environmental quality, CRC press, Inc., 98-131.
- Potter, H. A. B., and Yong, R. N. 1999. Influence of iron/aluminium ratio on the retention of lead and copper by amorphous iron–aluminium oxides. *Applied Clay Science*, 2 :1016-1317p.
- Qiu, H., Liang, C., Zhang, X., Chen, M., Zhao, Y., Tao, T., Xu, Z. and Liu, G. 2015. Fabrication of a Biomass-Based Hydrous Zirconium Oxide Nanocomposite for Preferable Phosphate Removal and Recovery. *American Chemical Society: Applied Materials and Interfaces*, 7: 20835-20844.

- Raven K. P. and Hossner, L. R. 1993. Phosphate desorption quantity-intensity relationships in soil. *Journal of Soil Science Society of America*, 57:1505-1508.
- Raven, K. P. and Hossner, L. R. 1994. Sorption and desorption quantity intensity parameters to plant available soil phosphorus. *Soil Science Society of American Journal*, 58: 405-410.
- Ren, Z. M., Zhang, G. S. and Chen, J. P. 2011. Adsorptive removal of arsenic by an iron zirconium binary oxide adsorbent from water. *Journal of Colloid and Interface Science*, 358, 230–237.
- Rhoades, J. D. 1982. Cation exchange capacity. pp. 149-157. In: Page, A.L., Miller, R.H. and Keeney, D.R. (eds.), Agronomy No. 9, *Methods of Soil Analysis, Part 2*.
- Rowell, D. L. 1994. Soil Science methods and applications. pp. 459. *Soil Science*, University of Reading.
- Ruttenberg, K. C. 2009 The global phosphorus cycle. *Treatise on Geochemistry* 9: 585-591.
- Samadi, A. 2006. Phosphorus sorption characteristics in relation to soil properties in some calcareous soils of Western Azerbaijan. *Province Journal Agricultural and Science Technology*, 8: 251-264.
- Sanchez, P. A., Palm, C. A. and Buol, S.W. 2003. Fertility capability soil classification: a tool to help assess soil quality in the tropics. *Geoderma*, 114: 157-185.
- Sato, S. 2003. Phosphorus sorption and desorption in a brazilian ultisol: effects of pH and organic anions on phosphorus bioavailability. PhD dissertation, University of Florida, Brazil.
- Shabani, A. M. H., Dadfarnia, S. and Dehghani, Z. 2009. On-line solid phase extraction system using 1, 10-phenanthroline immobilized on surfactant coated alumina for the FAAS determination of copper and cadmium. *Talanta*, 79: 1066-1070.
- Shaheen, W. M. and Hong, K. S. 2002. Thermal characterization and physic-chemical properties of Fe₂O₃-Mn₂O₃/Al₂O₃ system. *Thermochemica Acta*, 381: 153-164.
- Sharma, M. S. R. and Raju, N. S. 2013. Correlation of heavy metal contamination with soil properties of industrial areas Mysore, of Karnataka, India by Cluster Analysis. *International Research Journal of Environment Sciences*, 2: 22 27.
- Sharpley, A. N. 1985. The cycling of phosphorus in unfertilized and fertilized agricultural soils. *Soil Science Society of American Journal*, 49: 90–911.

- Sharpley, A. N. 1996. Availability of residual phosphorus in manure soils. *Soil Science Society of America Journal*, 60: 1459-1466.
- Shwe, W. M., Dr. Mya, Oo, Dr. SuSu and Hlaing. 2012. Preparation of iron oxide nanoparticles mixed with calcinated laterite for arsenic removal. *Chemical Engineering and its Applications*, 121-125.
- Soinne, H. 2009. Extraction methods in soil phosphorus characterisation: Limitations and applications. *Academic dissertation, University of Helsinki, Helsinki, Finland*.
- Song, X. and Sayari, A. 1996. Combustion synthesis and characterization of Fe₂O₃-ZrO₂ nanocomposite oxides. *Catalytic Review Science Engineering*, 38: 329-333.
- Sousa, A. F., Braga, E. C., Chagas T. P., Gomes, A., Valentini, E. and Longhinotti. 2012 Adsorption of phosphate using mesoporous spheres containing iron and aluminum oxide, *Journal of chemical Engineering*. 210 :143–149.
- Sparks, D. L. 2001. Elucidating the fundamental chemistry of soils: Past and recent achievements and future frontiers. *Geoderma*, 100: 303–319.
- Stumm, W., and J. J. Morgan, 1981. Aquatic Chemistry: An Introduction Emphasizing Chemical Equilibria in Natural Waters John Wiley & Sons, Toronto
- Su, Y., Yang, W., Sun, W., Li, Q., and Shang, J. K. 2015. Synthesis of mesoporous cerium zirconium binary oxide nano adsorbents by a solvothermal process and their effective adsorption of phosphate from water. *Chemical engineering Journal*, 268: 270–279
- Sujana, M. G and Anand, S. 2010. Iron and aluminum based mixed hydroxides: A novel sorbents for fluoride removal form aqueous solution. *Journal of Applied Surface Science*, 256: 6956-6962.
- Sujana, M. G. and Anand, S. 2010. Fluoride removal studies from contaminated ground water by using bauxite. *Desalination*, 267(2-3): 222-227.
- Taavoni-Gilan, A., Taheri-Nassaj, E., Naghizadeh, R. and Akhondi, H. 2010. Properties of sol-gel derived Al₂O₃-15 wt.% ZrO₂ (3 mol% Y₂O₃) nano powders using two different precursors. *Ceramics International*, 36: 1147–1153.
- Taddesse, A. M., Claassens, A. S. and de Jager, P. C. 2008a. Long-term phosphorus desorption using dialysis membrane tubes filled with iron hydroxide and its effect on phosphorus pools. *Journal of Plant Nutrition*, 31(8):1507-1522.

- Taddesse, A. M., Claassens, A.S. and de Jager, P. C. 2008b. Long term kinetics of phosphate desorption from soil and its relationship with plant growth. *South African Journal of Plant and Soil*, 25(3): 131-134.
- Tadjarodi, A., Kerdari, H. and Imani, M. 2012. Synthesis, Characterization and Adsorption Capability of CdO Microstructure for Congo red from Aqueous Solution, *Journal of natural science*, 2: 9-17.
- Tofik, A. S., Abi, T. M., Tesfahun, K. T. and Girma, G. G. 2016. Fe-Al binary oxide nanosorbent: Synthesis, characterization and phosphate sorption property. *Journal of Environmental Chemical Engineering*, 4: 2458-2468.
- Van der zee, S. E. A. T. M., L. G. J. Fokkink and W. H. A. Van Reimsdijk, 1987. A new technique for assessment of reversibly absorbed phosphate. *Soil Science Society of America Journal*, 51: 599-604.
- Verma, A., Samanta, S. B., Bakhshi, A. K. and Agnihotry, S. A. 2005. Effect of stabilizer on structural, optical and electrochemical properties of sol-gel derived spin coated TiO₂ films. *Solar Energy Materials and Solar Cells*, 88: 47-64.
- Vincent, T., Gross, M., Dotan, H. and Rothschild, A. 2012. Thermally oxidized iron oxide nano architectures for hydrogen production by solar-induced water splitting, *International Journal of hydrogen energy*, 37: 8102-8109.
- Walkley, A. and Black. I. A. 1934. An examination of Degtjareff method for determining soil organic matter and a proposed modification of the chromic acid titration method. *Soil Science*, 37: 29-37.
- Xiaofang, Y., Dongsheng, W., Zhongxi, S. and Hongxiao, T. 2007. Adsorption of phosphate at the aluminum hydroxide water interface: Role of the surface acid base properties. *Colloids Surface A*, 297: 84-90.
- Xu, Y., L. Axe. 2005. Synthesis and characterization of iron oxide-coated silica and its effect on metal adsorption. *J. Colloid Interface Sci.* 282, 11–19.
- Yang, J. J., Pickett, M.D., Li, X., Ohlberg, D. A. A., Stewart, D. R. and Williams, R. S. 2008. Memristive switching mechanism for metal/oxide/metal nano devices. *Nature Nanotechnology*, 3(7): 429-433.
- Yanjuan, D., Yanju, Z. Baoan, D. and Jingfeng, Z. 2008. Preparation of nano sized ZnFe₂O₄ powders by co-precipitation method, 10: 10-52.

- Yu, Y., and Chen, J. P. 2015. Key factors for optimum performance in phosphate removal from contaminated water by a Fe-Mg-La tri-metal composite sorbent. *Journal of Colloid Interface Science*, 445: 303–311.
- Yusran, F. 2010. The relationship between phosphate adsorption and soil organic carbon from organic matter addition. *Journal of Tropical Soils*, 15: 1-5.
- Zhang, G., Liu, H., Liu, R. and Qu, J. 2009. Removal of phosphate from water by a Fe-Mn binary oxide adsorbent. *Journal of Colloid and Interface Science*, 335: 168-174.
- Zhang, J. Z., Ch. Fischer, J. and Ortner, P. B. 2004. Potential availability of sedimentary phosphorus to sediment resuspension in Florida Bay. *Global Biogeochemical Cycles*, 18: GB4008, doi:10.1029/2004GB002255, 14p.
- Zhang, Y., Wu, X., Dou, X. and Yang, M. 2007. Fluoride removal performance of novel Fe-Al-Ce tri metal oxide adsorbents. *Chemosphere*, 69: 1758-1764.
- Zhou, Q., Wang, X., Liu, J., and Zhang, L. 2012. Phosphorus removal from wastewater using nano-particulates of hydrated ferric oxide doped activated carbon fiber prepared by Sol-Gel method. *Chemical Engineering Journal*, 200: 619–626.

7. APPENDIX

Appendix Tables

Appendix Table 1. Total correlation between soil properties and cumulative P desorbed for Bojji Dimeji (B) soil

CORR	pH H ₂ O	pH KCl	Ex.A	Ex. Al	C	OM	TN	AvP	TP
pH H ₂ O	1								
pHKCl	1.00**	1							
Ex. A	0.32	0.32	1						
Ex Al	0.97	0.97	0.09	1					
C	0.86	-0.86	0.75	0.72	1				
OM	0.32	0.32	-0.78	0.54	0.18	1			
TN	1.00**	1.00**	-0.32	-0.97	0.86	0.32**	1**		
AvP	1.00**	1.00**	0.34	0.96	0.87	0.31**	1.00**	1	
TP	0.98	0.98	0.15	0.99*	0.76	0.49	-0.98	0.98	1*
FeD	-0.42	-0.42	-0.99	-0.19	0.82	0.71	0.42	-0.44	-0.25
FeOx	0.93	0.93**	-0.03	0.99	0.62	0.64	-0.93**	0.92	0.98
MnD	0.89**	0.89	-0.12	0.97	0.55	0.70**	-0.89	0.89	0.96
MnOx	0.32	0.32	1.00	0.09	0.75	-0.78	-0.32	0.34	0.15
BP0	-0.94	-0.94	-0.61	-0.84	0.98	-0.01	0.94	-0.95	-0.87
BP1	0.99	0.99	0.27	0.98	0.83	0.38	-0.99	0.99	0.99
BP2	0.42**	0.42**	0.99	0.19	0.81	0.71**	-0.42**	0.43	0.25
BP3	0.72**	0.72**	0.85	0.59	0.98	0.34**	-0.77**	0.78	0.64
CORR	FeD	FeOx	MnD	MnOx	BP1	BP2	BP3		
FeD	1								
FeOx	-0.07	1							
MnD	0.01	0.99	1**						
MnOx	-0.99	-0.03	-0.12	1					
BP0	0.69	-0.77	-0.71	-0.61					
BP1	-0.37	0.95	0.92	0.27	1				
BP2	1.000	0.06	0.01**	0.99**	0.37	1**			
BP3	-0.904	0.49	0.41**	0.85**	0.73	0.90**	1**		

** . Correlation is significant at the 0.01 level (2-tailed). and * . Correlation is significant at the 0.05 level (2-tailed) ** . Correlation is significant at the 0.01 level (2-tailed). And * . Correlation is significant at the 0.05 level (2-tailed) , *Av.P* = Availability of P, *Ex.A* = Exchangeable acidity, *C* = carbon, *OM* =organic matter, *TN* = Total nitrogen,. *TP* = Total phosphorous, *Fe D* = Iron extracted by Dithionite, by Dithionite, *Mn D* extracted by Dithionite, *Fe Ox* = Iron extracted by Oxalate, *Mn Ox* = manganese extracted by oxalate.

Appendix Table 2. Total correlation between soil properties and cumulative P desorbed for Mana sibu (M) soil.

Corr	pHH ₂ O	pH KCl	Ex.A	Ex. Al	OM	TN	Av P	TP
pH H₂O	1							
pH KCl	1.00**	1						
Ex. A	-0.32	0.32	1					
Ex. Al	-0.98	0.98	0.50	1				
C	0.50	-0.50	0.65	-0.32				
OM	0.50	-0.50	-0.98	-0.65	1			
TN	-0.32	0.32	1.00**	0.50	-0.98	1		
Av P	0.88	-0.88	-0.72	-0.95	0.84	-0.72	1	
TP	-0.97	0.97	0.12	0.92	-0.31	0.12	-0.77	1
Fe_D	-0.94	0.94	0.00	0.86	-0.18	0.00	-0.68	0.99
Fe_{ox}	-0.94	0.94**	0.00	0.86	-0.18	0.00**	-0.68	0.99
Mn_D	0.93**	-0.93	0.03	-0.84	0.15**	0.03	0.65	-0.98
Mn_{Ox}	-0.16	0.16	0.98	0.35	-0.93	0.98	-0.60	-0.32
MP0	0.34	-0.34	-1.00	-0.51	0.98	-1.00	0.73	-0.14
MP1	-0.27	0.27	0.99	0.45	-0.97	0.99	-0.69	.071
MP2	0.18	-0.18	-0.99**	-0.37	0.94	-0.99	0.62**	.012
MP3	-0.28	0.28	0.99	0.45	-0.97	0.99	-0.69	.073
CORR	Fe_D	Fe_{Ox}	Mn_D	Mn_{Ox}	MP0	MP1	MP2	MP3
Fe _D	1							
Fe _{Ox}	1.00**	1						
Mn _D	-0.99**	-0.99	1**					
Mn _{Ox}	-0.16	-0.16	0.19	1				
MP0	-0.01	-0.01	-0.01	-0.98	1			
MP1	-0.05	-0.05	0.08	0.99	-0.99	1		
MP2	.014	.014	-0.17	1.00	0.98	-0.99	1	
MP3	-0.04	-0.04	0.08	0.99	-0.99	1.00	0.99**	1

** . Correlation is significant at the 0.01 level (2-tailed). And * . Correlation is significant at the 0.05 level (2-tailed) ** . Correlation is significant at the 0.01 level (2-tailed). And * . Correlation is significant at the 0.05 level (2-tailed), *Av.P* = Availability of P, *Ex.A* = Exchangeable acidity, *C* = carbon, *OM* =organic matter, *TN* = Total nitrogen., *TP* = Total phosphorous, *Fe_D* = Iron extracted by Dithionite, by Dithionite, *Mn_D* extracted by Dithionite, *Fe_{Ox}* = Iron extracted by Oxalate, *Mn Ox* = manganese extracted by oxalate.

Appendix Table 3. Total correlation between soil properties and cumulative P desorbed for Kara Kiltu (K) soil

Corr	pH H ₂ O	pH KCl	Ex A	Ex Al	OM	TN	AVP	TP
pH H₂O	1							
pH KCl	-0.50	1						
Ex A	0.41	-0.99	1					
Ex Al	0.79	0.12	-0.21	1				
C	-0.99	0.57	-0.50	-0.73				
OM	-0.24	0.96	-0.98	0.39	1			
TN	-0.72	-0.24	0.32	-0.99	-0.50	1		
AVP	-0.83	0.89	-0.85	-0.32	0.74	0.21	1	
TP	0.27	0.69	-0.75	0.80	0.86	-0.86	0.30	1
Fe_D	-0.75	-0.19	0.28	-0.99*	-0.46	0.99	0.25	0.84*
Fe_{Ox}	-0.81	-0.09	0.18	1.00	-0.37	0.99	0.34	-0.78
Mn_D	-0.88	0.84	-0.79	-0.41	0.66	0.30	0.99	0.20
Mn_{Ox}	0.05	-0.89	0.92	-0.56	-0.98	0.65	-0.60	-0.94
KP0	-0.98	0.32	-0.23	-0.89	0.04	0.84	0.70	-0.45
KP1	-0.39	0.99	-1.00	0.24	0.98	-0.35	0.83	0.77
KP2	-0.80	0.91	-0.87	-0.27	0.77	0.16	0.99	0.35
KP3	-0.50	-0.49	0.57	-0.92	-0.71	0.96	-0.06	-0.97
CORR	Fe_D	Fe_{Ox}	Mn_D	Mn_{Ox}	KP0	KP1	KP2	KP3
Fe_D	1							
Fe_{Ox}	0.99**	1						
Mn_D	0.35	0.44	1					
Mn_{Ox}	0.62	0.54	-0.51	1				
KP0	0.86	0.91	0.77	0.14	1			
KP1	-0.31	-0.21	0.78	-0.93	0.20	1		
KP2	0.20	0.30	0.98	-0.63	0.67	0.86	1	
KP3	0.94	0.91	0.03	0.83	0.65	-0.59	-0.11	1

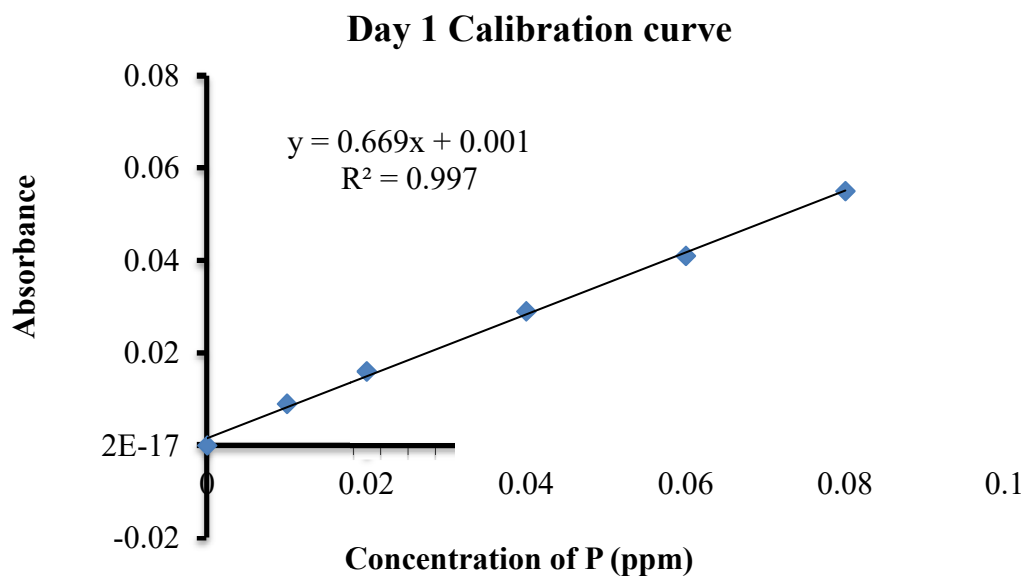
** . Correlation is significant at the 0.01 level (2-tailed). And * . Correlation is significant at the 0.05 level (2-tailed) , *Av.P* = Availability of P, *Ex.A* = Exchangeable acidity *C* = carbon, *OM* = organic matter, *TN* = Total nitrogen, *TP* = Total phosphorous, *Fe_D* = Iron extracted by Dithionite, *Mn_D* extracted by Dithionite, *Fe_{Ox}* = Iron extracted by Oxalate, *Mn_{Ox}* = manganese extracted by oxalate.

Appendix Table 4. Total correlation between soil properties and cumulative P desorbed for Nedjo (N) soil

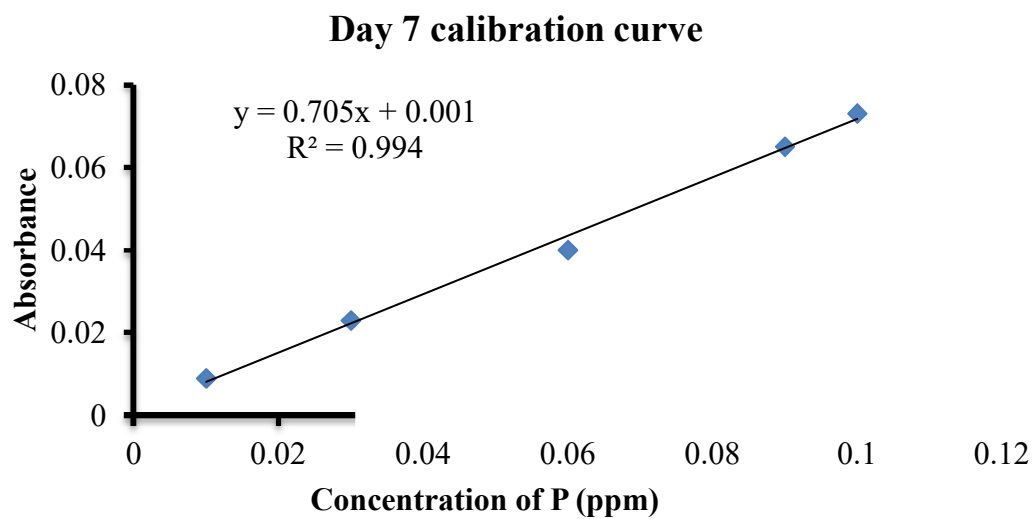
Corr	pH H ₂ O	pH KCl	ExA	Ex Al	OM	TN	AVP	TP
pH H₂O	1							
pH KCl	0.78	1						
Ex A	-0.85	-0.99	1					
Ex Al	0.89	0.41	-0.52	1				
C	0.50	0.92	-0.87	0.05				
OM	-0.50	-0.92	0.87	-0.05	1			
TN	-0.32	0.32	-0.21	-0.72	-0.65	1		
AvP	-0.50	-0.92	0.87	-0.05	1.00	-0.65	1	
TP	-0.62	-0.97	0.93	-0.19	0.98	-0.53	0.98	1
Fe_D	0.65	0.98	-0.95	0.24	-0.98	0.50	-0.98	-0.99
Fe_{Ox}	0.24	-0.40	0.29	0.66	0.71	-0.99	0.71	0.60
Mn_D	0.67	0.06	-0.18	0.93	0.30	-0.92	0.30	0.16
Mn_{Ox}	0.65	0.98	-0.95	0.24	-0.98	0.50	-0.98	-0.99
NP0	0.95	0.93	-0.97	0.71	-0.74	-0.02	-0.74	-0.83
NP1	0.73	0.99	-0.98	0.34	-0.95	0.39	-0.95	-0.98
NP2	0.97	0.63	-0.72	0.96	-0.30	-0.52	-0.30	-0.44
NP3	0.93	0.50	-0.60	0.99	-0.15	-0.64	-0.15	-0.29
CORR	Fe_D	Fe_{Ox}	Mn_D	Mn_{Ox}	NP0	NP1	NP2	NP3
Fe_D	1							
Fe_{Ox}	-0.56	1						
Mn_D	-0.12	0.88	1					
Mn_{Ox}	1.00	-0.56	-0.12	1				
NP0	0.85	-0.05	0.41	0.85	1			
NP1	0.99	0.47**	-0.01	0.99	0.90	1**		
NP2	0.47	0.45	0.81	0.47	0.86	0.57	1	
NP3	0.33	0.58**	0.89	0.33	0.77	0.43**	.098	1

** . Correlation is significant at the 0.01 level (2-tailed) and * . Correlation is significant at the 0.05 level (2-tailed) **. Correlation is significant at the 0.01 level (2-tailed). and * . Correlation is significant at the 0.05 level (2-tailed) , *Av.P* = Availability of P, *Ex.A* = Exchangeable acidity, *C* = carbon, *OM* =organic matter, *TN* = Total nitrogen,. *TP* = Total phosphorous, *Fe_D* = Iron extracted by Dithionite, by Dithionite, *Mn_D* extracted by Dithionite, *Fe_{Ox}* = Iron extracted by Oxalate, *Mn Ox* = manganese extracted by oxalate.

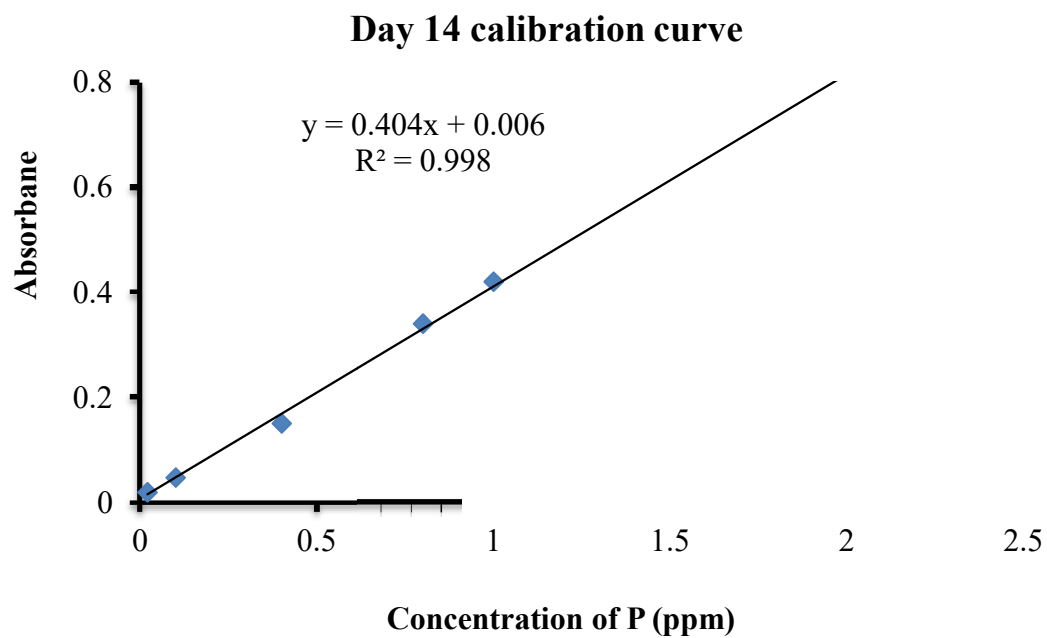
Appendix Figures



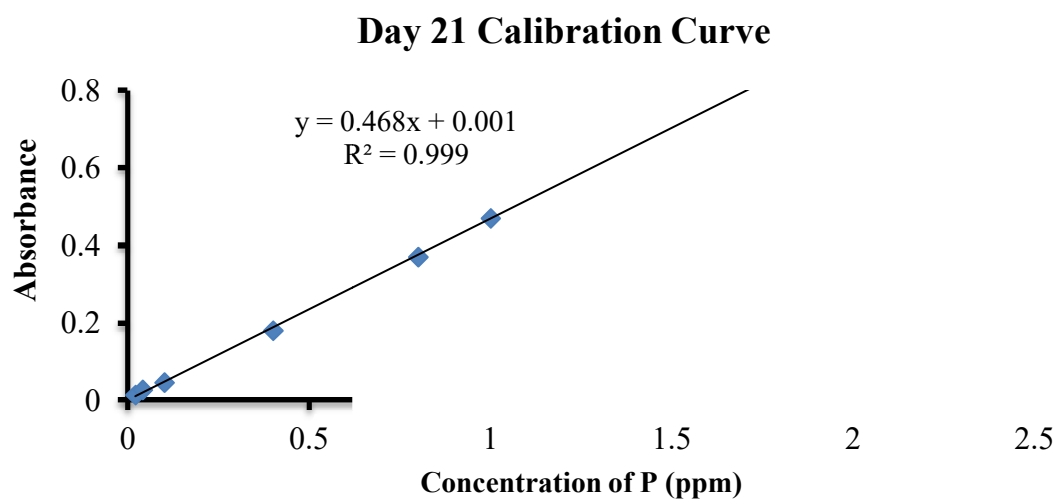
Appendix Figure 1. Calibration curve for day 1 P desorption



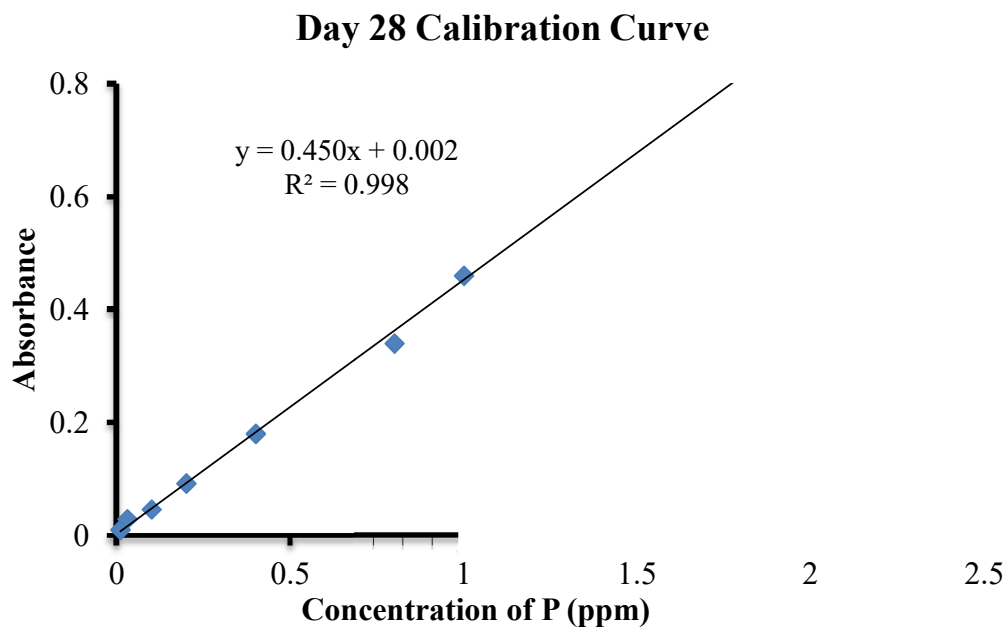
Appendix Figure 2. Calibration curve for day 7 P desorption



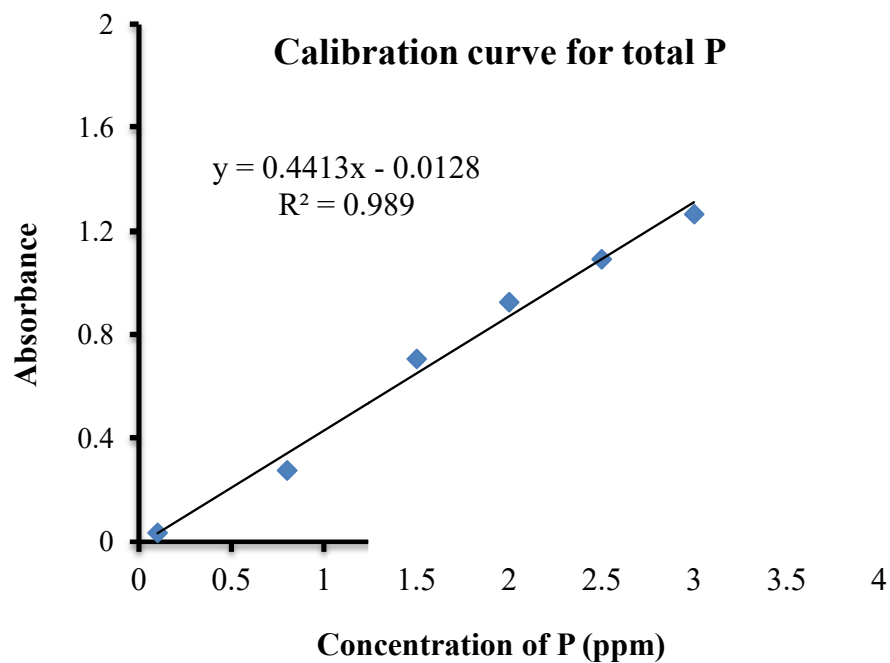
Appendix Figure 3. Calibration curve for day 14 P desorption.



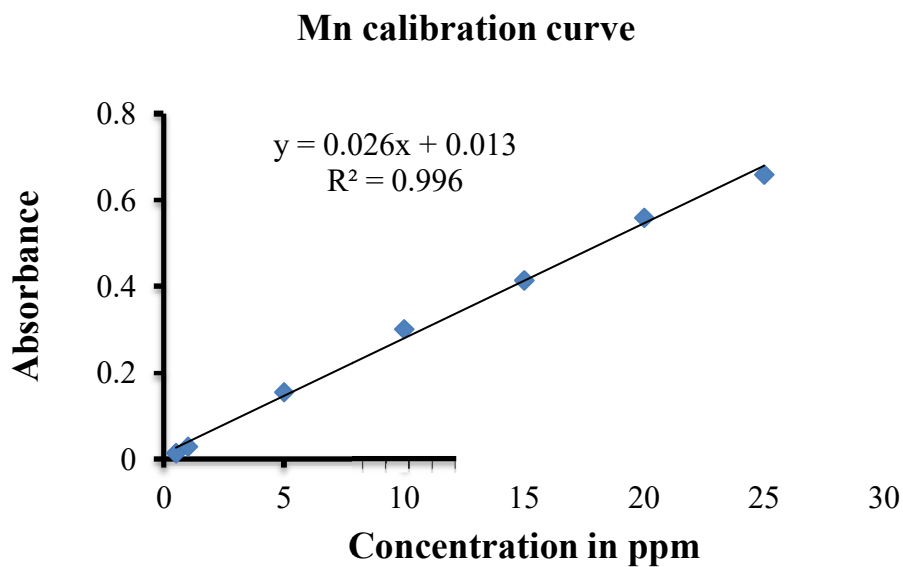
Appendix Figure 4. Calibration curve for day 21 P desorption.



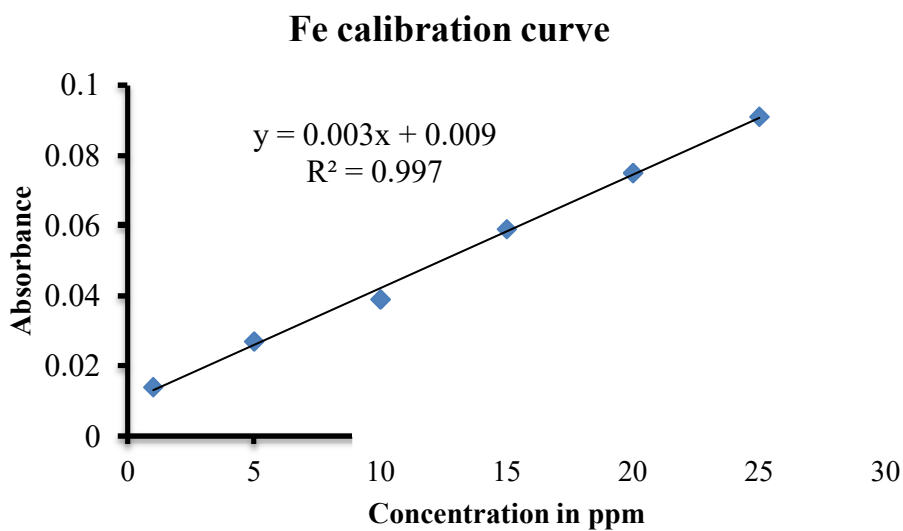
Appendix Figure 5. Calibration curve for day 28 P desorption.



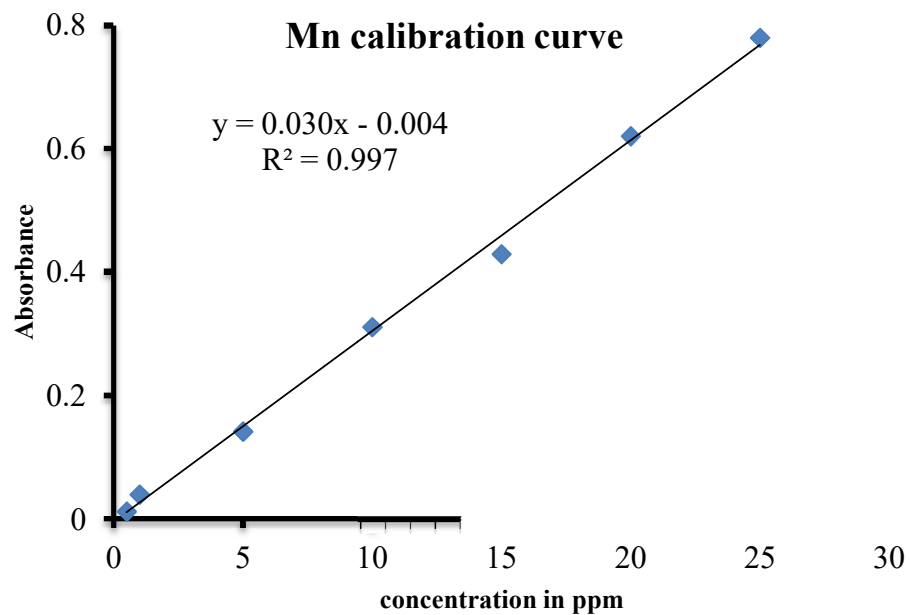
Appendix Figure 6. Calibration curve for total phosphorus



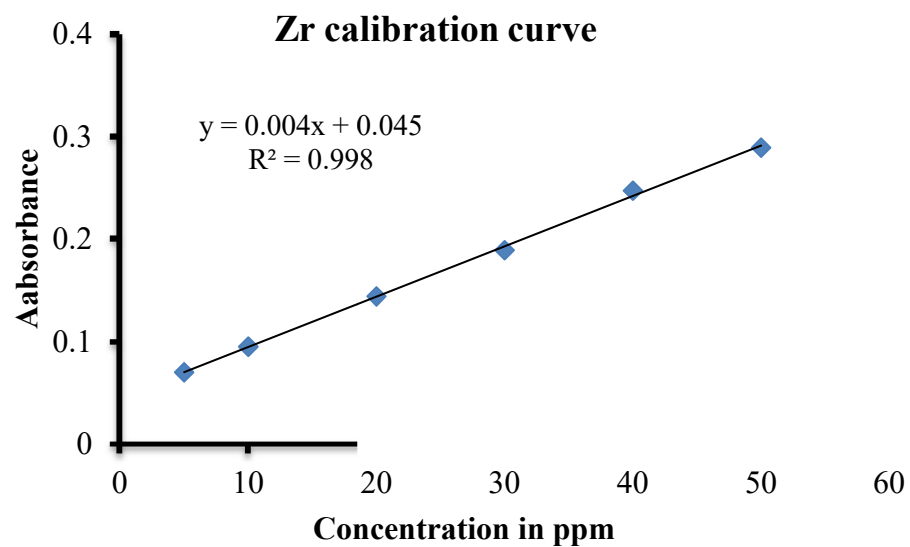
Appendix Figure 7. Calibration curve for Mn in soil for Dithionate extractants



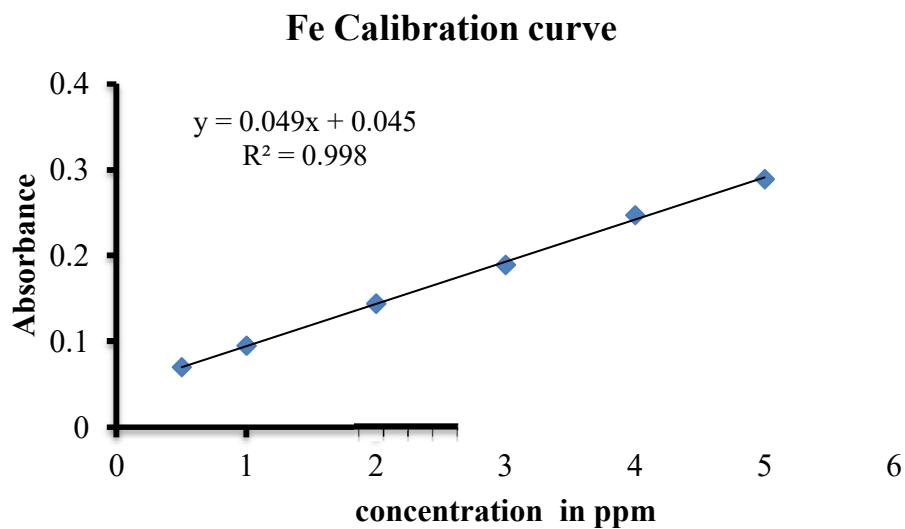
Appendix Figure 8. Calibration curve for Fe in soil for Dithionate and Oxalate extractants



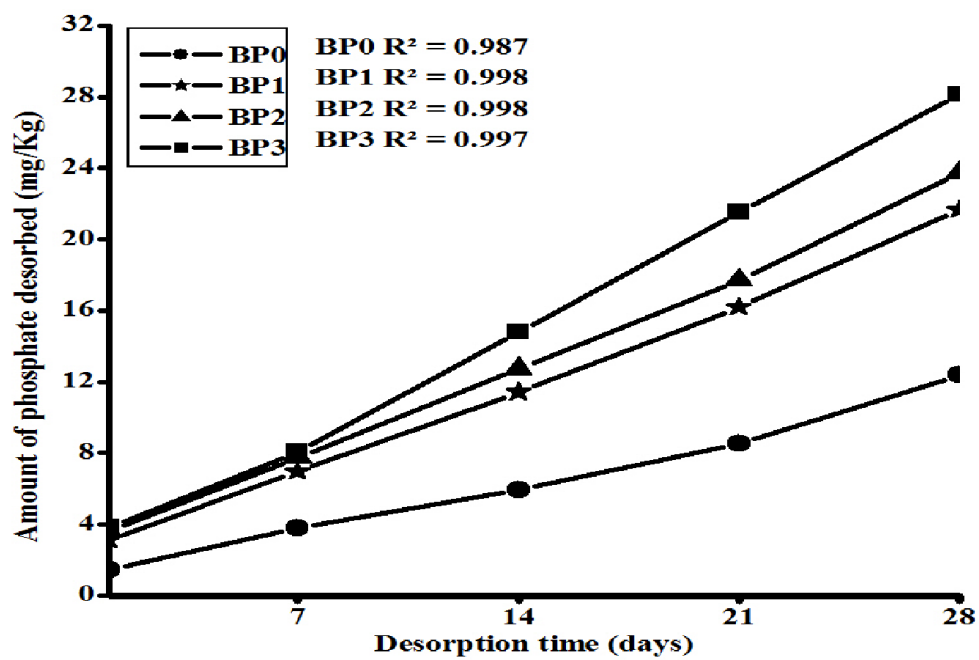
Appendix Figure 9. Calibration curve for Mn in soil for Oxalate extractants



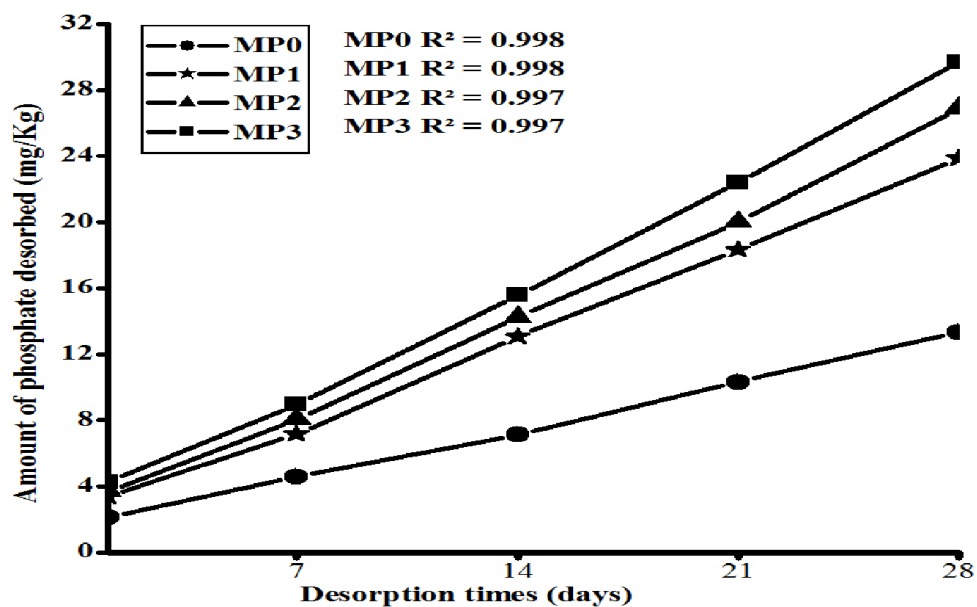
Appendix Figure 10. Calibration curve for Zr in synthesized nano composite



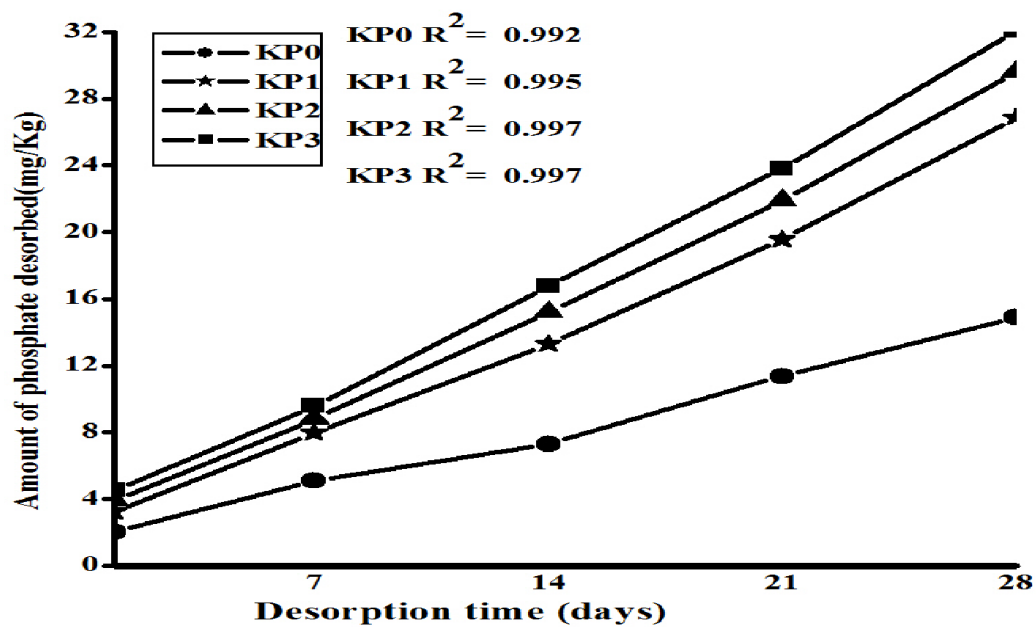
Appendix Figure 11. Calibration curve for Fe in synthesized nano composite



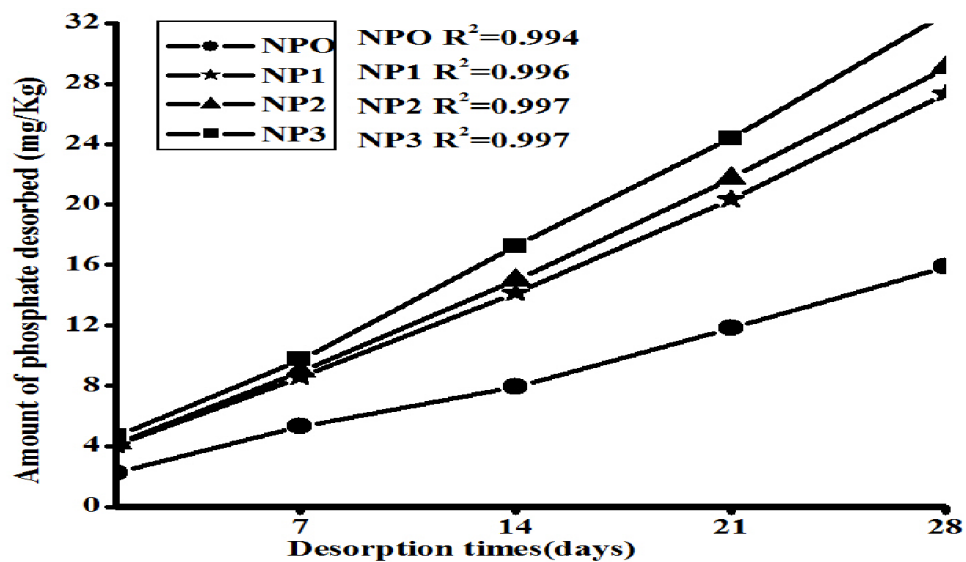
Appendix Figure 12. Cumulative desorbable P with time extracted using DMT-Fe-Al-Zr for the different treatments for Boji Dirmeji (B) soil sample over 28 days



Appendix Figure 13. Cumulative desorbable P with time extracted using DMT-Fe-Al-Zr for the different treatments for Mana Sibiu (M) soil sample) over 28 days



Appendix Figure 14. Cumulative desorbable P with time extracted using DMT-Fe-Al-Zr for the different treatments Kiltu Kara (K) for soil sample over 28 days



Appendix Figure 15. Cumulative desorbable P with time extracted using DMT-Fe-Al-Zr for the different treatments for Nedjo (N) soil sample over 28 days